FORM TI-12
07/1999

B-T-3387

Measuring the Fracture Toughness of TZM and ODS Molybdenum Alloys using Standard and Sub-Sized Bend Specimens

B.V. Cockeram

USDOE contract No. DE-AC11-98PN38206

BETTIS ATOMIC POWER LABORATORY WEST MIFFLIN, PENNSYLVANIA 15122-0079

Operated for the U.S. Department of Energy
by Bechtel Bettis, Inc.

Measuring the Fracture Toughness of TZM and ODS Molybdenum Alloys using Standard and Sub-Sized Bend Specimens

B.V. Cockeram

Bechtel-Bettis Atomic Power Laboratory, P.O. Box 79, West Mifflin, PA 15122-0079.

Abstract

Oxide Dispersion Strengthened (ODS) and TZM molybdenum have excellent creep resistance and strength at high temperatures in inert atmospheres. Fracture toughness and tensile testing was performed at temperatures between -150°C and 450°C to characterize 6.35 mm thick plate material of ODS and TZM molybdenum. A transition from low fracture toughness values (5.8 to 29.6 MPa$\sqrt{m}$) to values > 30 MPa$\sqrt{m}$ is observed for TZM molybdenum in the longitudinal orientation at 100°C and in the transverse orientation at 150°C. These results are consistent with data reported in literature for molybdenum. A transition to low fracture toughness values (< 30 MPa$\sqrt{m}$) was not observed for longitudinal ODS molybdenum at temperatures ≥ -150°C, while a transition to low fracture toughness values (12.6 to 25.4 MPa$\sqrt{m}$) was observed for the transverse orientation at room-temperature. The fine spacing of La-oxide precipitates that are present in ODS molybdenum result in a transition temperature that is significantly lower than any molybdenum alloy reported to date, with upper bound fracture toughness values that bound the literature data. A comparison of fracture toughness values obtained using a 1T, 0.5T, and 0.25T Charpy shows that a 0.5T Charpy could be used as a sub-sized specimen geometry.

I. INTRODUCTION

Molybdenum is a refractory metal that undergoes no phase change for the body-centered cubic (bcc) crystal structure from ambient to the melting temperature (2610°C (4730°F)). The good high-temperature strength, creep resistance, low coefficient of thermal

expansion, and high thermal conductivity are attractive properties for molybdenum-base alloys[1]. Molybdenum forms a volatile oxide at high temperature at high oxygen partial pressures, which limits long-term use in air at temperatures ≥ 500°C. However, molybdenum is widely used where the high-temperature strength and creep resistance are needed for applications that involve short-term exposures in air (i.e. forging dies, metalworking tooling, and glass-melting furnaces) or long-term exposures in a controlled atmosphere (i.e. vacuum furnace components). Molybdenum has also been considered for use in advanced nuclear power generation systems[2-3]. Metals with a bcc structure generally exhibit high levels of ductility and toughness at a homologous temperature (T/T_m (Kelvin)) ≥0.3, while a greater tendency for brittle fracture is observed at homologous temperatures < 0.2. The homologous temperature for molybdenum alloys at room-temperature is low ($T/T_m \leq 0.10$), and the Ductile to Brittle Transition Temperature (DBTT) is generally within 100°C of room-temperature, which indicates that brittle fracture can be a concern at ambient temperatures.

Since molybdenum is generally used for applications that are creep limited where brittle fracture is less of a concern, little data is available in literature on the fracture toughness of molybdenum and molybdenum-base alloys[4-13]. A review of some fracture toughness data for molybdenum and molybdenum-base alloys has been reported[4]. Most of the early work involved the use of Charpy specimens that were not pre-cracked, use of an EDM wire for pre-cracking, or specimen sizes that were too thin for a valid measurement, which indicates that these values may not be conservative. Only recently has a method of compression pre-cracking been developed to allow a more accurate and conservative measure of molybdenum fracture toughness[4,5,7-10]. Although some fracture toughness data have been reported for molybdenum, most of the data have been measured only at room-temperature. Little testing has been performed over a range of temperatures to define a transition temperature or DBTT.

Two important molybdenum-base alloys are molybdenum - 0.5% titanium - 0.1% zirconium (TZM)[14] and Oxide Dispersion Strengthened (ODS) molybdenum[15-18]. TZM has a

fine distribution of carbide precipitates that are rich in titanium and zirconium, which inhibits grain growth and recrystallization at high temperatures and results in good high-temperature strength. ODS molybdenum has a fine distribution of lanthanum-oxide (2 volume%), which also limits grain growth and recrystallization to result in excellent strength and creep resistance at high temperatures[15-18]. The fibrous grain structure with a fine grain size for ODS molybdenum results in a high level of tensile ductility. However, fracture toughness data for ODS molybdenum have not been reported. The purpose of this work is to measure the fracture toughness of TZM and ODS molybdenum from -150°C to 450°C to identify the DBTT. Since test volume space is limited in some cases, a comparison of fracture toughness data are made using various sized bend specimens to determine if a consistent measure of fracture toughness can be obtained.

II. EXPERIMENTAL PROCEDURES

A. *Materials*

Table I is a summary of the compositions for TZM and ODS molybdenum that were obtained from H.C. Starck (formerly known as CSM Industries), Cleveland, OH as 6.35 mm thick plate. Vacuum arc-cast TZM molybdenum was produced in accordance with ASTM B387 (type 363[14]) specifications. The TZM molybdenum was produced using a Press-Sinter-Melt process, where pre-alloyed TZM molybdenum powder is fed from a hopper, which is enclosed within a vacuum melting furnace that was used to produce the powder, into a pressing die, where it is pressed into a disc and fed into a melting furnace[4]. This process is repeated until an electrode is built-up. The electrode is then melted in vacuum using an AC arc and solidified in a water-cooled copper crucible. The cast ingot is then extruded at high temperature to break-up the large grain structure that is produced by arc casting. The rectangular extrusion is sectioned and given a heat treatment to recrystallize the material prior to hot rolling to a 6.35 mm thick plate. The rolling is performed perpendicular to the extrusion direction, which results in alignment of grains parallel to the direction of rolling (longitudinal direction). A final stress-relief

anneal was performed after rolling at 1150°C for 0.5 hour. The surface of the TZM plate was etched after the stress-relief heat treatment to remove the decarburized zone.

ODS molybdenum plate (6.35 mm) was produced at H.C. Starck using methods that have been reported[15-18]. Molybdenum-oxide powder (mostly MoO_2) is wet-doped with a lanthanum nitrate solution. The slurry is dried in air, and given a heat treatment in hydrogen at 1050 - 1100°C for 4.5 hours to reduce the molybdenum oxide and pyrolize the lanthanum nitrate. This process results in a nominal 2 volume% content of La_2O_3 in the powder. The powder was cold isostatically pressed at room temperature at a pressure of 220.6 MPa into a rectangular billet (63.5 cm X 25.4 cm X 7.6 cm) and then sintered in hydrogen at 1800°C for 16 hours. The billet was rolled at 1100°C to 12.4 mm thickness using multiple passes (reheating the bar at least once). The sheet was caustic/acid cleaned and then rolled at 1050°C to a nominal thickness of 6.35 mm for a final total reduction of 92%. The 6.35 mm plate was caustic/acid cleaned and then given a final stress-relief anneal at 910°C for 1 hour.

B. *Specimen Preparation*

Tensile specimens (Figure 1), and 1T, 0.5T, and 0.25T Charpy (Figure 2) specimens were machined from the TZM and ODS molybdenum plate. The tensile specimens, and 0.5T, and 0.25T Charpy specimens were machined after removing 0.6 mm of material from each face of the 6.35 mm thick plate. The tensile specimens were laser scribed with the appropriate identification and then electropolished at room temperature in a solution of four parts concentrated reagent grade sulfuric acid and one part distilled deionized water using a 0.25 mm thick Type 304 stainless steel cathode and a dc voltage of 6-7 volts to remove 51 μm to 76 μm from the gauge section. The Charpy specimens were machined from 6.35 mm thick plate with the notch oriented in the longitudinal direction (L-T orientation in accordance with ASTM E1823[19-21], notch perpendicular to the direction of rolling), transverse direction (T-L orientation in accordance with ASTM E1823, notch parallel to the direction of rolling), or through thickness

direction (T-S orientation in accordance with ASTM E1823, notch parallel to the plate thickness). The Charpy specimens were laser scribed for identification, and then pickled in a solution of 10 parts acetic acid, 4 parts nitric acid, and 1 part HF acid for 5-15 seconds to remove 25 μm to 51 μm of material followed by a rinse in HCl acid, and a rinse in DI water. The tensile and Charpy specimens were given a final stress-relief heat treatment in a vacuum furnace (vacuum < 10^{-6} torr) at 1150°C for 0.5 hour for TZM and 1200°C for 1 hour for ODS.

C. *Tensile and Fracture Toughness Testing Procedures*

Tensile testing was performed at Pittsburgh Materials Technology Inc (PMTI), Large, PA and Composite Testing and Analysis (CT&A), State College, PA in accordance with ASTM E8 from -150°C to 1000°C at an actuator displacement rate of 0.017 mm/sec (strain rate = 0.021 sec^{-1})[22-23]. All tensile data are reported in terms of engineering stress and engineering strain. For testing at CT&A, the strain was measured using a spring-loaded high-temperature extensometer that was equipped with pointed alumina rods, which contacted the face of the specimens just inside the grips. The grips were solid enough such that contact of the extensometer at this point ensured lateral support of the specimen to prevent bending while allowing free longitudinal movement of the material within the gauge length. The extensometer does meet the requirements of Class B-2 in accordance with ASTM-E8[22-23], and a good estimate of Young's modulus was obtained by a linear regression fit of the stress-strain data between stresses of 0 to 400 MPa for testing performed at temperatures < 600°C, and between stresses of 0 to 200 MPa for testing performed between 700°C and 1000°C. Ultimate tensile strength, 0.2% off-set yield strength, and total elongation were determined using standard methods[22-23]. Elongation for tensile testing performed at PMTI was determined using the cross-head displacement, so a measurement of Young's modulus could not be obtained. Tensile testing at temperatures > 600°C at PMTI was performed in a vacuum furnace at a vacuum $\leq 5 \times 10^{-5}$ torr.

Fracture toughness testing was performed at CT&A in accordance with the ASTM E399 method[20-21]. All specimens were fatigue pre-cracked prior to fracture toughness testing. Since molybdenum has a high hardness and fatigue characteristics at room-temperature that are similar to ceramic materials, the majority of fatigue pre-cracking was performed in compression (stress ratio, R = 0.1), which is the approach typically used for successful fracture toughness testing of molybdenum [4,5,7-10]. Fracture toughness testing was performed at a displacement rate of 0.0025 mm/s (K-rate = 33 to 154 MPa$\sqrt{m}$ / min), which satisfies the loading rate requirements for a valid test[20-21]. Testing at room-temperature to 100°C was performed in air. Tensile or fracture toughness testing at temperatures from 100°C to 1000°C was performed in an inert argon atmosphere with less than 10 ppm oxygen, after equilibrating the specimens at temperature for ½ hour. Testing below room-temperature was performed in an isolated stainless steel chamber with a large thermal mass that was cooled with a mixture of ambient air and nitrogen gas from a liquid nitrogen source. The specimens were cooled to below the desired test temperature, and the chamber was then allowed to heat up and the test was run at the test temperature. The large thermal mass of the chamber allowed control of temperature within 2 °C during testing at temperatures ≤ 0°C. Fracture toughness testing was also performed at a higher displacement rate of 0.25 mm/s (K-rate = 330 to 15,400 MPa$\sqrt{m}$ / min) and lower displacement rate of 0.00025 mm/s (K-rate = 1.1 to 15.3 MPa$\sqrt{m}$ / min), which are outside the loading rate specified in the standard, to evaluate the influence of loading rate.

A fracture toughness test is valid ($K_{IC} = K_Q$) if all 14 checks are satisfied. Three of the more important requirements for a valid K_{IC} test are thought to be overly conservative for hard materials that have a more limited plastic zone size[24-25]:

$$a, B \geq 2.5 \left[K_Q^2 / \sigma_y^2 \right] \quad [1]$$

$$0.6\, K_Q \geq K_{max} \quad [2]$$

$$1.1 \geq \left[P_{max} / P_Q \right] \quad [3]$$

where σ_y is the yield stress, K_{max} is the maximum stress intensity for the final 2.5% of fatigue pre-cracking, P_Q is the load at 5% secant offset, and P_{max} the maximum applied load. The requirements define in Eqs. (1) and (3) are most important to assure plane strain conditions and linear-elastic conditions, respectively. However, it is still possible to get meaningful data when these criteria are relaxed. Since the method of compression-compression fatigue pre-cracking results in a small residual plastic zone size where the fatigue pre-crack has been grown into a decreasing stress intensity (K) field such that crack arrest occurs, the intent of Eq. (2), which only applies to tension-tension fatigue pre-cracking, is not applicable. The K_{IC} results were considered to be conditionally valid (K_{CV}), if the following relaxed criteria were met.

$$a,B \geq [K_Q^2 / \sigma_y^2] \qquad [4]$$

$$1.15 \geq [P_{max} / P_Q] \qquad [5]$$

Conditionally valid means that the criteria defined by ASTM E399 have not been satisfied, but the data are a reasonable estimate of the fracture toughness of molybdenum materials. K_{CV} values are not valid lower-bound toughness values. Due to the crack-arrest behavior associated with compression-compression fatigue pre-cracking, the fatigue precrack length beyond the notch was only 0.36 mm to 0.51 mm and the total length (a/W) was nominally 0.37 to 0.46 for most of the tests, which does not strictly meet the ASTM E399 requirements of $0.45 \leq a/W \leq 0.55$. Solutions for the stress-intensity factor at these shorter crack lengths are well known, and the pre-crack lengths for the TZM and ODS molybdenum specimens are judged to be sufficient in length for a meaningful fracture toughness result. The microstructure of the longitudinal and transverse sections from fractured K_{IC} specimens were metallographically evaluated with a Murakami's etch. Fractographic examinations were also performed using Scanning Electron Microscopy (SEM).

III. REVIEW OF MOLYBDENUM FRACTURE TOUGHNESS DATA

A summary of fracture toughness data reported in literature for molybdenum, TZM, and a molybdenum – 1% zirconium alloy is given in Table II. Some of the results were obtained using specimens that were not pre-cracked or specimens that were pre-cracked using a wire EDM[5,6], which violates the intent of the standard[20,21] and may not provide the most accurate measure of fracture toughness. High fracture toughness values were obtained from thin molybdenum sheet stock specimens were too thin to maintain plane-strain conditions[7], which results in a non-conservative overestimate of fracture toughness. Use of compressive pre-cracking is shown in Table II to provide a measure of fracture toughness that is relatively consistent for various product forms and metallurgical conditions for molybdenum.

The plot of fracture toughness values versus temperature shows in Figure 3 that a transition from low fracture toughness values ranging from 8 to 22 MPa$\sqrt{m}$ to higher values (30 to 96 MPa$\sqrt{m}$) is observed for a number of molybdenum materials at temperatures between 200°C and 500°C. Use of a Charpy test method for arc-cast molybdenum specimens that were not pre-cracked has indicated that the transition temperature from ductile to brittle behavior is -60°C to 30°C[11], which is significantly lower than the DBTT shown in Figure 3 for fracture toughness data. Thus, a more conservative measure of DBTT is obtained for molybdenum using fracture toughness testing of pre-cracked specimens. Lower fracture toughness values were observed for molybdenum produced by powder metallurgy methods in comparison to arc-cast material. Powder metallurgy processing results in higher residual oxygen and carbon contents, which produces lower toughness values and a higher DBTT in comparison to molybdenum produced by arc-casting[1-11].

IV. TENSILE TESTING RESULTS

The tensile results for TZM molybdenum obtained in the longitudinal and transverse direction are summarized in Tables III and IV, respectively. Tensile data for ODS molybdenum are given in Tables V and VI for the longitudinal and transverse orientation, respectively. Representative stress-strain curves for TZM and ODS molybdenum are shown in Figures 4 and

5. Some banding was observed in the microstructure of ODS (Figures 6g and 6h) and TZM (Figure 7c), which likely results from the mechanical working used to form the plate. A coarser grain size and coarser precipitate density is present in the banded region. Banding may result from inhomogeneity in the chemistry or working of the metal, but precise identification of the source of the banding will require additional examinations. The use of a tensile specimen that is significantly thinner (0.51 to 0.76 mm) than the 6.35 mm thick plate stock that contained some amount of banding and microstructural variation (grain size, spacing of precipitates, etc.) likely explains the data scatter. However, the tensile properties are within the range of values reported in literature for TZM molybdenum[14,26-32].

Comparison of tensile properties for TZM and ODS molybdenum shows in Figures 8 and 9, respectively, that the strength and elongation of the two materials are generally comparable between temperatures of -150°C and 1000°C, with the exception of a slightly lower yield strength for ODS molybdenum between 200°C and 1000°C. The fine distribution of La-oxide particles in ODS molybdenum provides a higher recrystallization temperature ($T \geq 1600$°C), and better high-temperature strength and creep resistance compared to TZM at temperatures > 1000°C[15-18]. ODS molybdenum has a fine grain size with elongated grains and fine La-oxide particles orientated in the direction of working (Longitudinal), see Figure 6. TZM molybdenum consists of sheet-like grains that are elongated in the direction of working with equiaxed Ti,Zr-rich carbides (Figure 7). The grain size of ODS molybdenum is significantly finer than TZM molybdenum. Recrystallization of TZM molybdenum to form a large grain size typically occurs at temperatures ≥1300°C, which explains the significant decrease in tensile strength that is observed at 1400°C.

The yield strength of the longitudinal and transverse orientations were generally comparable within the data scatter for both TZM and ODS molybdenum, see Figures 8a and 9a, respectively. Significantly lower total elongation values are observed for the transverse

orientation in comparison to the longitudinal orientation for both TZM (Figure 8b) and ODS (Figure 9b). The fracture surface of TZM molybdenum tested at room-temperature is shown in Figure 10 to consist of a ductile laminate failure with necking of sheet-like grains. The microstructure of TZM molybdenum consists of sheet-like grains (Figure 7), and fracture initiation at grain boundaries by the formation of micro-cracks likely leaves ligaments of sheet-like grains that neck down to failure, which gives the ductile laminate appearance for the fracture surface. The fracture surface of ODS molybdenum tested at room-temperature is shown in Figure 11 to consist of a ductile laminate failure with necking of sheet-like grains. Fracture initiation at grain boundaries, La-oxides, and La-oxide/matrix boundaries by the formation of micro-cracks leaves ligaments of sheet-like grains that neck down to failure, which gives the ductile laminate appearance for ODS. The fine grain size and fine spacing of La-oxides and La-oxide/matrix boundaries for ODS molybdenum (Figure 6) results in a smaller size for the laminate features on the fracture surface in comparison to TZM. Thicker and wider laminates were observed on the fracture surface of the transverse specimens in comparison to the longitudinal fracture surfaces for both TZM and ODS. Alignment of grains and oxide precipitates in the longitudinal direction results in more grain boundary and/or precipitate area for fracture initiation in the transverse direction, which likely explains the lower total elongation in the transverse direction for both TZM and ODS.

Tensile testing of longitudinal TZM molybdenum at -100°C results in measurable ductility and a ductile failure was observed, while tensile testing at -150°C resulted in no ductility with a brittle fracture. High elongation and a ductile failure were observed for tensile testing of transverse TZM at room-temperature, while tensile testing at -50°C resulted in brittle cleavage. Based on these results, the DBTT of TZM molybdenum is -100°C for the longitudinal orientation and room-temperature for the transverse orientation. High amounts of total elongation were observed for tensile testing of longitudinal ODS molybdenum at -100°C, while low elongation

and brittle failure were observed at -150°C. A transition from high total elongation and ductile failures was observed for the tensile testing of transverse ODS molybdenum at -50°C. Based on these tensile test results, the DBTT for longitudinal and transverse ODS molybdenum is -100°C and -50°C, respectively.

The stress-strain curves for TZM molybdenum show in Figure 4 that a low work hardening rate was observed for both the longitudinal and transverse orientations over a range of test temperatures. Lower yield strength and total elongation are observed for TZM molybdenum at test temperatures > room-temperature, as is reported for molybdenum in literature[26-33]. The low work-hardening rate for TZM molybdenum likely results in low resistance to plastic instability or necking. The lower strength for TZM molybdenum at higher temperatures with a low resistance to necking likely results in lower total elongation at higher test temperatures, until recrystallization occurs at 1400°C and higher total elongation is observed. The fracture surface of TZM tested at higher temperatures (Figure 10) exhibits a higher degree of necking with true dimpling rather than the ductile laminate failure observed at room-temperature. This identifies a change in the fracture and deformation mechanism for TZM molybdenum at higher test temperatures.

An upper and lower yield point with a Lüders' plateau is observed for ODS molybdenum at test temperatures between -100°C and 100°C followed by a low work-hardening rate. The upper / lower yield point is produced by the trapping of dislocations by atmospheres of impurity solute atoms (i.e. carbon) to result in a higher stress for the initiation of dislocation movement than the stress required to maintain dislocation movement, which has been observed for molybdenum[27]. The loss of the upper/lower yield point corresponds to the temperature at which a decrease in yield strength and total elongation are observed for ODS. The low work hardening rate for ODS molybdenum results in low resistance to plastic instability or necking, which likely explains the decrease in total elongation observed at higher test temperatures.

Tensile testing of ODS at higher temperatures is shown in Figure 11 to result in a higher degree of necking and dimpling in comparison to the ductile laminate failure observed for room-temperature testing. This indicates that this response is a general effect that is related to the inherent properties of molybdenum, and likely results from the low work hardening rate and low necking resistance.

V. FRACTURE TOUGHNESS RESULTS

A. *Fatigue Pre-Cracking Method*

A summary of the parameters used for the fatigue pre-cracking of TZM and ODS molybdenum specimens prior to fracture toughness testing is given in Table VII. Most of the specimens were fatigue pre-cracked using a compression-compression technique, which is the method typically for molybdenum[4-6,9,10]. One TZM molybdenum specimen was fatigue pre-cracked using the standard method of tension-tension loading, and the fracture toughness value was within the range of data obtained using the compression-compression technique. Since molybdenum exhibits fatigue crack growth characteristics at room-temperature that are similar to a ceramic material with little fatigue crack growth observed until the applied stress intensity factor is 90% of the fracture toughness value, standard tension-tension methods are not a viable approach for fatigue pre-cracking. Compression-compression pre-cracking involves the application of an overload cycle that produces a residual tensile stress zone ahead of the crack tip, and further compressive-compressive cycling results in crack propagation through a zone of decreasing residual tensile stresses with crack arrest occurring when the local tensile stress intensities fall below the threshold value[33]. Although high levels of compressive load are applied using the compressive-compressive method of pre-cracking, propagation of the fatigue cracks to the point of crack arrest results in a small residual plastic zone size that is expected to have no influence on the fracture toughness results[33]. This is shown in Table VII by comparable fracture toughness values observed for the 0.5T Charpy specimens pre-cracked using tension-tension and compression-compression methods, which indicates that the intent of

the standard has been satisfied[20-21]. The side-to-side variations of the fatigue cracks were within the range specified by the standard.

B. *Fracture Toughness Results*

The majority of fracture toughness results for TZM molybdenum (Tables VIII to XI) were valid or conditionally valid. Fracture toughness results that do not meet all the validity requirements (K_Q) are considered to be an estimate of fracture toughness for molybdenum materials in some cases[5-10]. Most of the fracture toughness tests for TZM molybdenum performed above room-temperature did not meet the Eq. (5) criteria and plasticity rather than crack extension was observed in the load displacement curves in Figure 12a. This indicates that a significant deviation from linear-elastic behavior due to plastic deformation was observed, and the fracture toughness value that was determined using the E399 method[21] is a conservative measure of toughness. Most of the fracture toughness values determined for ODS molybdenum at temperatures ≥ room-temperature (Tables XII to XV) did not satisfy the Eq. (5) criteria, and extensive plastic deformation was observed in Figure 12b for the load displacement curves. Fracture toughness values for test results that did not meet Eq. (5) were determined by integration of the load displacement curves at the maximum load using the J-integral method[20], where J_{IC} is determined at the maximum load, and known modulus (E) and Poisson's ratio (ν) are used for the given test temperature:

$$K_{JIC} = (J_{IC} E / (1 - \nu^2))^{0.5} \quad (6)$$

$K_{J\text{-}max}$ was determined using Eq. (6). Fracture toughness values determined using the J-integral method ($K_{J\text{-}max}$) are shown in Tables VIII thru XV to be a factor of 1.4 to 4.7 higher. The true fracture toughness value for molybdenum materials that violate the Eq. (5) criteria is likely higher than the K_Q value and slightly lower than the $K_{J\text{-}max}$ value. The $K_{J\text{-}max}$ value is expected to be slightly non-conservative because cracking is expected to initiate slightly before the maximum load is achieved. However, the $K_{J\text{-}max}$ values are consistent with literature data that were determined for TZM molybdenum using a J_{IC} test method shown in Figure 3[4], which

supports the use of $K_{J\text{-}max}$ as a close measure of the fracture toughness. A J_{IC} test method is needed to provide a more accurate measure of fracture toughness.

The Eq. (4) criteria for plane-strain conditions can be difficult to satisfy for small sized specimens, which can result in a non-conservative measure of fracture toughness. The Eq. (4) criteria was not satisfied for a few of the fracture toughness tests performed at higher temperatures or with the 0.5T or 0.25T Charpy specimens. Plane-strain conditions can be satisfied for smaller-sized specimens using the J_{IC} test method. Since the fracture toughness tests that did violate the Eq. (4) criteria were typically in violation of Eq. (5), the use of the $K_{J\text{-}max}$ method, which allows plane strain conditions to be maintained for a smaller sized specimen, provides a more accurate measure of fracture toughness. All other validity requirements for the fracture toughness tests were satisfied.

VI. DISCUSSION OF FRACTURE TOUGNESS RESULTS

A. *Results Obtained Using a 1T Charpy*

Fracture toughness results for TZM molybdenum in the transverse and longitudinal orientation as a function of temperature are shown in Figure 13. Results for ODS molybdenum are shown in Figure 14. The $K_{J\text{-}max}$ values are used for fracture toughness in Figures 13 and 14 when the Eq. (5) requirement is not satisfied.

The lower bound K_{IC} fracture toughness values for TZM molybdenum (5.8 to 21.1 MPa$\sqrt{m}$), which were measured at temperatures < room-temperature, are within the range of values reported in literature (Figure 3). The K_{IC} fracture toughness values determined at temperatures ≤ room-temperature for the longitudinal and transverse orientation are similar for TZM molybdenum. The $K_{J\text{-}max}$ fracture toughness values for longitudinal TZM molybdenum are higher than the transverse orientation at temperatures ≥ 250°C. A transition from high toughness values (K_Q > 30 MPa$\sqrt{m}$) to low values (K_Q = 21 to 5.8 MPa$\sqrt{m}$) is observed for longitudinal TZM at 100°C. Brittle transgranular cleavage is observe on the fracture surface of the longitudinal TZM specimen tested at room-temperature (Figure 15a), while a ductile failure

mode is observed for fracture toughness testing at temperatures ≥ 100°C (Figure 15b). The ductile laminate failure with necking of sheet-like grains for fracture toughness testing of longitudinal TZM molybdenum at temperatures ≥ 100°C is similar in appearance to the ductile failure observed for tensile specimens at room-temperature. Transgranular cleavage is observed as the crack length is increased. This result indicates that the DBTT for longitudinal TZM molybdenum is 100°C.

High fracture toughness values (K_Q > 30 MPa$\sqrt{m}$) with a ductile fracture (Figure 15d) are observed for transverse TZM in Figure 13 at temperatures ≥ 150°C, while low toughness values (K_Q = 29.6 to 7.7 MPa$\sqrt{m}$) and brittle transgranular cleavage (Figure 15c) are observed at temperatures ≤ 100°C. This indicates that the DBTT for the transverse orientation of TZM is 150°C. The ductile laminate failure with necking of sheet-like grains observed for the transverse TZM fracture toughness specimen is similar to that observed for the tensile specimen. Crack growth during the fracture toughness tests likely occurs along the grain boundaries between the sheet-like grains to leave ligaments that are pulled to failure with a high degree of localized necking, which produces the ductile laminate failures shown for TZM in Figures 15b and 15d. A longer length of sheet-like grains is observed for ductile failures in the longitudinal orientation of TZM compared to the transverse orientation, which relates to the microstructure of TZM with long sheet-like grains in the longitudinal orientation (Figure 7). The higher fraction of grain boundary area, which serve as a weak area of the structure for fracture propagation, in the transverse orientation of TZM molybdenum results in a higher DBTT and lower upper bound fracture toughness values compared to the longitudinal orientation.

Based on the limited results shown in Figure 3 for literature data, the DBTT for molybdenum would be between 250°C and 500°C[4,5,12,26]. Performing fracture toughness testing for TZM molybdenum at finer temperature increments between 100°C and 300°C in this work has indicated that the DBTT for the longitudinal (DBTT = 100°C) and transverse

orientation (DBTT = 150°C) are lower than reported in literature. However, the upper bound (Test temperatures > 150°C) and lower bound (Test temperatures < 100°C) fracture toughness values determined in this work are within the range of values reported in literature[4-12]. The fracture toughness values for TZM molybdenum determined here at temperatures > 150°C are consistent with results for arc-cast TZM[4,12], and significantly higher than other results reported for powder metallurgy molybdenum[5,6,12]. The use of vacuum arc cast processing to produce the TZM molybdenum used in this work and other work[4,12] minimizes the amount of impurities (oxygen and nitrogen) that can lead to lower toughness values, which explains the high fracture toughness values for arc cast TZM.

The upper bound fracture toughness values for longitudinal ODS molybdenum are significantly higher than the results for TZM molybdenum and literature data for molybdenum alloys. A transition from a ductile to a brittle failure on the fracture surface was previously observed for TZM molybdenum near a fracture toughness value of 30 MPa$\sqrt{m}$, which will be used as the basis to define a transition temperature or DBTT for both TZM and ODS molybdenum. A transition to fracture toughness values < 30 MPa$\sqrt{m}$ was not observed in Figure 14 for longitudinal ODS molybdenum at temperatures between -150°C to 350°C. A ductile laminate failure with necking of sheet-like grains is observed for fracture toughness testing of ODS molybdenum at -150°C, -100°C, and room-temperature in Figures 16a, 16b, and 16c, respectively. This indicates that the DBTT for longitudinal ODS molybdenum is at a temperature ≤ -150°C. The ductile laminate failure observed for longitudinal ODS molybdenum likely results from crack propagation along grain boundaries, La-oxide precipitates, and La-oxide/matrix boundaries to leave sheet-like grains that are stretched to failure. The fine spacing of grain boundaries and La-oxide/matrix boundaries in ODS molybdenum serves to produce fine regions of sheet-like grains that are pulled to failure, which produces a fracture surface that is more similar to the classic dimple rupture observed for metals. The fine spacing of grain

boundaries and La-oxide/matrix boundaries produces a significantly finer spacing of ductile laminate features on the fracture surface of ODS toughness specimens than observed for TZM. Fine grain sizes are produced during the mechanical working and stress-relief heat treatment of TZM molybdenum, but the coarser spacing of precipitates observed in TZM results in a coarser size of ductile laminate features on the fracture surface. Thus, the fine distribution of La-oxide/matrix boundaries that are present in ODS molybdenum likely explain the significantly lower DBTT and higher upper bound fracture toughness values in comparison to other molybdenum alloys.

A transition from high fracture toughness values to low values < 30 MPa$\sqrt{m}$ is observed for transverse ODS molybdenum at room-temperature, see Figure 14. Brittle cleavage fracture is shown in Figure 16d on the fracture surface of transverse ODS molybdenum tested at temperatures $\leq$ 0°C. Ductile laminate failure of sheet-like grains is observed for transverse ODS at temperatures $\geq$ 25°C, see Figure 16e and 16f. These results indicate that the DBTT for transverse ODS molybdenum is room-temperature. Crack initiation and propagation likely occurs at grain and La-oxide/matrix boundaries to leave ligaments that are pulled to failure, which produces the ductile laminate failure observed for transverse ODS in Figure 16. The mechanical working used to form ODS molybdenum produces alignment of grain boundaries and La-oxides in the longitudinal direction, which leaves a high fraction of grain and La-oxide/matrix boundary area in the transverse direction that are weak paths for crack propagation, and likely explains the higher DBTT and lower upper bound fracture toughness values for transverse ODS in comparison to the longitudinal orientation. Although ODS molybdenum is not isotropic with a significant difference in fracture toughness values between the longitudinal and transverse orientations, the DBTT for transverse ODS molybdenum is room-temperature, which is lower than TZM molybdenum or any other molybdenum alloy reported to date in Figure 3. The lower bound fracture toughness values for transverse ODS *molybdenum* are similar to lower bound fracture toughness values for other alloys, and the

upper bound fracture toughness values are at the low end of the range of values reported in literature for other molybdenum alloys. The fine spacing of La-oxide particles that are present in ODS molybdenum results in a fine grain size being maintained through all levels of processing, which results in a DBTT for the transverse and longitudinal orientation that are significantly lower than any molybdenum alloy reported to date with upper bound fracture toughness values that bound the data reported in literature.

The DBTT determined from tensile testing for TZM molybdenum in the longitudinal (DBTT = -100°C) and transverse (room-temperature) orientation are much lower than determined from fracture toughness testing for the longitudinal (100°C) and transverse (150°C) orientations. The DBTT determined from the tensile testing of ODS molybdenum for the longitudinal (-100°C) and transverse (-50°C) orientations are more similar to the values that were determined from fracture toughness testing for the longitudinal (T < -150°C) and transverse (room-temperature) orientations. As has been commonly reported for a number of bcc metals such as steels[34], the triaxial stress state that is associated with a notch or defect results in a greater tendency toward brittle fracture and higher DBTT. Thus, fracture toughness testing method provides a conservative estimate of DBTT that accounts for the presence of a defect. Additionally, fracture toughness data can be used for a brittle fracture analysis of a structure. ODS molybdenum consists of a much finer grain size and La-oxide/matrix boundary spacing that disrupts the fracture path and produces a ductile laminate failure mode that is finely spaced, which could explain why the DBTT determined from tensile testing that is more similar to the value determined from fracture toughness testing.

A limited amount of fracture toughness testing was performed at higher and lower loading rates to evaluate the influence of strain rate. Molybdenum materials, which have a bcc crystal structure, are known to have some degree of strain-rate sensitivity and higher ductility and fracture toughness would be expected for tests performed at slow strain rates near the DBTT. The fracture toughness values for transverse TZM molybdenum obtained at the higher

and slower loading rates are shown in Table VIII to be within the scatter of values. For longitudinal TZM, the use of a higher loading rate resulted in little change in the fracture toughness values, but use of a lower loading rate resulted in slightly higher fracture toughness values for the limited data sets. No shift in the DBTT of TZM molybdenum could be resolved from this limited data. Similarly, limited fracture toughness testing of transverse (Table XII) and longitudinal (Table XIII) ODS molybdenum at room-temperature and 350°C, which is above the DBTT, at high and low loading rates revealed no significant difference in the upper-shelf fracture toughness values. The limited amount of data indicates that there is little strain rate sensitivity for the upper-shelf fracture toughness of TZM and ODS molybdenum over the range of loading rates and temperatures tested. More data would be needed to further define the influence of strain rate sensitivity on the toughness and DBTT of ODS and TZM molybdenum.

B. *Results Obtained Using a 0.5T and 0.25T Charpy*

The fracture toughness values obtained for TZM molybdenum using a 0.5T Charpy specimen are shown in Figure 13a to be comparable to results obtained using a 1T specimen. The room-temperature fracture toughness values obtained for the 0.5T longitudinal and transverse TZM specimens are within the range of values for the 1T specimen, and the brittle transgranular cleavage shown in Figure 17a is similar to that observed for the 1T Charpy (Figure 15a). The fracture toughness values determined for the 0.5T longitudinal TZM specimens at 100°C and 200°C are higher than the values measured using a 1T specimen at 100°C and 200°C, but are within the range of upper bound fracture toughness values measured at 250°C to 450°C. These differences could be associated with the scatter that results from fracture toughness measurements near the DBTT. The ductile laminate failure shown in Figure 17b for the 0.5T longitudinal TZM specimen is similar to the 1T Charpy shown in Figure 15b. The upper bound fracture toughness value that was measured at 150°C for the 0.5T transverse TZM Charpy was also comparable to results obtained with a 1T specimen, and a ductile

laminate fracture was observed for both specimens. The DBTT and fracture toughness results for 0.5T specimens are consistent with results for a 1T Charpy for TZM molybdenum.

The fracture toughness values measured for longitudinal TZM using a 0.25T Charpy at room-temperature, 100°C, and 200°C are shown in Figure 13b to be within the range of upper bound fracture toughness values and significantly higher than the values determined using the 1T specimens at room-temperature. Ductile laminate failures are observed in Figures 17c and 17d for testing of the 0.25T longitudinal specimens at room-temperature and 100°C, respectively, which is not consistent with the brittle transgranular cleavage fractures that were observed for room-temperature testing of the 0.5 and 1T Charpy specimens. Plane strain conditions were not established using the 0.25T Charpy for longitudinal TZM, which results in fracture toughness data and a DBTT that is not consistent with results obtained using 0.5T or 1T Charpy. The fracture toughness results obtained using the 0.25T Charpy for transverse TZM are shown in Figure 13b to be consistent with results obtained using the 1T specimen, and the DBTT is correctly identified at 150°C. However, these results indicate that an accurate measure of the DBTT of TZM molybdenum may not be obtained using the 0.25T Charpy specimens.

The fracture toughness values that were obtained for longitudinal and transverse ODS molybdenum using a 0.5T specimen at room-temperature, 100°C, and 200°C are within the range of the respective upper bound values that were determined using a 1T Charpy. The ductile laminate fracture observed for the 0.5T longitudinal and transverse ODS specimen tested at room-temperature in Figures 18a and 18b, respectively, are similar to the fracture surfaces for the 1T specimens (Figure 16). This indicates that the DBTT determined for longitudinal and transverse ODS molybdenum using the 0.5T Charpy is $\leq$ room-temperature. Thus, the fracture toughness results obtained for ODS molybdenum using the 0.5T specimen are consistent with the data obtained using a 1T Charpy.

The fracture toughness values obtained for the 0.25T transverse ODS specimen are a close match to values obtained using the 1T Charpy specimen, see Figure 14b. However, the fracture toughness values determined for the 0.25T longitudinal ODS specimen were at the low end of the range of upper bound fracture toughness values that were determined using the 1T Charpy. The ductile laminate fracture observed at room-temperature for the 0.25T longitudinal ODS specimen in Figure 18c is consistent with the fracture surfaces observed for the 0.5T and 1T specimens. The results for the 0.25T Charpy specimens indicate that the DBTT for longitudinal and transverse ODS is ≤ room-temperature, which is consistent with the results obtained for the 0.5T and 1T specimens. Plane strain conditions are less valid for the smaller 0.25T specimen, which may explain why the fracture toughness results for the longitudinal 0.25T ODS specimens are less consistent with the results obtained using a 0.5T and 1T Charpy. Therefore, the most accurate and consistent measure of fracture toughness of both ODS and TZM molybdenum is obtained using a 0.5T and 1T Charpy specimen.

Fracture toughness measurements through the thickness (T-S orientation) of the TZM and ODS molybdenum plates were performed using a 0.5T and 0.25T Charpy specimens. Monotonic loading of the 0.5T specimens for the T-S orientation resulted in crack growth that was perpendicular to the notch and along the boundaries between sheet-like grains. Since crack growth was not parallel to the notch for fracture toughness testing of 0.5T specimens, the equations developed for linear elastic fracture mechanics do not apply[20,21] and a valid measurement of fracture toughness was not obtained. The toughness values reported in Tables X and XIV for TZM and ODS molybdenum, respectively, for the T-S orientation are not an accurate fracture toughness value, but are listed as a possible estimate. Cracking of 0.25T Charpy specimens in the T-S orientation did occur parallel to the notch for both TZM and ODS molybdenum, but splitting of the cracks into two separate paths was observed, which indicates that the fracture toughness results obtained in the T-S orientation for TZM and ODS molybdenum in Tables XI and XV, respectively, are not a valid result. The low estimate for the

room-temperature toughness value obtain using the 0.25T ODS specimen in the T-S orientation is not consistent with the ductile fracture and stretching of laminate ligaments shown in Figure 18d. Alternative test methods are needed to provide an accurate measure of fracture toughness through the thickness of a molybdenum plate.

VII. SUMMARY

Fracture toughness testing of TZM and ODS molybdenum in the longitudinal and transverse orientation was performed at temperatures ranging from -150°C to 450°C to define the DBTT. A transition from low fracture toughness values (K_Q = 29.6 to 5.8 MPa$\sqrt{m}$) to values > 30 MPa$\sqrt{m}$ is observed for TZM molybdenum in the longitudinal orientation at 100°C and transverse orientation at 150°C. A ductile laminate fracture with necking of sheet-like grains is observed for TZM molybdenum at these temperatures, while brittle transgranular cleavage is observed at test temperatures < 100°C. This indicates that the DBTT for longitudinal and transverse TZM molybdenum is 100°C and 150°C, respectively. The DBTT determined from tensile testing for TZM molybdenum in the longitudinal (DBTT = -100°C) and transverse (room-temperature) orientation are much lower than determined using the fracture toughness testing, which indicates that the triaxial stress state that is produced by the presence of the notch of a fracture toughness specimen results in a more relevant and conservative measure of DBTT. Crack growth during the fracture toughness tests likely occurs along the grain boundaries between the sheet-like grains to leave ligaments that are pulled to failure with a high degree of localized necking, which produces the ductile laminate failures observed for TZM fracture toughness and tensile specimens. The higher fraction of grain boundary area for fracture propagation in the transverse orientation of TZM molybdenum results in a higher DBTT, lower tensile elongation, and lower upper bound fracture toughness values in comparison to the longitudinal orientation. The upper and lower bound fracture toughness values determined in this work for TZM are within the range of values reported in literature[4-12].

A transition to low fracture toughness values (< 30 MPa$\sqrt{m}$) was not observed for longitudinal ODS molybdenum at temperatures ≥ -150°C, while a transition to low fracture toughness values (25.4 to 12.6 MPa$\sqrt{m}$) was observed for the transverse orientation at room-temperature. The fine spacing of grain boundaries and La-oxide/matrix boundaries produces a significantly finer spacing of ductile laminate features on the fracture surface of ODS molybdenum tensile and fracture toughness specimens than observed for TZM molybdenum. The grain boundaries and La-oxides are aligned in the longitudinal direction of ODS molybdenum, which leaves a high fraction of grain and La-oxide/matrix boundary area in the transverse direction for crack propagation, and likely explains the higher DBTT, lower tensile elongation, and lower upper bound fracture toughness values for the transverse orientation. Although the fracture toughness values for ODS molybdenum are not isotropic, the DBTT for transverse ODS molybdenum is room-temperature, which is lower than TZM molybdenum or any other molybdenum alloy reported to date. The upper bound fracture toughness values for transverse ODS molybdenum are at the low end of the range of values for TZM, while the values for longitudinal ODS molybdenum are significantly higher than TZM. The fine spacing of La-oxide precipitates that are present in ODS molybdenum result in a DBTT that is significantly lower than any molybdenum alloy reported to date with upper bound fracture toughness values that bound the data reported in literature.

The fracture toughness values and DBTT that were obtained using a 0.5T Charpy specimen were consistent with fracture toughness results obtained using a 1T Charpy for both TZM and ODS molybdenum in the transverse or longitudinal orientation. Plane strain conditions were not maintained using the 0.25T Charpy and the fracture toughness results were not consistent with data obtained using the 0.5T and 1T specimens for both TZM and ODS. Thus, the 0.5T Charpy could be used as a sub-sized specimen geometry to provide fracture toughness results that are consistent with a 1T Charpy at room-temperature to 200°C.

VIII. ACKNOWLEDGEMENTS

This work was supported under USDOE Contract No. DE-AC11-98PN38206. The advice and direction from W.J. Mills and J.W. Holmes (CT&A) regarding this work was much appreciated. Thanks to R.A. Ramaley, A. Stinson, and M.J. Warnock for assistance with SEM and metallography. The technical comments and review of J. L. Hollenbeck are much appreciated.

REFERENCES

1. J.B. Lambert and J.J. Rausch: *Non-Ferrous Alloys and Special-Purpose Materials, Materials Handbook, Vol. 2,* ASM International, Materials Park, OH, 1992, pp. 557-582.
2. R.E. Gold, and D.L. Harrod: *J. of Nuclear Materials*, 1979, vol. 85-85, pp. 805-815.
3. B.L. Cox, and F.W. Wiffen: *J. of Nuclear Materials*, 1979, vol. 85-85, pp. 901-905.
4. J.A. Shields, P. Lipetzky, and A.J. Mueller*: Proc. 15th Int. Plansee Seminar, Vol. 1*, Metallwerk Plansee, Reutte, Austria, 2001. Available as B-T-3326, DOE/OSTI, Oak Ridge, TN, April 4, 2001, pp. 1-13.
5. M. Scibetta, R. Chaouadi, and J.L. Puzzolante: *J. of Nuclear Materials*, 2000, vol. 283-287, pp. 455-460.
6. A.Yu. Koval, A.D. Vasilev, and S.A. Firstov: *Int.J. Refractory Metals and Hard Materials*, 1997, vol. 15, pp. 223-226.
7. M. Danylenko: *Modeling the Mechanical Response of Structural Materials,* E.M. Taleff and R.K. Mahidhara, Eds., The Minerals, Metal & Materials Society, Warrendale, PA, 1997, pp. 229-235.
8. M. Rödig, H. Derz, G. Pott, and B. Werner: *Proc. 14th Int. Plansee Seminar, Vol. 1*, G. Kneringer, P. Rödhammer, and P. Wilharitz, Eds, Metallwerk Plansee, Reutte, Austria, 1997, pp. 781-791.
9. D.L. Chen, B. Weiss, R. Stickler, M. Witwer, G. Leichtfried, and H. Hödl: *High Temperature Materials and Processes*, 1994, Vol. 13, pp. 75-85.
10. D.L. Chen, B. Weiss, R. Stickler, M. Witwer, and G. Leichtfried: *Proc. 13th Int. Plansee Seminar, Vol. 1*, H. Bildstein and R. Eck, Eds, Metallwerk Plansee, Reutte, Austria, 1993, pp. 621-631.
11. M. Semchyshen, and R.Q. Barr: *J. Less-Common Metals*, 1966, vol. 11, pp. 1-13.

12. C.W. Marschall and F.C. Holden: *High Temperature Refractory Metals,* L. Richardson, et. al., Eds., Gordon-Breach Science Publishers, New York, 1964, pp. 129-159.

13. H.E. Romine: *Fracture Toughness at room Temperature of some refractory metals based on Tungsten, Molybdenum or Columbium which are being considered for use in the nozzles of large solid propellant rockets,* NWL Report No. 1873, U.S. Naval Weapons Laboratory, Dahlgren, VA, 1963.

14. *Standard Specification for Molybdenum and Molybdenum Alloy Bar, Rod, and Wire*, ASTM B387-95, American Society for Testing and Materials, Philadelphia, PA, 1995.

15. R. Bianco, R.W. Buckman, Jr., and C.B. Geller: *High Strength, Creep-Resistant Molybdenum Alloy and Process For Producing the Same*, US Patent #5,868,876, February 9, 1999.

16. A.J. Mueller, J.A. Shields, and R.W. Buckman: *Proc. 15th Int. Plansee Seminar, Vol. 1,* Metallwerk Plansee, Reutte, Austria, 2001. Available as B-T-3325, DOE/OSTI, Oak Ridge, TN, February 8, 2001, pp. 1-13.

17. R.Bianco and R.W. Buckman, Jr.: "Evaluation of Oxide Dispersion Strengthened (ODS) Molybdenum Alloys", *1995 Spring ASM/TMS Symposium on High Temperature Materials*, May 19, 1995, GE CR&D Center, Schenectady, NY (Available as WAPD-T-3073, DOE/OSTI, Oak Ridge, TN, 1995).

18. R. Bianco and R.W. Buckman, Jr.: *Molybdenum and Molybdenum Alloys*, A. Crowson, E. S. Chen, J. A. Shields, and P. R. Subramanian, Eds., The Minerals, Metals & Materials Society, Warrendale, PA, 1998, pp. 125-142.

19. *Standard Terminology Relating to Fatigue and Fracture Testing*, ASTM E1823-96, American Society for Testing and Materials, Philadelphia, PA, 1996.

20. *Standard Test Method for Measurement of Fracture Toughness*, ASTM E1820-01, American Society for Testing and Materials, Philadelphia, PA, 2001.

21. *Standard Test Method for Plane-Strain Fracture Toughness of Metallic Materials*, ASTM E399-90, American Society for Testing and Materials, Philadelphia, PA, 1997.

22. *Standard Test Method for Tension Testing of Metallic Materials*, ASTM E8-00, American Society for Testing and Materials, Philadelphia, PA, 2000.

23. *Standard Test Methods for Elevated Temperature Tension Tests of Metallic Materials*, ASTM E21-98, American Society for Testing and Materials, Philadelphia, PA, 1998.

24. B.V. Cockeram: *Surface and Coatings Technology*, 1998, vol. 108-109, pp. 377-384.

25. B. V. Cockeram: *Met. Trans.*, 2002, Vol. 33A, pp. 33-56.

26. A. Lawley, J. Van den Sype, and R. Maddin, *J of the Institute of Metals*, 162-1963, vol. 91, pp. 23-27.

27. G.W. Brock: *Trans. Met. Soc. AIME*, 1961, vol. 221, pp. 1055-1062.

28. K. Furuya and J. Moteff, *J. of Nuclear Materials*, 1981, Vol. 99, pp 306-316.

29. I. V. Gorynin et al., *J. of Nuclear Materials*, 1992, Vol. 191 – 194, pp. 421-42.

30. B. N. Singh et al., *J. of Nuclear Materials*, 1998, Vol. 258 – 263, pp. 865-87.

31. B. N. Singh et al., *J. of Nuclear Materials*, 1994, Vol. 212 - 215, pp. 1292-1297.

32. K. Abe et al., *J. of Nuclear Materials*, 1981, Vol. 99, pp. 25-37.

33. S. Suresh and J.R. Brockenbrough: *Acta Met.*, 1988, Vol. 36, pp. 1455-1470.

34. R. W. Hertzberg: *Deformation and Fracture Mechanics of Engineering Materials, Second Edition,* John Wiley & Sons, New York, 1983, pp. 269-348.

Table I. Composition of the TZM and ODS molybdenum 6.35 cm thick plates used in this work (in weight percent) provided in material certification reports, as compared to ASTM B386-95[14] specifications.

Material / Lot#	C	O	N	Ti	Zr	Fe	Ni	Si	La	Al	Ca	Cr	Cu	Other
ODS Molybdenum / Ingot #382 Heat# LA22963	0.001	NA	NA	<.001	NA	.0074	.0012	.0024	1.6	.0021	0.032	.0024	.001	<.001 Mg <.001 Mn <.001 Pb <.001 Sn
TZM Molybdenum / Ingot 61722B Lot# TZM24080	0.0223	.0017	.0009	0.50	0.114	<.001	<.001	<.001	NA	NA	NA	NA	NA	NA
ASTM B386 (Type 363) TZM Specification	0.01 / 0.03	≤.0030	≤.002	0.40 / 0.55	0.06 / 0.12	≤.010	≤.002	≤.010	NA	NA	NA	NA	NA	NA

Notes to Table I:
(1) NA = Not available.
(2) All material was obtained from H.C. Stark, which was formally known as CSM Industries, Inc., Cleveland, OH.

Table II. Summary of Fracture Toughness Data reported in literature for Molybdenum and Molybdenum-base Alloys.

Ref[1]	Material / Product Form	Condition / Orientation	Type of Specimen	Validity of Data	Test Temp.	Fracture Toughness Values [MPa√m]
4	AC Molybdenum / Plate	Stress-relieved / Longitudinal	Square CT	Valid	20°C	20, 20
					300°C	73, 76
		Stress-relieved / Transverse			20°C	21, 22
					300°C	69, 77
		Recrystallized / Longitudinal			20°C	18, 21[2]
					300°C	59, 60
		Recrystallized / Transverse			20°C	19, 19
					300°C	66, 68
	AC TZM Molybdenum / Plate	Stress-relieved / Longitudinal			20°C	19, 20
					300°C	84, 89
		Stress-relieved / Transverse			20°C	15, 18
					300°C	88, 93
		Recrystallized / Longitudinal			20°C	15, 18
					300°C	58, 64
		Recrystallized / Transverse			20°C	18, 19
					300°C	67, 67
5	TZM / Rod	Stress-relieved / Radial	Disc CT	Not Pre-cracked	20°C	16, 17
					200°C	18, 29
					450°C	20, 30, 34, 36, 37, 39

Table II. (Continued) Summary of Fracture Toughness Data reported in literature for Molybdenum and Molybdenum-base Alloys.

Ref[1]	Material / Product Form	Condition / Orientation	Type of Specimen	Validity of Data	Test Temp.	Fracture Toughness Values [MPa√m]
6	Molybdenum – 1% Zr / Sheet	Recrystallized	Two-edged notched flat	Pre-cracked by EDM	-196°C	7
					-75°C	8
					-50°C	9
					-40°C	10
					0°C	12, 13
					20°C	14, 15, 16, 17
					50°C	12, 12
					100°C	12, 12
					150°C	12, 13
					210°C	13, 14
					250°C	12, 14
					300°C	11, 14
7	Molybdenum / Sheet	Longitudinal	?	Invalid[4]	20°C	15 – 60[3]
		Transverse	?		20°C	10 – 40[3]
8	P/M TZM / Bar	Stress-relieved / Radial	Disc CT	Valid	20°C	15 – 17[3]
					200°C	17 – 19[3]
					450°C	26 – 28[3]
9, 10	P/M Molybdenum / Forged Bar	As-worked / Radial	Disc CT	Valid	20°C	8 ± 5%[5]
			Surface-Cracked		20°C	17[5]
	P/M Molybdenum / Swaged Bar	As-worked / Radial	Surface-Cracked	Valid	20°C	11, 17[5]
		Recrystallized / Radial			20°C	11, 18[5]

Table II. (Continued) Summary of Fracture Toughness Data reported in literature for Molybdenum and Molybdenum-base Alloys.

Ref[1]	Material / Product Form	Condition / Orientation	Type of Specimen	Validity of Data	Test Temp.	Fracture Toughness Values [MPa√m]
9,10	P/M TZM / Forged Bar	As-worked / Radial	Disc CT	Valid	20°C	19 ± 5%[5]
			Surface-Cracked		20°C	17[5]
	P/M TZM / Swaged Bar	Recrystallized / Radial	Surface-Cracked	Valid	20°C	31 ± 7%[5]
12	AC Molybdenum / Sheet	Stress-relieved / Transverse	Notched Flexure Bar	Valid	25°C	12
					100°C	13, 22
					250°C	32, 75, 80
		Recrystallized / Transverse			25°C	10
					100°C	10, 12
					250°C	10, 11
					400°C	13, 15
13	AC Molybdenum / Extruded Bar	As-Worked / Center of Bar	Notched Flexure Bar	Invalid[6]	20°C	17.6[5]
	AC Molybdenum / Extruded Bar	As-Worked / OD of Bar			20°C	20.6[5]

Notes:
1. The reference number for the data is listed.
2. Conditionally valid result. Violated the Eq. (1) criteria.
3. The range of toughness values are reported.
4. Since the sheet use for testing was thin, this data are judged to be invalid.
5. These are average values.
6. These values were calculated from measurements of G_{IC}.
7. AC = Arc-Cast processing method; P/M = Powder-Metallurgy processing method. EDM = Electro-discharge machining; CT = compact tension specimen; OD = Outer diameter.

Table III. Tensile Data for TZM Molybdenum in the **Longitudinal** Direction.

Temperature [°C]	Yield stress [MPa]	Ultimate Tensile Strength [MPa]	Total Elongation [%]	Young's modulus [GPa]
-149	N/A	1487	0.0	
-98	1251	1251	4	
-50	1075	1088	4.8	na
-50	1008	1021	9.7	262.0
-48	1043	1043	15	
RT	662.8	777.9	na	313.8
RT	733.0	765.9	14.9	269.8
RT	732.8	807.4	15.2	291.1
RT	754.4	841.0	12.8	289.3
RT	725.3	789.5	17	
RT	738.5	815.0	22	
100	653.1	771.4	12.4	270.2
100	666.8	774.4	10.6	274.9
100	629.5	721.2	14	
200	572.8	654.6	8.8	244.0
200	567.8	678.1	8.2	255.4
200	590.9	689.5	10	
300	599.9	668.9	8	
400	615.0	673.0	7	
600	569.7	618.2	4.6	235.8
600	573.9	637.9	4.9	248.3
702	509.5	555.7	5	
800	512.2	565.2	4.3	240.9
800	482.5	512.2	3.6	245.8
976	448.2	486.8	5	
1000	461.4	501.4	4.1	246.3
1000	504.4	535.5	3.4	204.8
1000	499.2	533.2	3.5	225.3
1000	490.4	527.6	3.2	214.6
1201	402.0	414.4	7	
1406	106.9	172.4	30	

Notes: 1. A measurement of Young's modulus was made for the testing performed at CT&A.
2. All other testing was performed at PMTI.
3. RT = room-temperature.

Table IV. Tensile Data for TZM Molybdenum in the **Transverse** Direction.

Temperature [°C]	Yield stress [MPa]	Ultimate Tensile Strength [MPa]	Total Elongation [%]	Young's modulus [GPa]
-50	N/A	1093.5	0	
RT	858.4	889.0	12.3	278.7
RT	821.2	858.3	9.5	305.5
RT	819.5	858.1	11.8	307.6
RT	812.0	835.9	10.9	283.9
RT	738.5	817.1	10	
100	786.7	834.9	6.8	295.5
100	744.0	805.3	11.1	295.9
99	752.2	803.3	8	
200	643.8	711.5	7.5	257.9
200	637.1	698.9	5.4	281.6
200	706.0	751.6	6	
299	651.6	693.6	5	
400	606.8	648.1	6	
600	631.1	655.4	2.2	263.3
600	644.1	684.1	2.8	273.3
701	544.0	610.9	4	
800	555.0	584.9	2.2	na
800	565.2	587.2	2.9	242.3
800	603.7	627.6	2.9	241.5
1000	509.4	528.0	2.6	204.8
1000	556.4	572.9	2.2	226.2
1000	591.2	614.4	2.6	240.6
1000	545.0	566.0	3.1	221.1

Notes: 1. A measurement of Young's modulus was made for the testing performed at CT&A.
2. All other testing was performed at PMTI.
3. RT = room-temperature.

Table V. Tensile Data for ODS Molybdenum in the **Longitudinal** Direction.

Temperature [°C]	Yield stress [MPa]	Ultimate Tensile Strength [MPa]	Total Elongation [%]	Young's modulus [GPa]
-100	1250.0	1374.9	12	
-50[4]	1116.0	1118.0	5.6	na
RT	715.8	769.6	14.7	273.6
RT	678.8	692.0	4.91	291.0
RT	720.7	771.7	17.2	292.8
RT	762.5	798.7	9.7	274.3
RT	658.5	677.1	14	
100	637.4	688.3	18.5	257.2
100	668.6	702.4	9.7	270.5
200	462.8	496.8	12.0	243.5
200	503.2	591.5	14.0	286.5
600	446.4	477.4	4.3	236.4
600	462.3	491.4	3.0	226.4
800	359.6	379.3	6.9	216.1
800	331.1	340.4	3.3	206.0
1000	278.9	296.3	5.2	183.3
1000	310.1	333.0	5.1	177.9
1000	322.5	345.9	4.8	181.7
1000	316.3	342.7	6.2	204.2

Notes:
1. A measurement of Young's modulus was made for the testing performed at CT&A.
2. All other testing was performed at PMTI.
3. RT = room-temperature.
4. The upper/lower yield point observed for this test results in a high value for the yield stress, see Figure 5a. Ultimate tensile stress is the highest stress following the upper/lower yield point, which can be lower than the yield stress in some cases.

Table VI. Tensile Data for ODS Molybdenum in the **Transverse** Direction.

Temperature [°C]	Yield stress [MPa]	Ultimate Tensile Strength [MPa]	Total Elongation [%]	Young's modulus [GPa]
-50	1062.0	1070.0	4.2	253.0
RT[4]	825.3	805.0	13.0	292.7
RT	678.6	687.0	3.7	263.0
RT	752.9	790.6	13.4	291.0
RT	770.9	808.6	9.7	278.4
RT	668.8	682.6	5	
100	716.7	754.1	13.1	213.6
100	676.7	722.9	11.7	264.3
200	499.2	525.4	4.7	230.1
200	519.7	577.7	4.5	236.8
600	454.7	479.0	2.6	267.4
600	500.3	514.9	1.6	231.8
800	395.2	417.5	2.8	209.0
800	382.7	406.2	3.3	214.3
800	265.7	283.6	3.7	158.2
1000	274.0	282.7	5.1	175.0
1000	300.4	315.2	5.9	150.2
1000	274.0	333.3	4.7	129.1
1000	305.5	320.2	3.8	169.9

Notes: 1. A measurement of Young's modulus was made for the testing performed at CT&A.
2. All other testing was performed at PMTI.
3. RT = room-temperature.
4. The upper/lower yield point observed for this test results in a high value for the yield stress, see Figure 5b. Ultimate tensile stress is the highest stress following the upper/lower yield point, which can be lower than the yield stress in some cases.

Table VII. Summary of conditions used for the fatigue pre-cracking of TZM molybdenum and ODS molybdenum Charpy specimens used for fracture toughness testing (K_{max} and fracture toughness values are reported for room-temperature data only).

Material / orientation	Specimen Type / Method[1]	Total Cycles	Loads Used for Precracking[2] [kN]		K_{max} values used for pre-cracking (final value)[2] [MPa √m]	Range of K_{IC} values[3] [MPa √m]
			Initial	Final		
TZM molybdenum / Transverse	1T Charpy / C	150,000 to 35,000	–18 + 10 Blocks –23 to –18	–18	-270 to -282	10.0 to 15.2
	0.5T Charpy / C	50,000	1 cycle at –10	–9	–176 to –197	11.6 to 14.0
	0.5T Charpy / C	200,000	Cycles at –13	–13	–345	15.9
	0.5T Charpy / C + Tension	1,000,000	1 cycle at –10 + cycles at –9	0.44	11.5	12.6
	0.25T Charpy / C	100,000	20 Blocks –2.2 to –1.8	–1.8	–272	20.0
TZM molybdenum / Longitudinal	1T Charpy / C	120,000 to 40,000	–18 + 10 Blocks –23 to –18	–18	–272 to –282	14.2 to 38.2
	0.5T Charpy / C	50,000	1 cycle at –10	–9	–187	24.8
	0.25T Charpy / C	100,000	20 Blocks –2.2 to –1.8	–1.8	–324	45.3
ODS molybdenum / Transverse	1T Charpy / C	100,000	20 Blocks –16 to –11	–11	–186 to –198	30.2 to 52.2
	0.5T Charpy / C	100,000	20 Blocks –11.5 to –9	–9	–224	41.0
	0.25T Charpy / C	100,000	20 Blocks –2.5 to –2	–2	–281 to –361	24.7 to 27.1
ODS molybdenum / Longitudinal	1T Charpy / C	100,000	20 Blocks –16 to –11	–11	–174 to –158	39.8 to 147.4
	0.5T Charpy / C	100,000	20 Blocks –11.5 to –9	–9	–224	82.8
	0.25T Charpy / C	100,000	20 Blocks –2.75 to –2.2	–2.2	–320	38.8

Notes:

1. C = compression-compression method of pre-cracking. Tension = tension-tension method of fatigue pre-cracking.
2. Negative numbers for the load indicate that compressive pre-cracking was used. Pre-cracking was performed in blocks, where 1 block = 1 over-load cycle followed by 5000 cycles at the lower load.
3. The final fracture toughness values (K_{IC}, K_{CV}, K_Q, K_{JIC}) that were measured at room-temperature are indicated.

Table VIII. Fracture Toughness Values Determined for TZM Molybdenum using a 1T Charpy Specimen with the **transverse** orientation (T-L orientation in accordance with ASTM E1823).

Test Temperature [°C]	Fracture Toughness [MPa √m]			$\frac{B}{(K_Q^2/\sigma_{YS}^2)}$	$\frac{P_{Max}}{P_Q}$	$\frac{a}{W}$	$K_{J\text{-}max}$ Determined from J integral[1] [MPa √m]
	K_Q	K_{CV}	K_{IC}				
Tests Performed at a Standard Displacement Rate (0.0025 mm/s)							
-100	7.7	--	7.7	100.7	1.00	0.40	--
-50	9.1	--	9.1	72.1	1.00	0.38	--
25	10.0	--	10.0	27.0	1.00	0.39	--
25	10.7	--	10.7	23.3	1.00	0.39	--
25	15.2	--	15.2	11.7	1.00	0.37	--
100	29.0	29.0	--	3.6	1.13	0.40	--
150	45.8	45.8	--	1.4	1.05	0.44	--
200	44.0	--	--	1.1	1.28	0.43	74.2
250	47.0	--	--	1.4	1.18	0.40	83.4
250	47.6		--	0.9	1.14	0.44	--
300	47.8		--	0.9	1.09	0.44	--
350	44.4	--	--	1.1	1.22	0.42	91.5
400	44.7	--	--	0.9	1.26	0.40	99.0
450	45.1	--	--	0.9	1.29	0.43	102.0
Tests Performed at a Displacement Rate of 0.00025 mm/s							
150	43.2	43.2	--	1.6	1.00	0.41	--
Tests Performed at a Displacement Rate of 0.25 mm/s							
150	46.8	46.8	--	1.4	1.13	0.42	--

Notes:

1. An estimate of fracture toughness was obtained for tests with a ratio of P_{max} to $P_Q > 1.15$ by taking the integral of the load displacement curve at P_{max}, calculating the J_Q value[20], and then calculating K_Q.
2. The range of compressive loads used for pre-cracking, as defined by the ratio of K_{max} to K_Q, ranged from –36.6 to –6.4.

Table IX. Fracture Toughness Values Determined for TZM Molybdenum using a 1T Charpy Specimen for the **longitudinal** orientation (L-T orientation in accordance with ASTM E1823).

Test Temperature [°C]	Fracture Toughness [MPa √m]			$\frac{B}{(K_Q^2/\sigma_{YS}^2)}$	$\frac{P_{Max}}{P_Q}$	$\frac{a}{W}$	$K_{J\text{-}max}$ Determined from J integral[1] [MPa √m]
	K_Q	K_{CV}	K_{IC}				
Tests Performed at a Standard Displacement Rate (0.0025 mm/s)							
-100	6.7	--	6.7	172.3	1.00	0.44	--
-50	5.8	--	5.8	162.2	1.00	0.41	--
25	21.1	--	21.1	6.1	1.00	0.40	--
25	38.2	38.2	--	1.8	1.00	0.38	--
100	40.2	40.2	--	1.3	1.00	0.39	--
150	45.1	45.1	--	1.1	1.04	0.41	--
200	51.0	--	--	0.6	1.13	0.41	--
250	45.5	--	--	0.8	1.20	0.40	97.0
300	42.6	--	--	1.0	1.28	0.42	99.5
350	41.9	--	--	1.0	1.30	0.40	103.9
400	41.7	--	--	1.1	1.31	0.38	119.8
450	39.9	--	--	1.2	1.39	0.41	129.8
Tests Performed at a Displacement Rate of 0.00025 mm/s							
25	33.1	33.1	--	2.4	1.00	0.39	--
150	37.4	--	--	1.5	1.24	0.44	95.4
Tests Performed at a Displacement Rate of 0.25 mm/s							
25	14.2	--	14.2	13.3	1.00	0.40	--
150	48.6	--	--	0.9	1.16	0.40	114.4

Notes:

1. An estimate of fracture toughness was obtained for tests with a ratio of P_{max} to P_Q > 1.15 by taking the integral of the load displacement curve at P_{max}, calculating the J_Q value[20], and then calculating K_Q.
2. The range of compressive loads used for pre-cracking, as defined by the ratio of K_{max} to K_Q, ranged from –50.6 to –5.8.

Table X. Fracture Toughness Values Determined for TZM Molybdenum using a 0.5T Charpy Specimen for the transverse, longitudinal, and through thickness orientations. All testing was performed at a displacement rate of 0.0025 mm/s.

Test Temperature [°C]	Fracture Toughness [MPa √m]			$\frac{B}{(K_Q^2/\sigma_{YS}^2)}$	$\frac{P_{Max}}{P_Q}$	$\frac{a}{W}$	$K_{J\text{-}max}$ Determined from J integral[1] [MPa √m]
	K_Q	K_{CV}	K_{IC}				
Transverse Orientation (T-L)							
25	11.6	--	11.6	19.6	1.00	0.34	--
25[3]	12.6	--	12.6	16.8	1.00	0.45	--
25	15.9	--	15.9	10.5	1.00	0.46	--
25	14.0	--	14.0	13.5	1.04	0.39	--
150[4]	32.8	--	--	2.5	1.39	0.42	57.0
Longitudinal Orientation (L-T)							
25	24.8	--	24.8	4.3	1.00	0.37	--
100	30.4	--	--	2.4	1.52	0.40	86.8
150	31.8	--	--	2.2	1.42	0.41	86.9
Through Thickness Orientation (T-S)							
25[5]	17.9	--	--	--	--	--	--
100[5]	23.8	--	--	--	--	--	--
200[5]	25.3	--	--	--	--	--	--

Notes:

1. An estimate of fracture toughness was obtained for tests with a ratio of P_{max} to P_Q > 1.15 by taking the integral of the load displacement curve at P_{max}, calculating the J_Q value J_Q value[20], and then calculating K_Q.
2. The range of compressive loads used for pre-cracking, as defined by the ratio of K_{max} to K_Q, ranged from –15.1 to –6.5.
3. This specimen was pre-cracked using a tension-tension method at a ratio of K_{max} to K_Q = 0.91.
4. Branching of the crack was observed, making this test invalid.
5. Crack travel perpendicular to the notch along the grain boundaries between sheet-like grains. The data for the through thickness specimens should be treated as an estimate of fracture toughness that is not a valid measurement.

Table XI. Fracture Toughness Values Determined for TZM Molybdenum using a 0.25T Charpy specimen for the transverse, longitudinal, and through thickness orientations. All testing was performed at a displacement rate of 0.0025 mm/s.

Test Temperature [°C]	Fracture Toughness [MPa √m]			$\frac{B}{(K_Q^2/\sigma_{YS}^2)}$	$\frac{P_{Max}}{P_Q}$	$\frac{a}{W}$	$K_{J\text{-}max}$ Determined from J integral[1] [MPa √m]
	K_Q	K_{CV}	K_{IC}				
Transverse Orientation (T-L)							
25	20.0	--	20.0	3.3	1.00	0.46	--
100[4]	24.4	--	--	1.9	1.19	0.44	--
150	23.3	--	--	2.1	1.37	0.45	47.3
Longitudinal Orientation (L-T)							
25	18.7	--	--	3.8	2.06	0.51	45.3
100	17.1	--	--	3.8	1.94	0.49	46.7
150	21.2	--	--	2.5	1.61	0.48	56.9
Through Thickness Orientation (T-S)							
25[3,4]	12.3	--	--	8.8	1.63	0.33	--
100[3]	2.7	--	--	148.1	7.69	0.33	13.0
200[3]	18.0	--	--	3.5	1.59	0.32	54.5

Notes:

1. An estimate of fracture toughness was obtained for tests with a ratio of P_{max} to P_Q > 1.15 by taking the integral of the load displacement curve at P_{max}, calculating the J_Q value (Reference (9)), and then calculating K_Q.
2. The range of compressive loads used for pre-cracking, as defined by the ratio of K_{max} to K_Q, ranged from –17.3 to –10.5.
3. Branching of the crack was observed, making this test invalid. The data for the through thickness specimens should be treated as an estimate of fracture toughness that is not a valid measurement.
4. Pop-in of cracks are observed on the load displacement curves, which indicates that this value is a more conservative estimate of the fracture toughness value.

Table XII. Fracture Toughness Values Determined for ODS Molybdenum using a 1T Charpy Specimen for the **transverse** orientation (T-L orientation in accordance with ASTM E1823).

Test Temperature [°C]	Fracture Toughness [MPa √m]			$\frac{B}{(K_Q^2/\sigma_{YS}^2)}$	$\frac{P_{Max}}{P_Q}$	$\frac{a}{W}$	$K_{J\text{-}max}$ Determined from J integral[1] [MPa √m]
	K_Q	K_{CV}	K_{IC}				
Tests Performed at a Standard Displacement Rate (0.0025 mm/s)							
-150	13.4	--	13.4	31.2	1.00	0.43	--
-100	12.6	--	12.6	35.4	1.01	0.41	--
-50	13.6	13.6	--	30.3	1.15	0.41	--
0	25.4	--	25.4	5.9	1.00	0.43	--
25	35.8	--	--	2.1	1.18	0.43	52.2
50	32.6	--	32.6	2.5	1.00	0.45	--
100	35.6	--	--	1.9	1.23	0.43	56.2
150	31.3	--	--	2.5	1.32	0.43	63.5
200	30.7	--	--	1.4	1.33	0.45	71.3
250	31.3	--	--	1.4	1.35	0.44	71.5
300	29.8	--	--	1.5	1.33	0.39	69.1
350	30.0	--	--	1.5	1.35	0.40	80.2
Tests Performed at a Displacement Rate of 0.00025 mm/s							
25	43.3	43.3	--	1.4	1.04	0.42	--
350	31.5	--	--	1.3	1.20	0.42	60.1
Tests Performed at a Displacement Rate of 0.25 mm/s							
25	30.2	--	30.2	2.9	1.00	0.42	--
350	34.7	--	--	1.1	1.17	0.42	67.9

Notes:

1. An estimate of fracture toughness was obtained for tests with a ratio of P_{max} to P_Q > 1.15 by taking the integral of the load displacement curve at P_{max}, calculating the J_Q value (Reference (9)), and then calculating K_Q.
2. The range of compressive loads used for pre-cracking for all tests, as defined by the ratio of K_{max} to K_Q, ranged from –14.3 to –4.3.

Table XIII. Fracture Toughness Values Determined for ODS Molybdenum using a 1T Charpy Specimen for the **longitudinal** orientation (L-T orientation in accordance with ASTM E1823).

Test Temperature [°C]	Fracture Toughness [MPa √m]			$\frac{B}{(K_Q^2/\sigma_{YS}^2)}$	$\frac{P_{Max}}{P_Q}$	$\frac{a}{W}$	$K_{J\text{-}max}$ Determined from J integral[1] [MPa √m]
	K_Q	K_{CV}	K_{IC}				
Tests Performed at a Standard Displacement Rate (0.0025 mm/s)							
-150	38.2	--	38.2	5.4	1.02	0.39	--
-100	47.9	--	47.9	3.4	1.00	0.38	--
25	39.8	--	--	1.7	1.44	0.39	147.4
50	44.2	--	--	1.4	1.25	0.38	117.2
100	37.4	--	--	1.4	1.24	0.37	111.7
150	31.5	--	--	2.0	1.45	0.39	109.7
200	31.3	--	--	1.3	1.43	0.40	133.1
250	30.3	--	--	1.4	1.56	0.40	122.4
300	27.8	--	--	1.6	1.47	0.37	104.5
350	29.6	--	--	1.5	1.45	0.38	139.5
Tests Performed at a Displacement Rate of 0.00025 mm/s							
25	41.9	--	--	1.5	1.24	0.38	119.7
350	28.2	--	--	1.6	1.41	0.39	96.3
Tests Performed at a Displacement Rate of 0.25 mm/s							
25	54.3	--	--	0.9	1.03	0.37	--
350	33.0	--	--	1.2	1.28	0.37	154.5

Notes:

1. An estimate of fracture toughness was obtained for tests with a ratio of P_{max} to $P_Q > 1.15$ by taking the integral of the load displacement curve at P_{max}, calculating the J_Q value (Reference (9)), and then calculating K_Q.
2. The range of compressive loads used for pre-cracking for all tests, as defined by the ratio of K_{max} to K_Q, ranged from –6.0 to –2.9.

Table XIV. Fracture Toughness Values Determined for ODS Molybdenum using a 0.5T Charpy Specimen for the transverse, longitudinal, and through thickness orientations. All testing was performed at a displacement rate of 0.0025 mm/s.

Test Temperature [°C]	Fracture Toughness [MPa √m]			$\frac{B}{(K_Q^2/\sigma_{YS}^2)}$	$\frac{P_{Max}}{P_Q}$	$\frac{a}{W}$	$K_{J\text{-}max}$ Determined from J integral[1] [MPa √m]
	K_Q	K_{CV}	K_{IC}				
Transverse Orientation (T-L)							
25	41.0	41.0	--	1.3	1.15	0.43	--
100	29.0	--	--	2.6	1.42	0.45	58.6
200	30.7	--	--	2.4	1.32	0.44	59.0
Longitudinal Orientation (L-T)							
25	36.9	--	--	2.0	1.41	0.44	82.8
100	25.8	--	--	3.3	1.77	0.40	84.6
200	28.1	--	--	2.8	1.56	0.43	86.1
Through Thickness Orientation (T-S)							
25[3]	12.0	--	--	--	--	--	--
100[3]	19.6	--	--	--	--	--	58.6
200[3]	18.6	--	--	--	--	--	

Notes:

1. An estimate of fracture toughness was obtained for tests with a ratio of P_{max} to P_Q > 1.15 by taking the integral of the load displacement curve at P_{max}, calculating the J_Q value (Reference (9)), and then calculating K_Q.
2. The range of compressive loads used for pre-cracking, as defined by the ratio of K_{max} to K_Q, ranged from –11.6 to –5.5.
3. Crack travel perpendicular to the notch along the grain boundaries between sheet-like grains. The data for the through thickness specimens should be treated as an estimate of fracture toughness that is not a valid measurement.

Table XV. Fracture Toughness Values Determined for ODS Molybdenum using a 0.25T Charpy Specimen for the transverse, longitudinal, and through thickness orientations. All testing was performed at a displacement rate of 0.0025 mm/s.

Test Temperature [°C]	Fracture Toughness [MPa √m]			$\frac{B}{(K_Q^2/\sigma_{YS}^2)}$	$\frac{P_{Max}}{P_Q}$	$\frac{a}{W}$	$K_{J\text{-}max}$ Determined from J integral[1] [MPa √m]
	K_Q	K_{CV}	K_{IC}				
Transverse Orientation (T-L)							
25	23.6	--	--	2.0	1.27	0.44	24.7
25	19.5	--	--	2.9	1.48	0.52	27.1
100	16.6	--	--	4.1	1.64	0.45	48.1
150	16.7	--	--	4.0	1.40	0.46	38.1
Longitudinal Orientation (L-T)							
25	38.8	38.8	--	0.9	1.02	0.45	--
100	15.5	--	--	4.7	1.95	0.44	54.1
150	11.6	--	--	8.3	2.17	0.43	52.2
Through Thickness Orientation (T-S)							
25[3]	9.9	--	--	--	--	--	18.5
100[3]	13.1	--	--	--	--	--	20.2
200[3]	15.2	--	--	--	--	--	--

Notes:

1. An estimate of fracture toughness was obtained for tests with a ratio of P_{max} to P_Q > 1.15 by taking the integral of the load displacement curve at P_{max}, calculating the J_Q value (Reference (9)), and then calculating K_Q.
2. The range of compressive loads used for pre-cracking, as defined by the ratio of K_{max} to K_Q, ranged from –25.6 to –8.2.
3. Branching of the crack was observed, making this test invalid. The data for the through thickness specimens should be treated as an estimate of fracture toughness that is not a valid measurement.

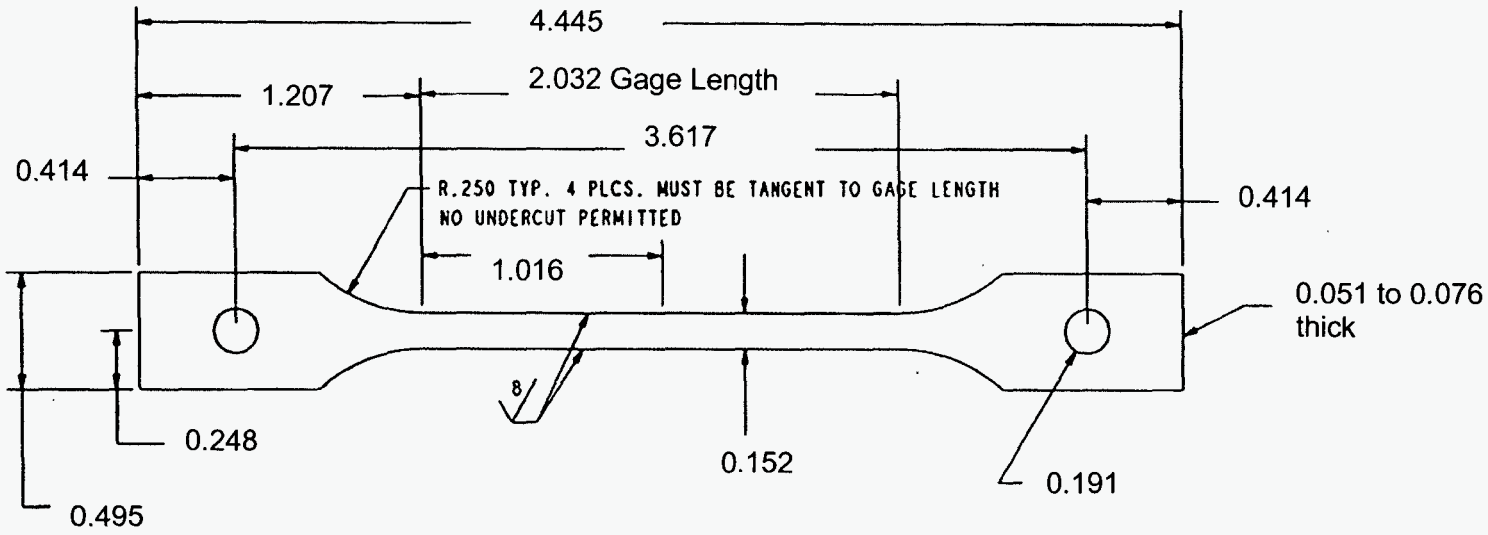

Figure 1. Schematic of the specimen used for tensile testing with the nominal dimensions. All dimensions in cm.

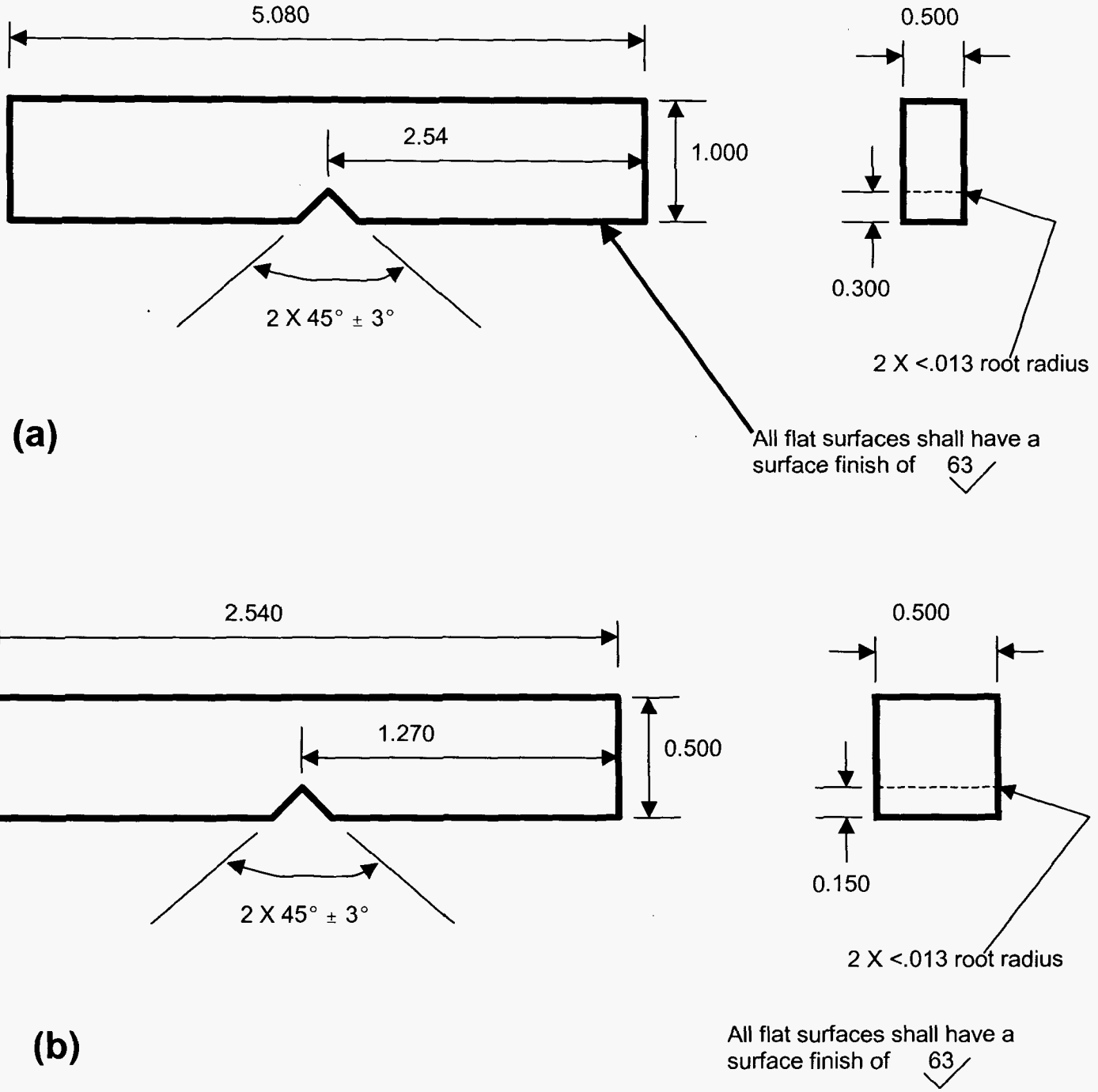

Figure 2. Schematic of the Charpy specimen used for fracture toughness testing: (a) 1T Charpy, (b) 0.5T Charpy, and (c) 0.25T Charpy. The nominal dimensions are shown with all dimensions in cm. Drawing not to scale.

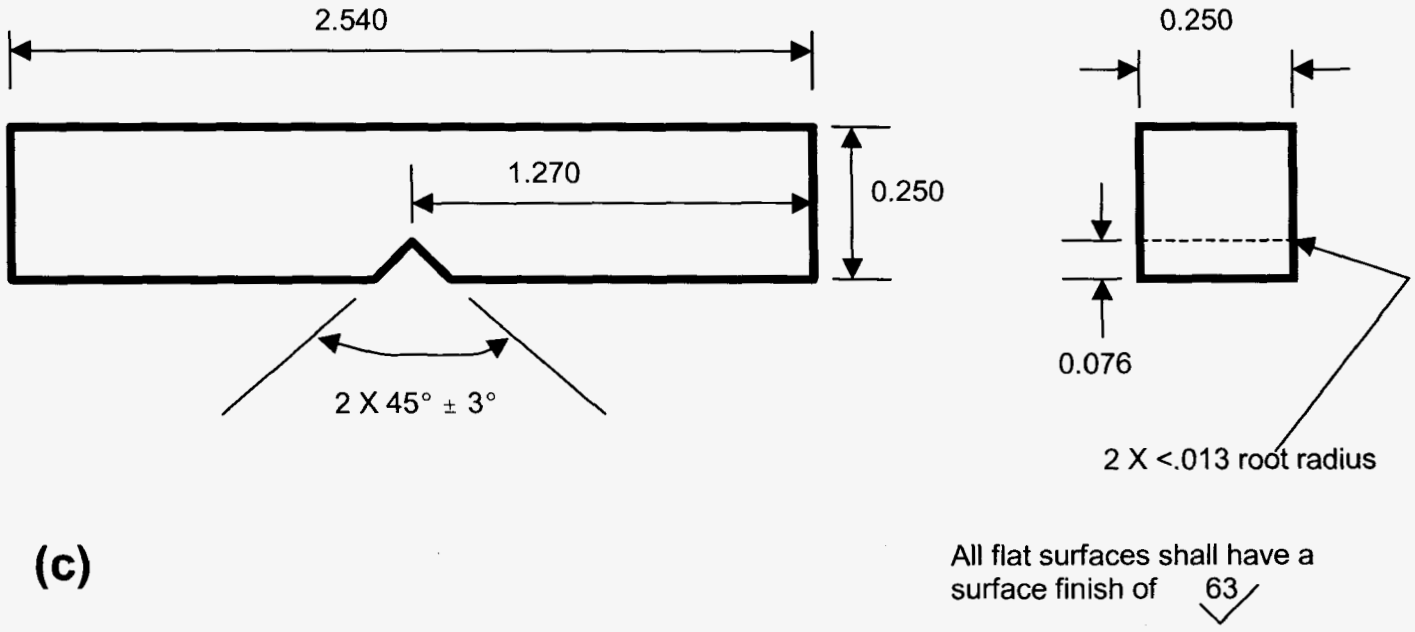

(c)

Figure 2. (Continued) Schematic of the Charpy used for fracture toughness testing: (a) 1T Charpy, (b) 0.5T Charpy, and (c) 0.25T Charpy. The nominal dimensions are shown with all dimensions in cm. Drawing not to scale.

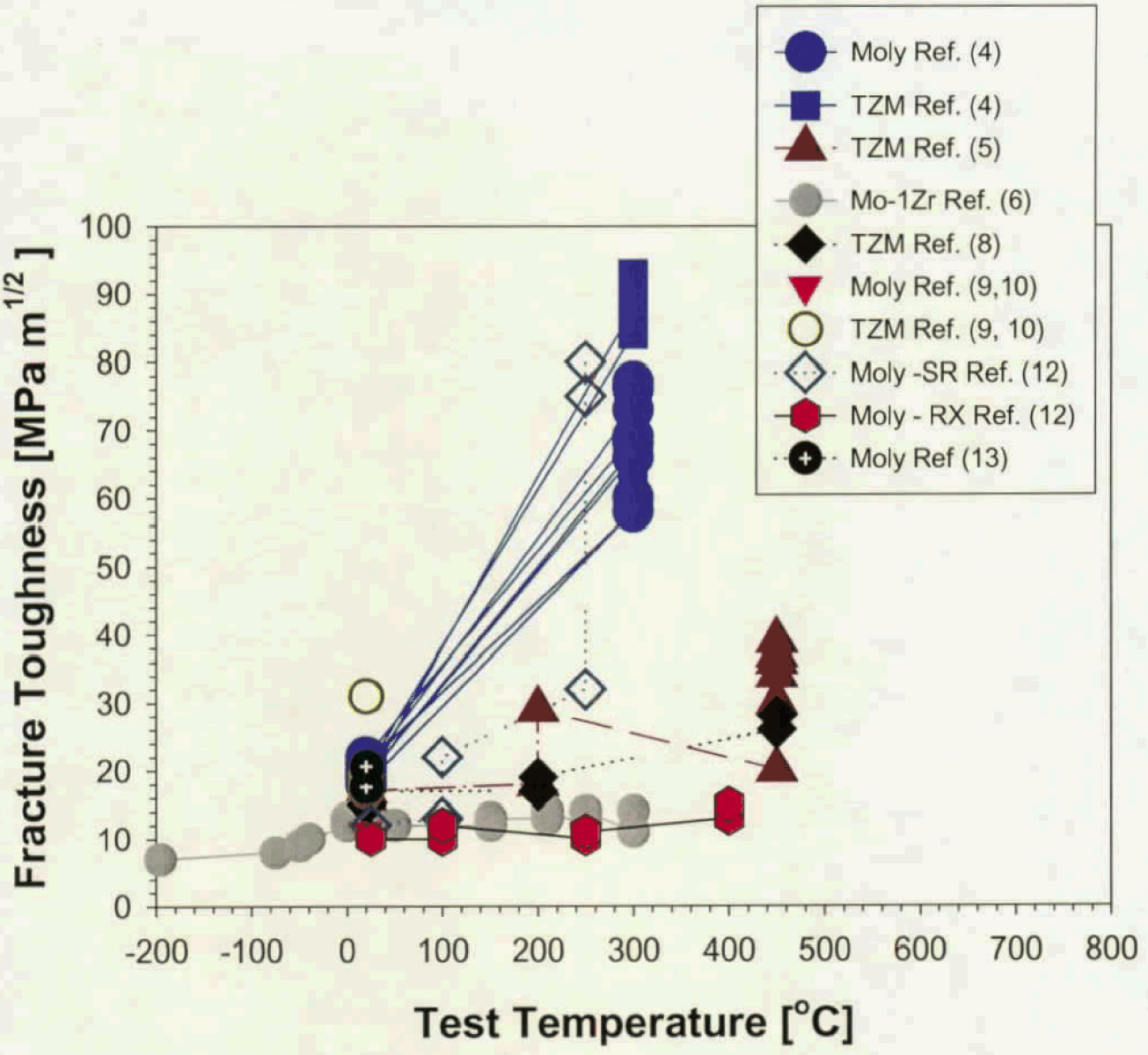

Figure 3. Plot of fracture toughness values versus temperature for data reported in literature for molybdenum, TZM, and molybdenum – 1% Zr[4-13]. The fracture toughness values are summarized in Table II.

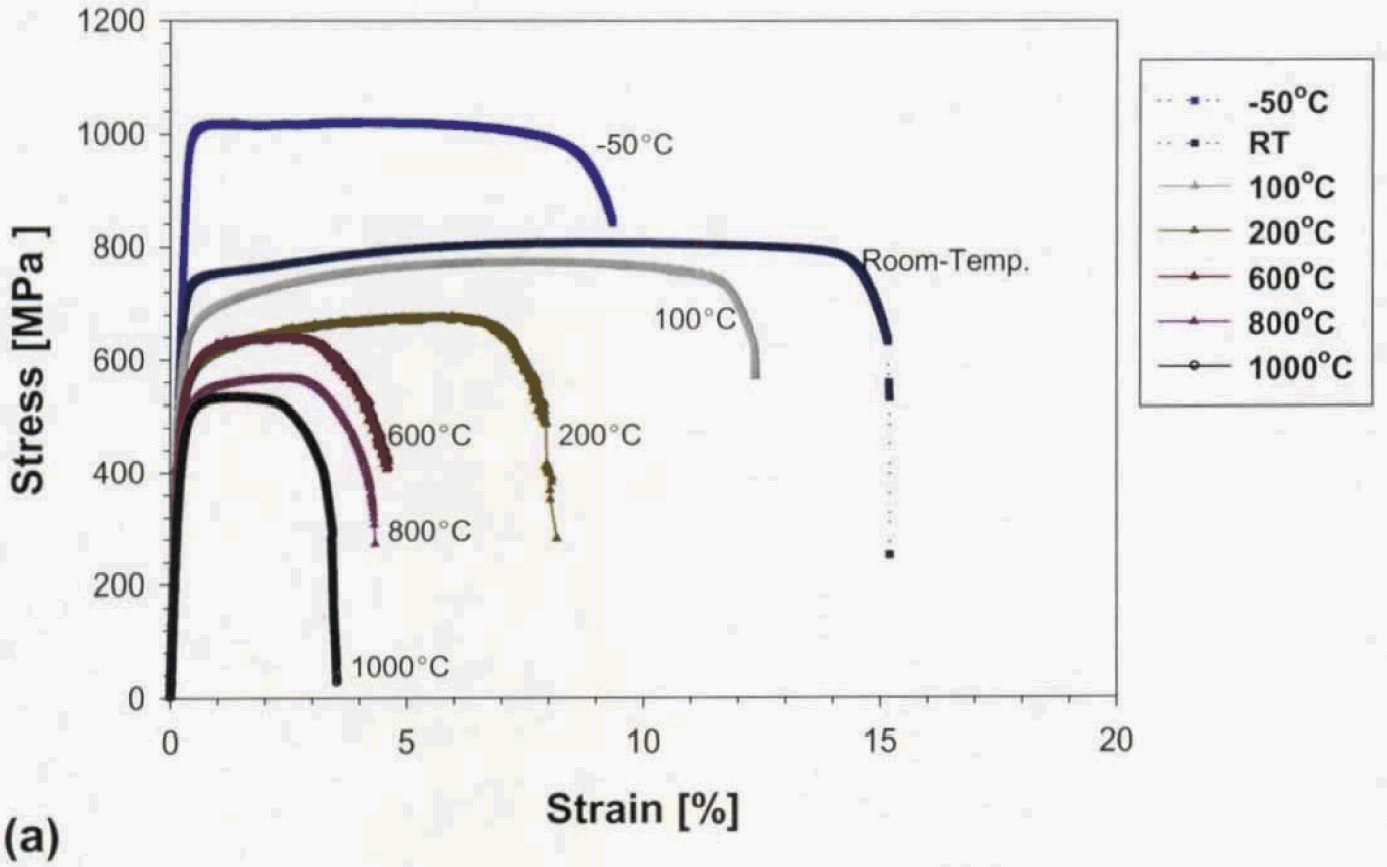

Figure 4. Representative stress-strain curves for tensile testing of TZM molybdenum from -50°C to 1000°C for the: (a) longitudinal orientation, and (b) transverse orientation. The tensile data are summarized in Tables III and IV. Engineering stress and engineering strain values are plotted. Note: the scales of both graphs in Figures 4 and 5 are identical.

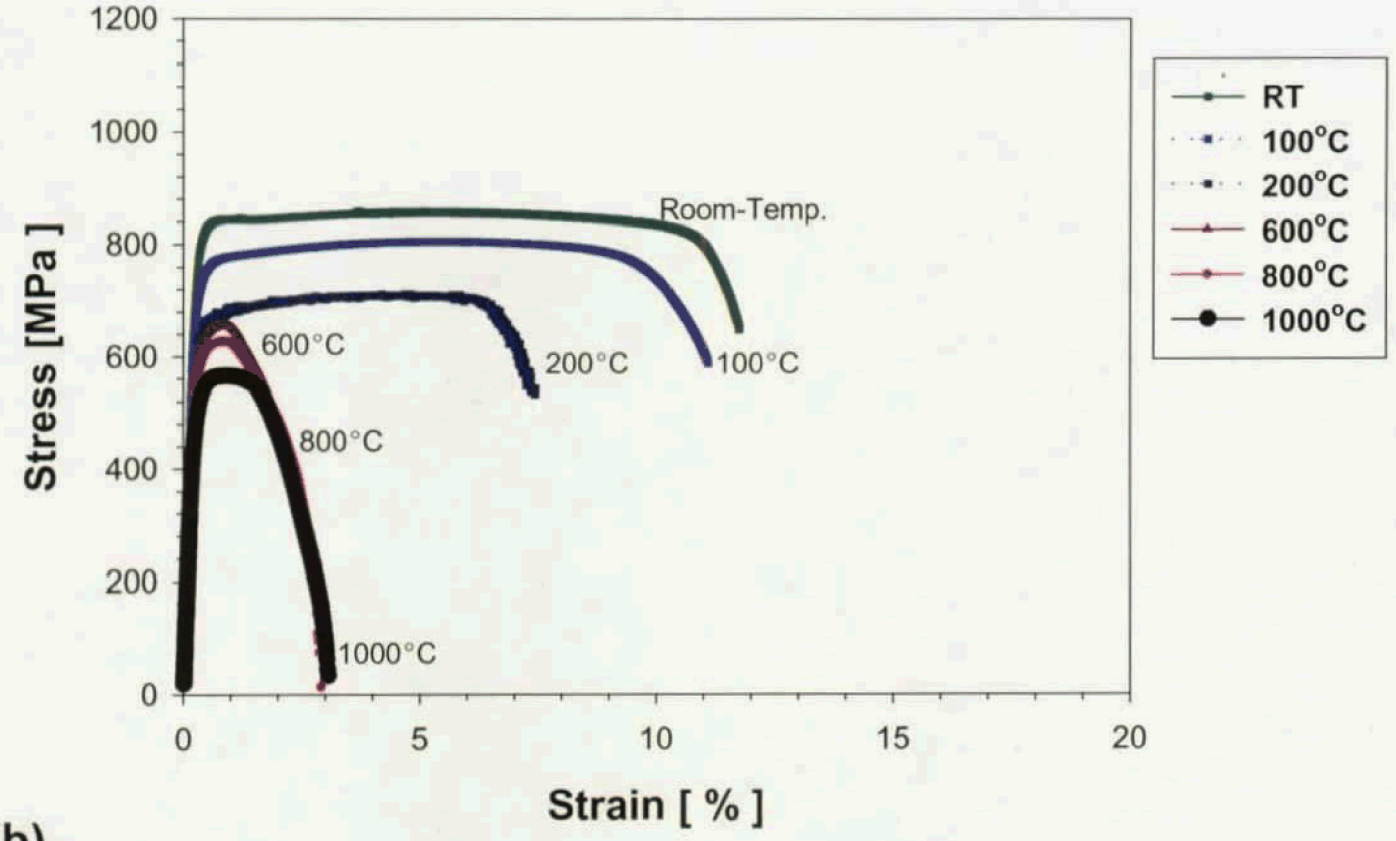

(b)

Figure 4. (Continued) Representative stress-strain curves for tensile testing of TZM molybdenum from -50°C to 1000°C for the: (a) longitudinal orientation, and (b) transverse orientation. The tensile data are summarized in Tables III and IV. Engineering stress and engineering strain values are plotted. Note: the scales of both graphs in Figures 4 and 5 are identical.

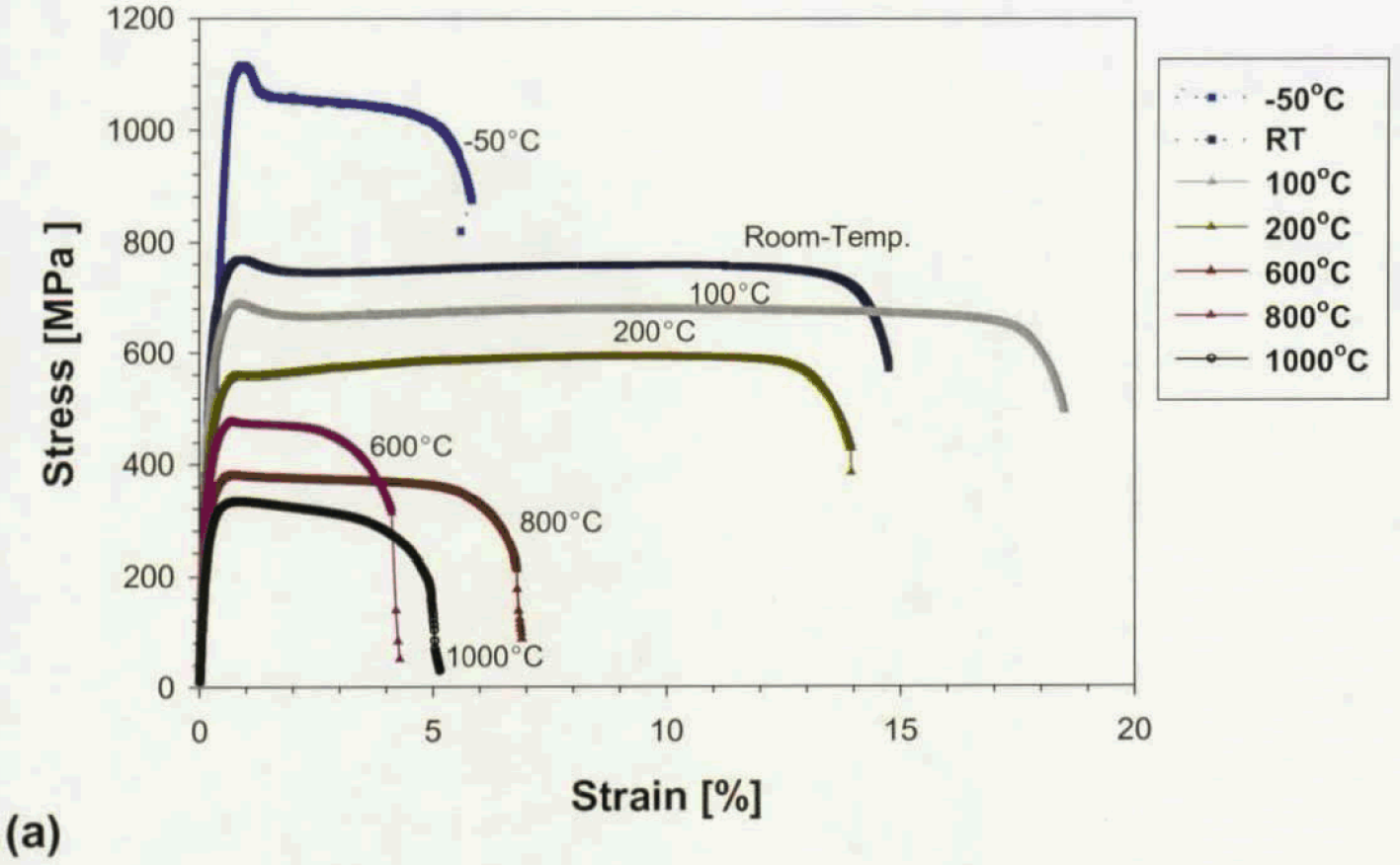

(a)

Figure 5. Representative stress-strain curves for tensile testing of ODS molybdenum from -50°C to 1000°C for the: (a) longitudinal orientation, and (b) transverse orientation. The tensile data are summarized in Tables V and VI. Engineering stress and engineering strain values are plotted. Note: the scales of both graphs in Figures 4 and 5 are identical.

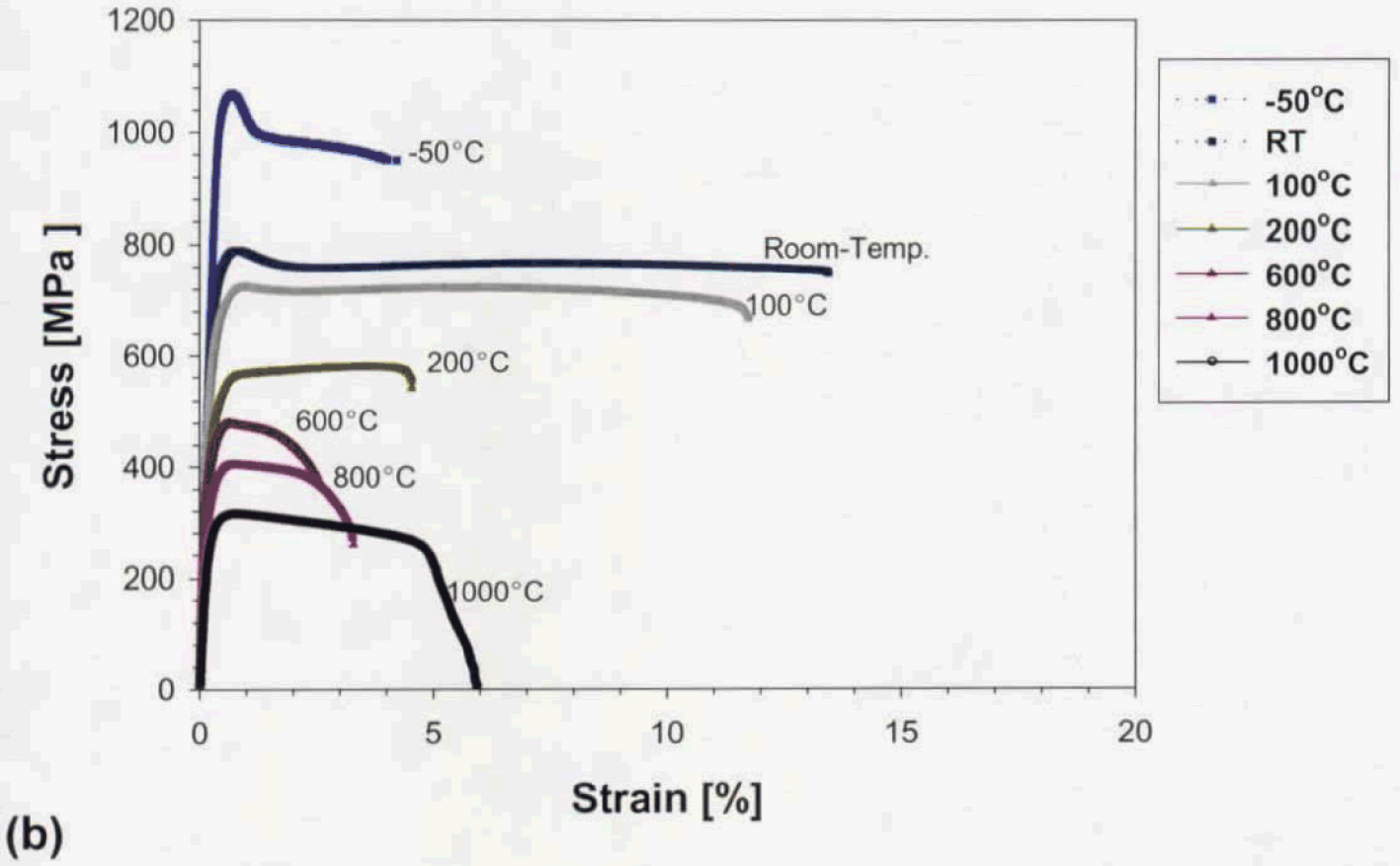

(b)

Figure 5. (Continued) Representative stress-strain curves for tensile testing of ODS molybdenum from -50°C to 1000°C for the: (a) longitudinal orientation, and (b) transverse orientation. The tensile data are summarized in Tables V and VI. Engineering stress and engineering strain values are plotted. Note: the scales of both graphs in Figures 4 and 5 are identical.

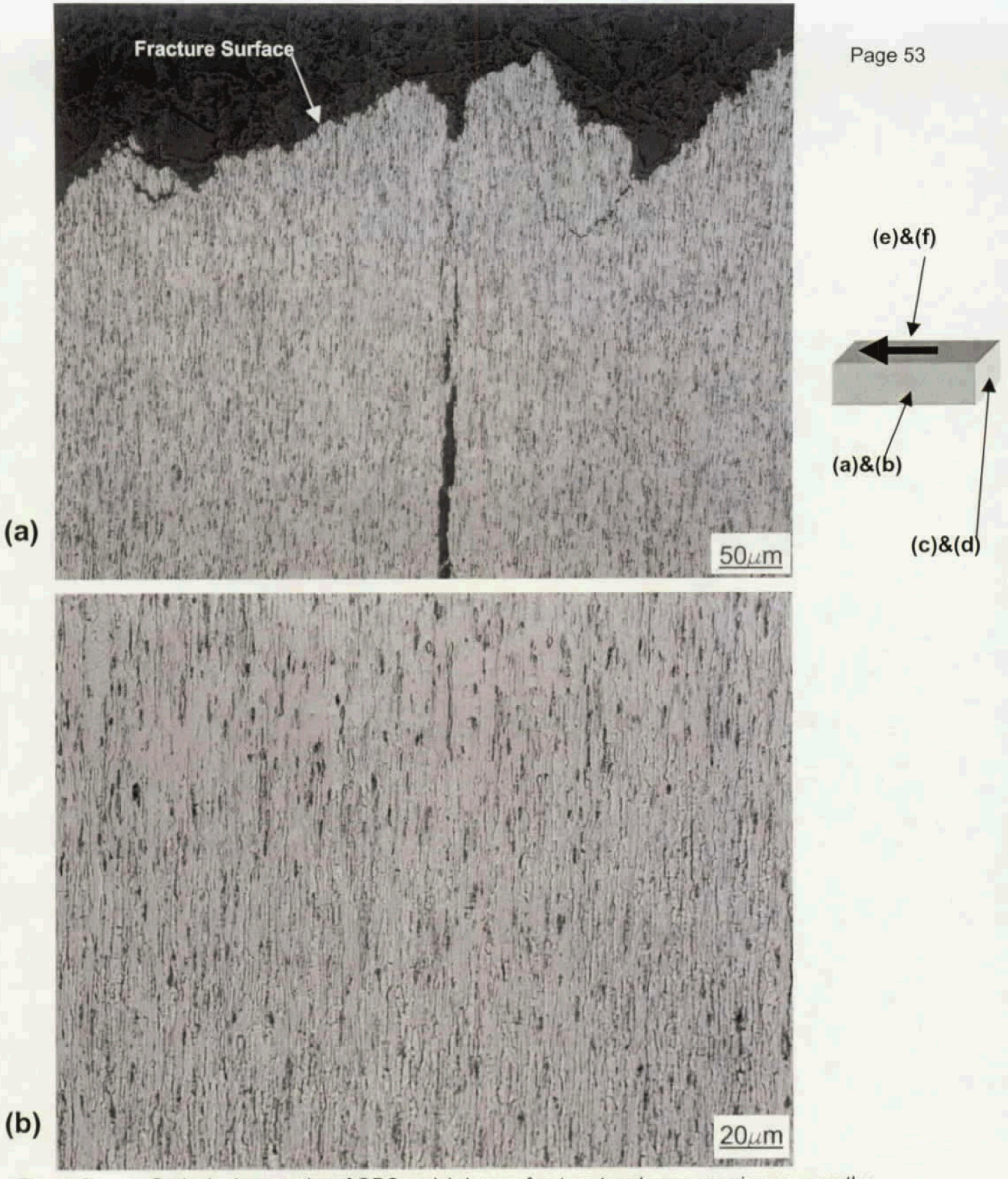

Figure 6. Optical micrographs of ODS molybdenum fracture toughness specimens near the fracture surface from the: (a) longitudinal orientation from a longitudinal specimen, (b) longitudinal orientation at higher magnification, (c) transverse section from a transverse specimen, (d) transverse section at high magnification, (e) surface of the ODS molybdenum plate, (f) high magnification image of plate surface, (g) transverse section showing banding that was observed in some regions of the plate, and (h) high magnification image of banding. The schematic of the plate with an arrow identifying the direction of working (longitudinal) shows the orientations used for the metallographic sections.

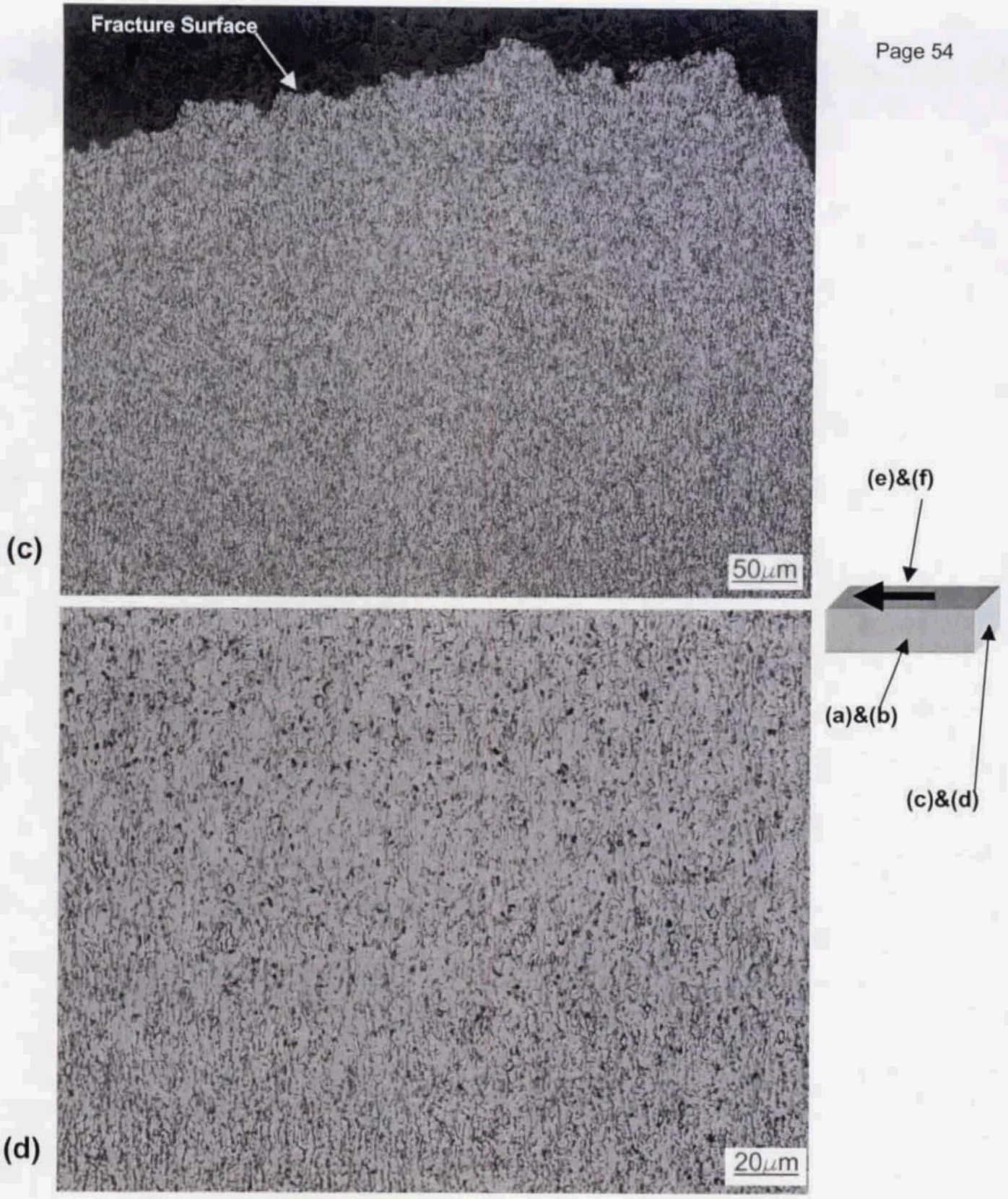

Figure 6. (Continued) Optical micrographs of ODS molybdenum fracture toughness specimens near the fracture surface from the: (a) longitudinal orientation from a longitudinal specimen, (b) longitudinal orientation at higher magnification, (c) transverse section from a transverse specimen, (d) transverse section at high magnification, (e) surface of the ODS molybdenum plate, (f) high magnification image of plate surface, (g) transverse section showing banding that was observed in some regions of the plate, and (h) high magnification image of banding. The schematic of the plate with an arrow identifying the direction of working (longitudinal) shows the orientations used for the metallographic sections.

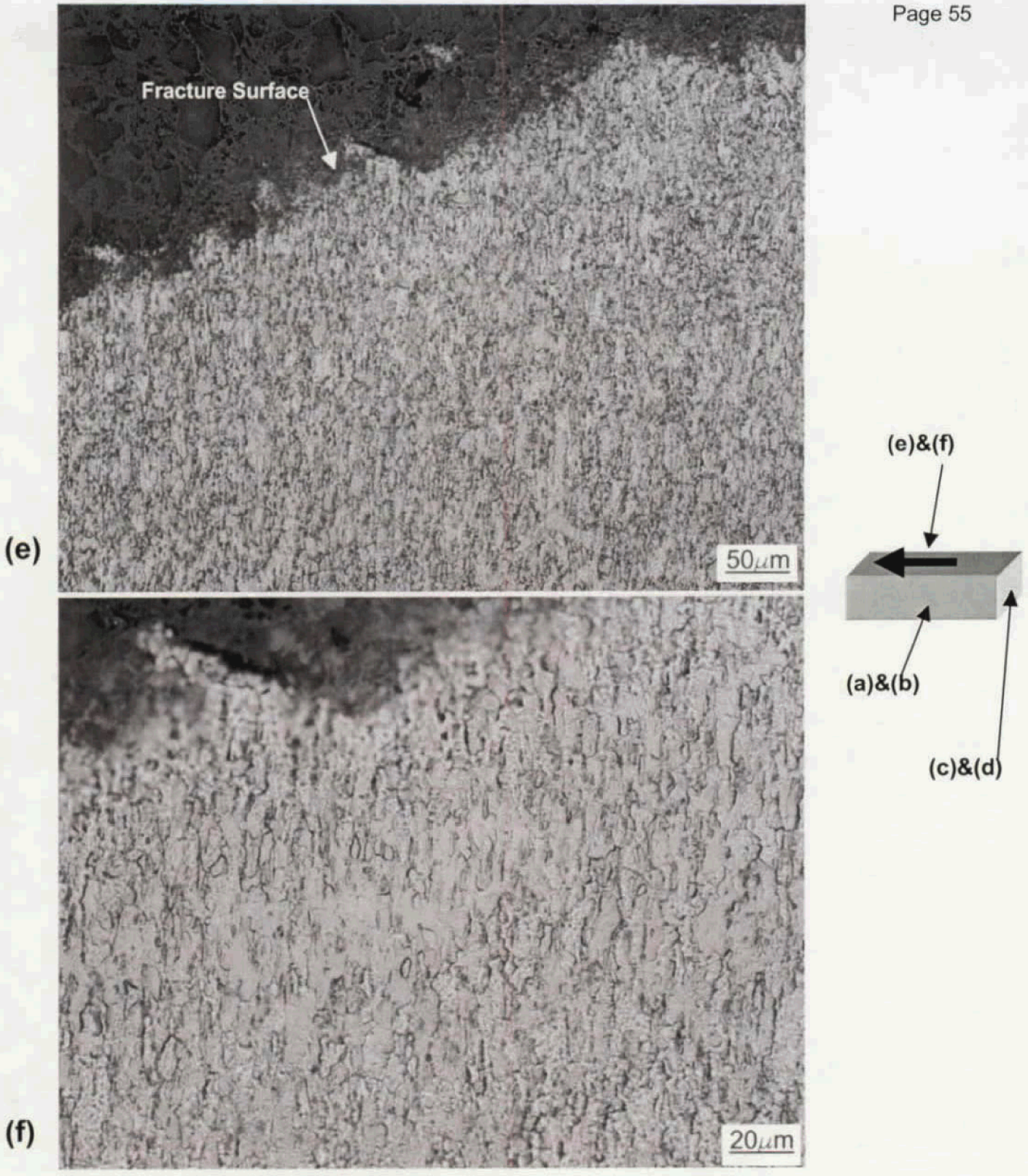

Figure 6. (Continued) Optical micrographs of ODS molybdenum fracture toughness specimens near the fracture surface from the: (a) longitudinal orientation from a longitudinal specimen, (b) longitudinal orientation at higher magnification, (c) transverse section from a transverse specimen, (d) transverse section at high magnification, (e) surface of the ODS molybdenum plate, (f) high magnification image of plate surface, (g) transverse section showing banding that was observed in some regions of the plate, and (h) high magnification image of banding. The schematic of the plate with an arrow identifying the direction of working (longitudinal) shows the orientations used for the metallographic sections.

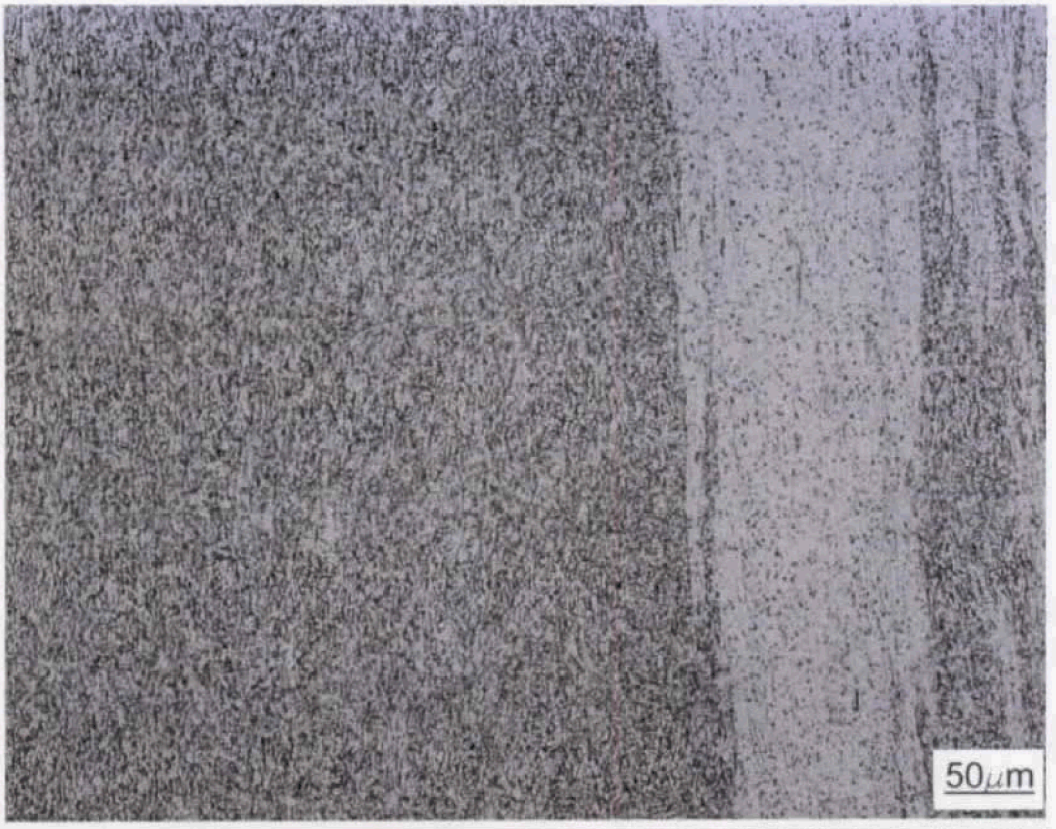

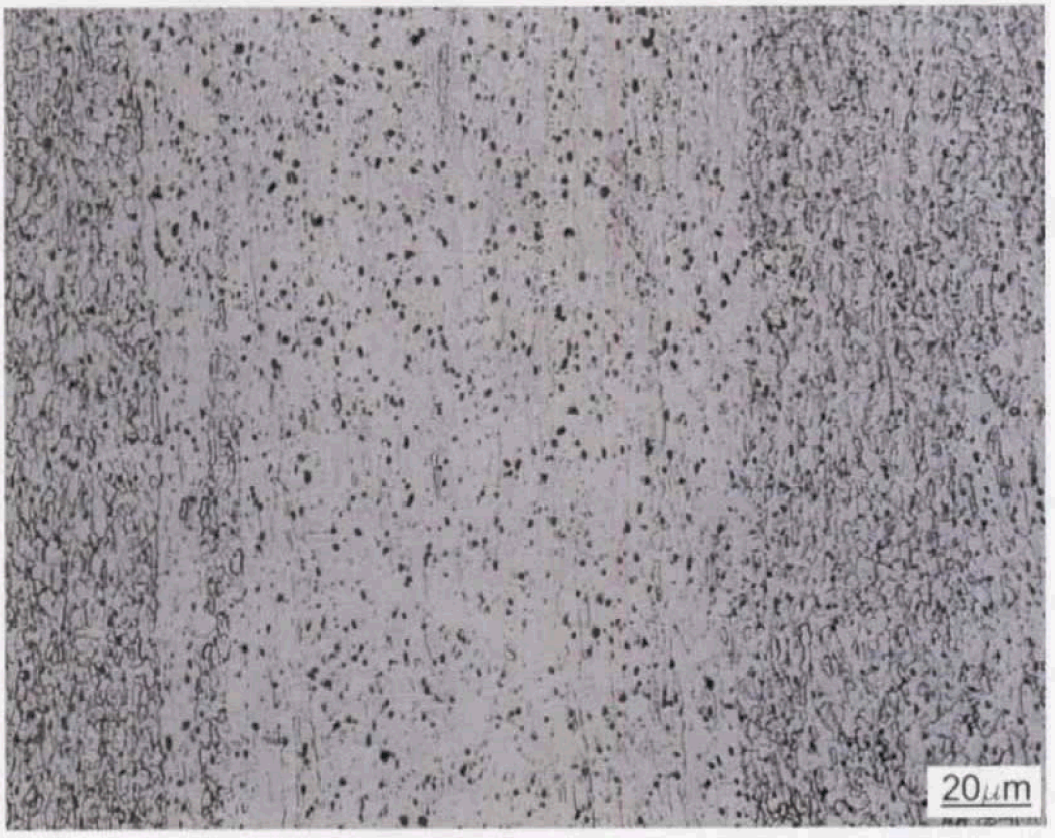

Figure 6. (Continued) Optical micrographs of ODS molybdenum fracture toughness specimens near the fracture surface from the: (a) longitudinal orientation from a longitudinal specimen, (b) longitudinal orientation at higher magnification, (c) transverse section from a transverse specimen, (d) transverse section at high magnification, (e) surface of the ODS molybdenum plate, (f) high magnification image of plate surface, (g) transverse section showing banding that was observed in some regions of the plate, and (h) high magnification image of banding. The schematic of the plate with an arrow identifying the direction of working (longitudinal) shows the orientations used for the metallographic sections.

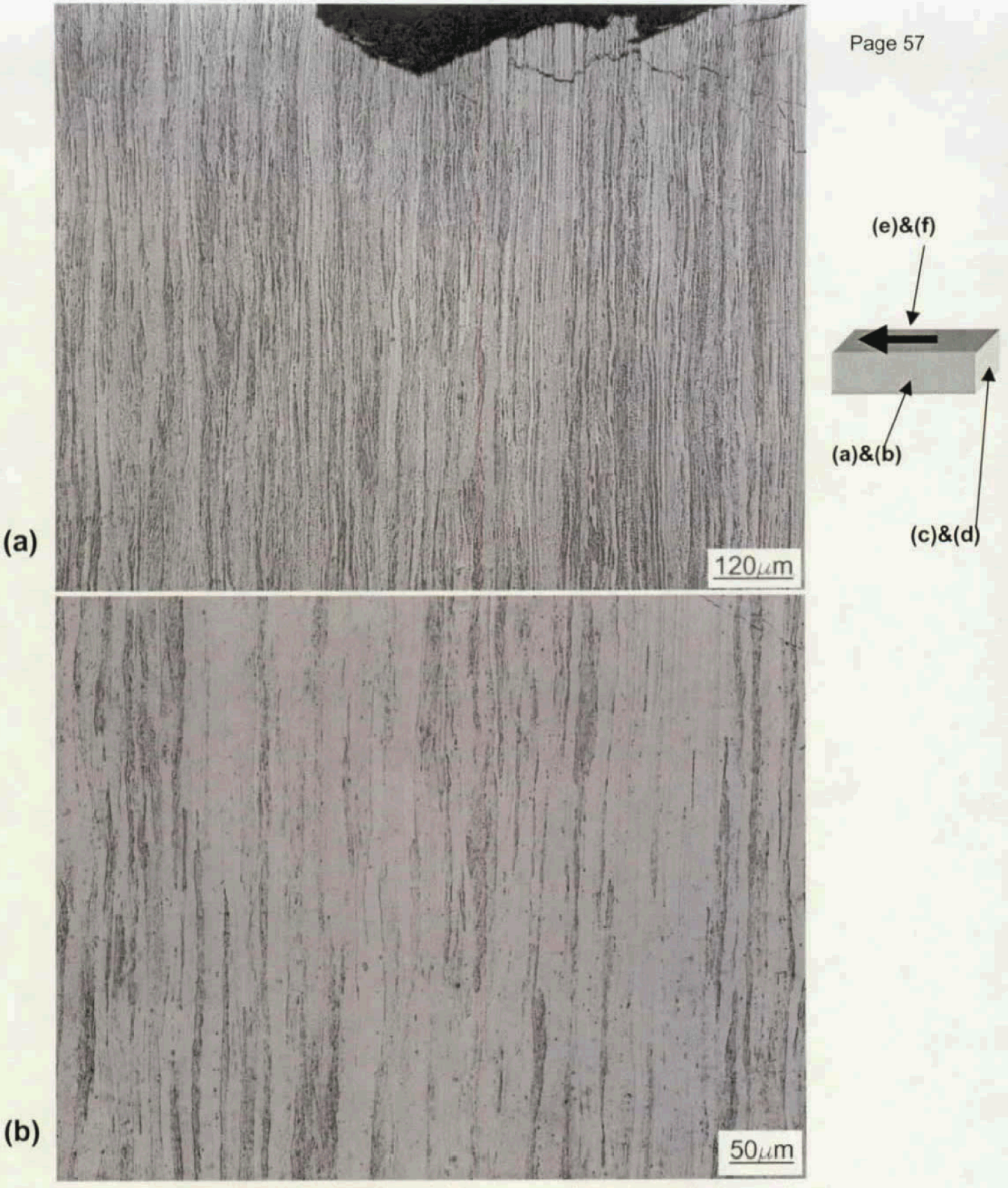

Figure 7. Optical micrographs of TZM molybdenum near the surface of a fracture toughness specimen from the: (a) longitudinal orientation from a longitudinal specimen, (b) longitudinal orientation at higher magnification, (c) transverse section from a transverse specimen, (d) transverse section at high magnification, (e) surface of the TZM plate, and (f) high magnification image of plate surface. The schematic of the plate with an arrow identifying the direction of working (longitudinal) shows the orientations used for the metallographic sections.

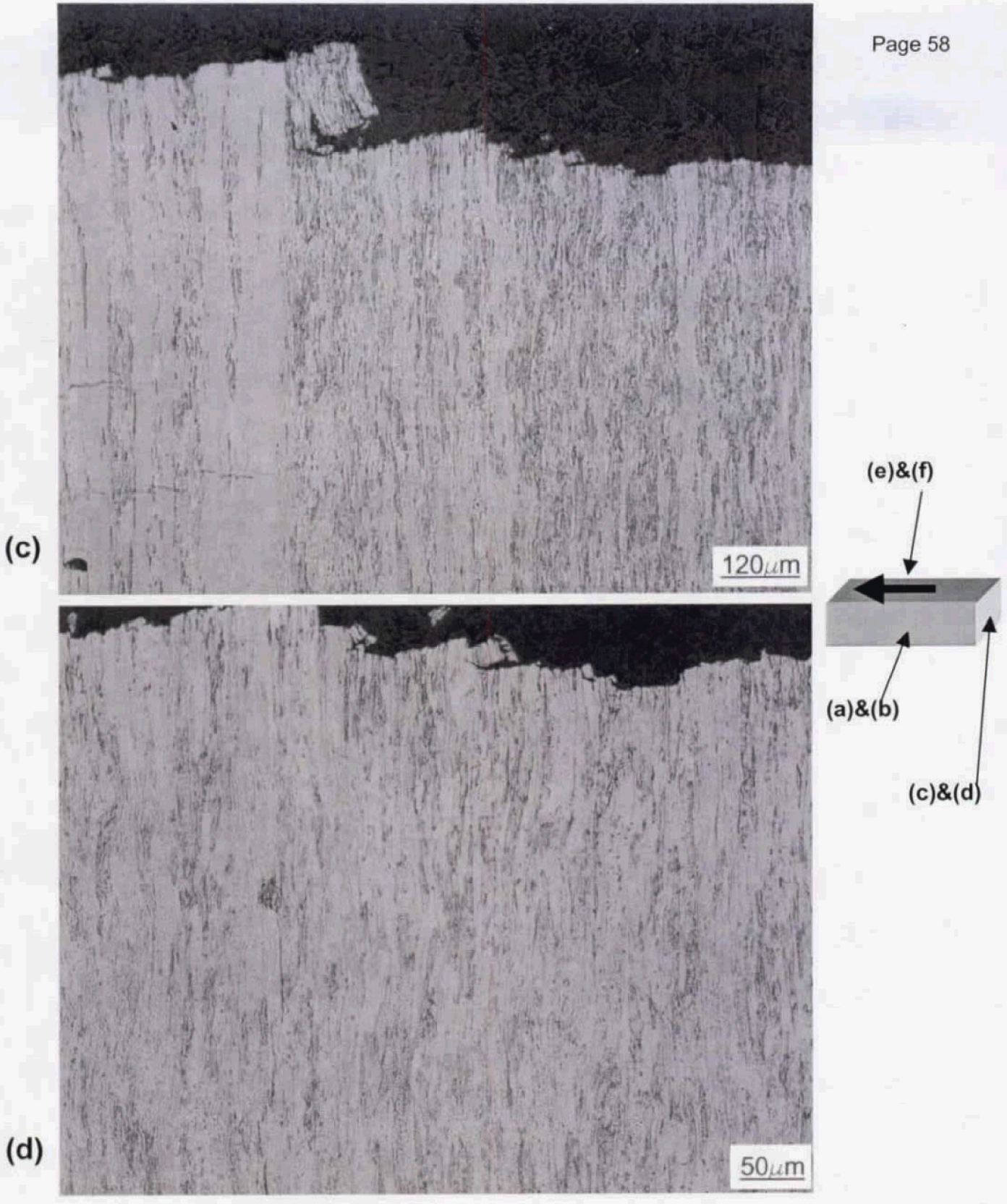

Figure 7. (Continued) Optical micrographs of TZM molybdenum near the surface of a fracture toughness specimen from the: (a) longitudinal orientation from a longitudinal specimen, (b) longitudinal orientation at higher magnification, (c) transverse section from a transverse specimen, (d) transverse section at high magnification, (e) surface of the TZM plate, and (f) high magnification image of plate surface. The schematic of the plate with an arrow identifying the direction of working (longitudinal) shows the orientations used for the metallographic sections.

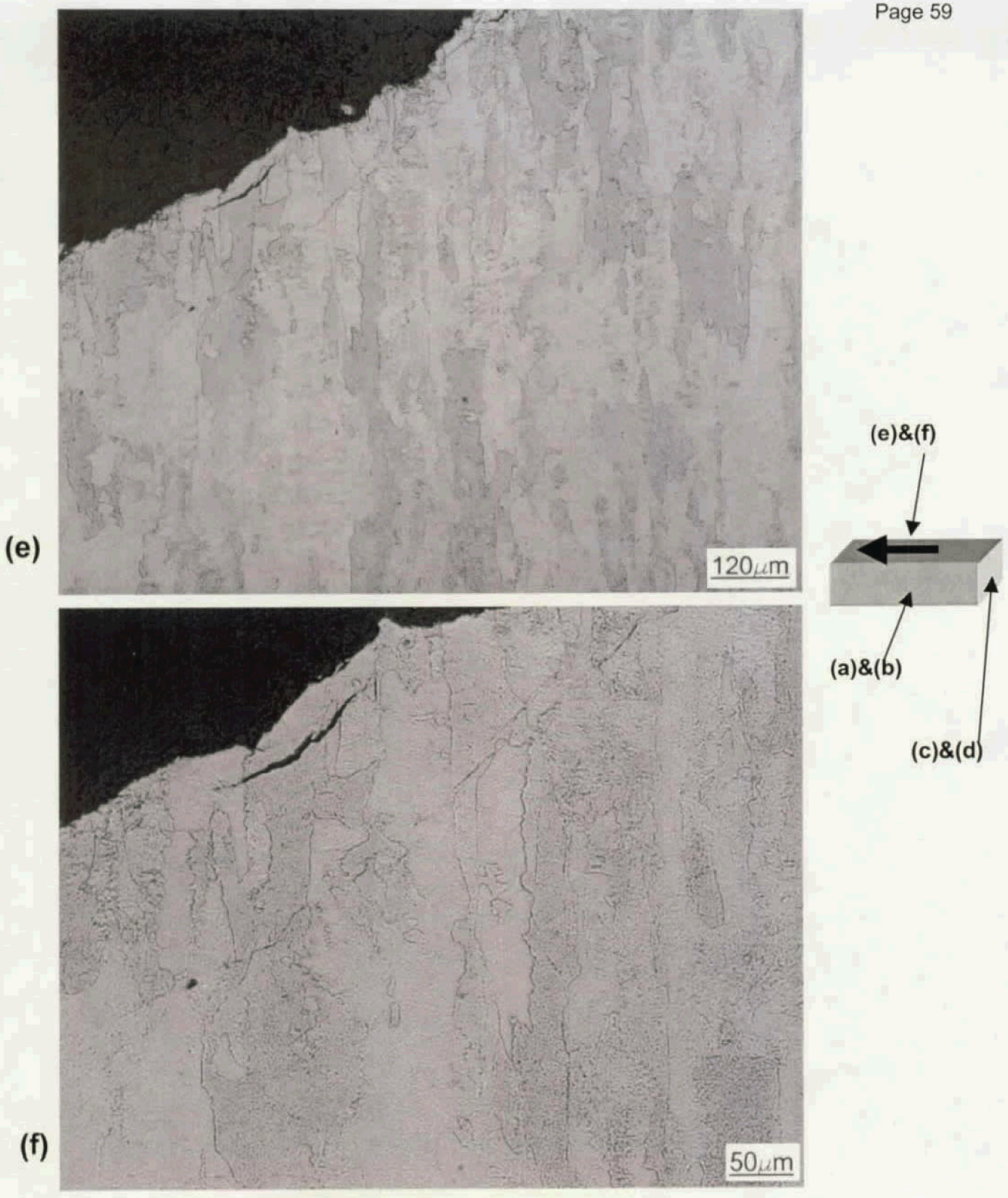

Figure 7. (Continued) Optical micrographs of TZM molybdenum near the surface of a fracture toughness specimen from the: (a) longitudinal orientation from a longitudinal specimen, (b) longitudinal orientation at higher magnification, (c) transverse section from a transverse specimen, (d) transverse section at high magnification, (e) surface of the TZM plate, and (f) high magnification image of plate surface. The schematic of the plate with an arrow identifying the direction of working (longitudinal) shows the orientations used for the metallographic sections.

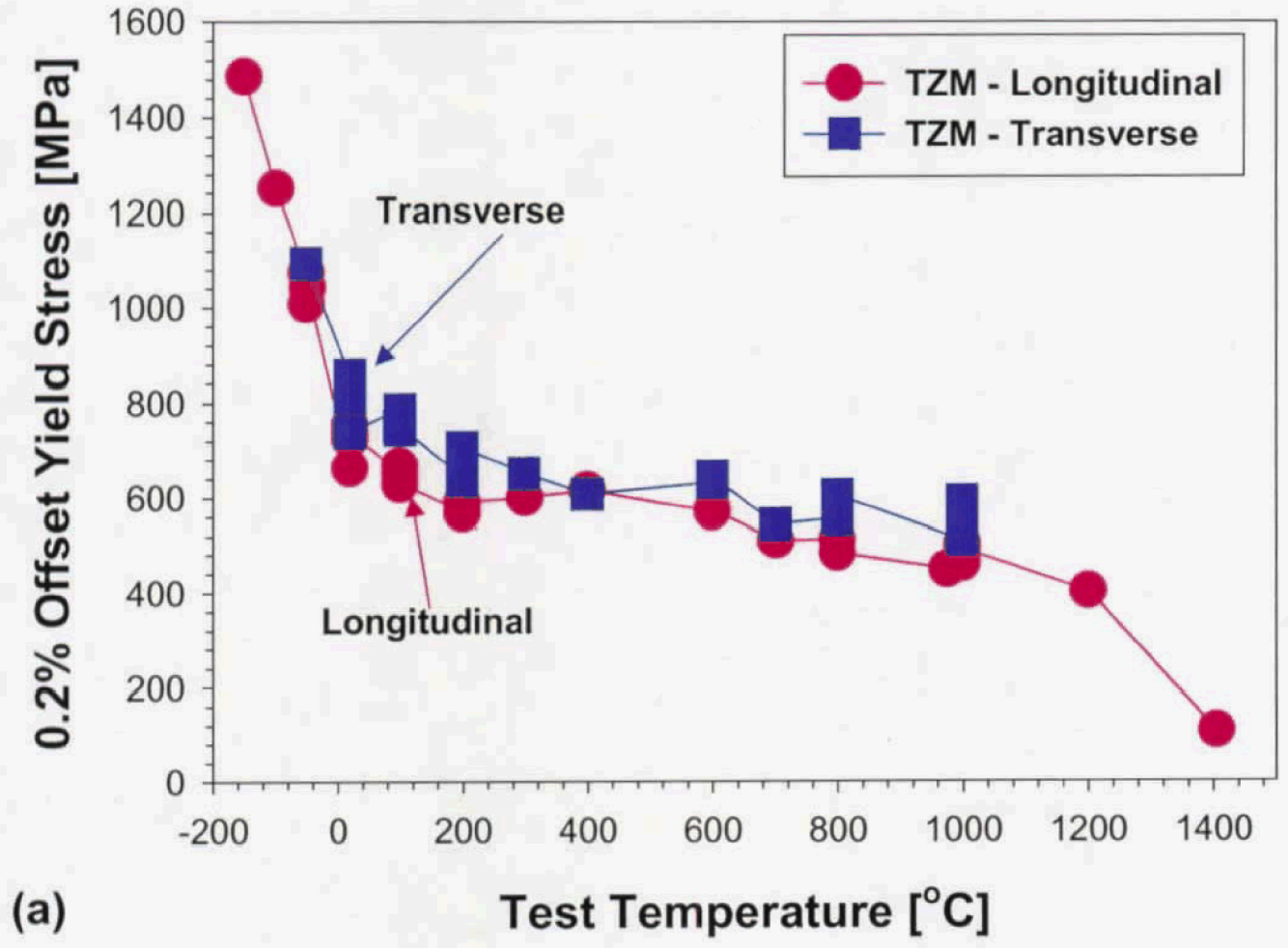

Figure 8. Comparison of tensile properties as a function of temperature for TZM molybdenum from -150°C to 1400°C for longitudinal (circle) and transverse (square) directions: (a) yield stress, and (b) total elongation. The tensile data are summarized in Tables III and IV. Engineering stress and engineering strain values are plotted. The scales for Figures 8 and 9 are the same.

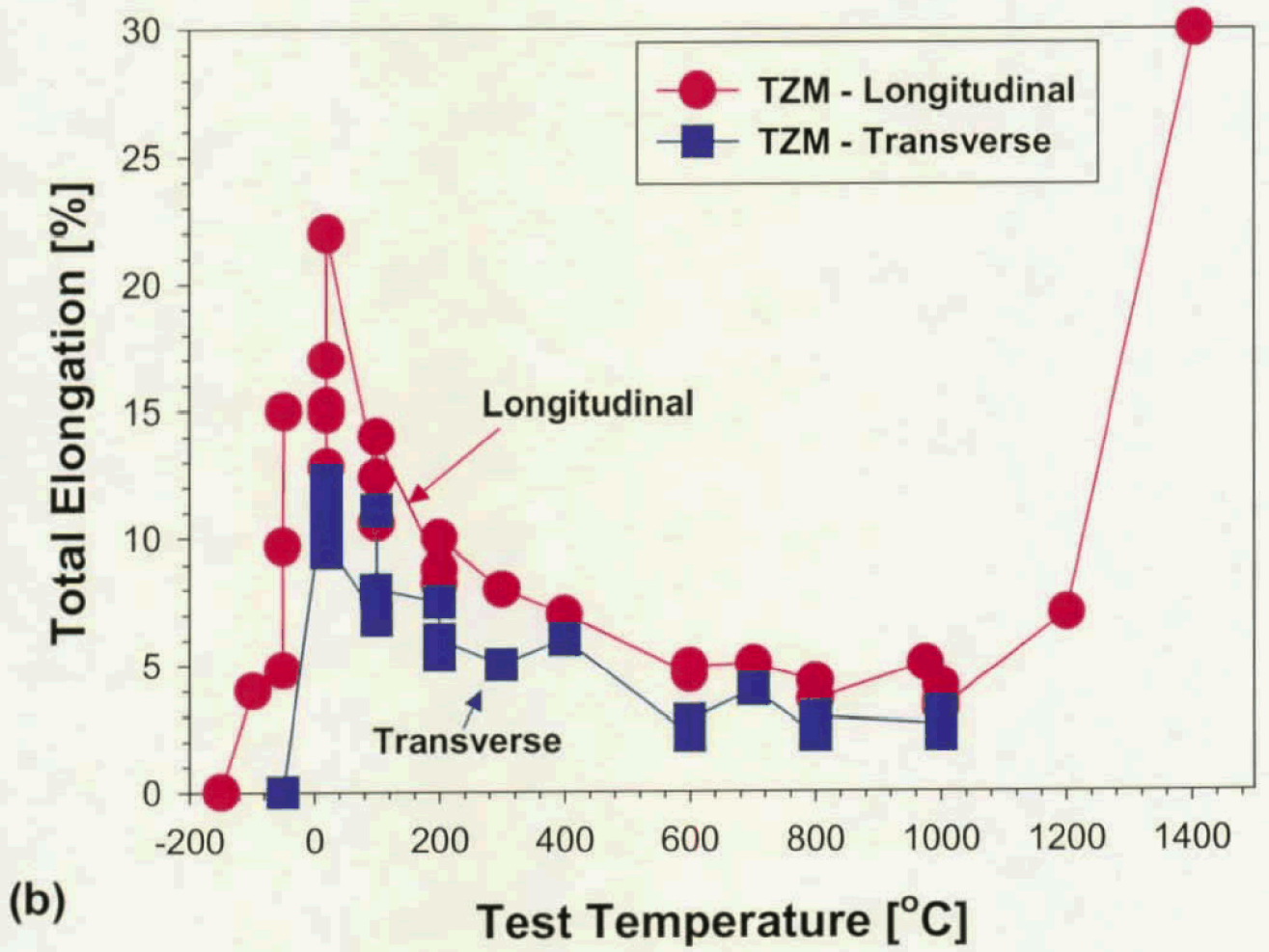

(b)

Figure 8. (Continued) Comparison of tensile properties as a function of temperature for TZM molybdenum from -150°C to 1400°C for longitudinal (circle) and transverse (square) directions: (a) yield stress, and (b) total elongation. The tensile data are summarized in Tables III and IV. Engineering stress and engineering strain values are plotted. The scales for Figures 8 and 9 are the same.

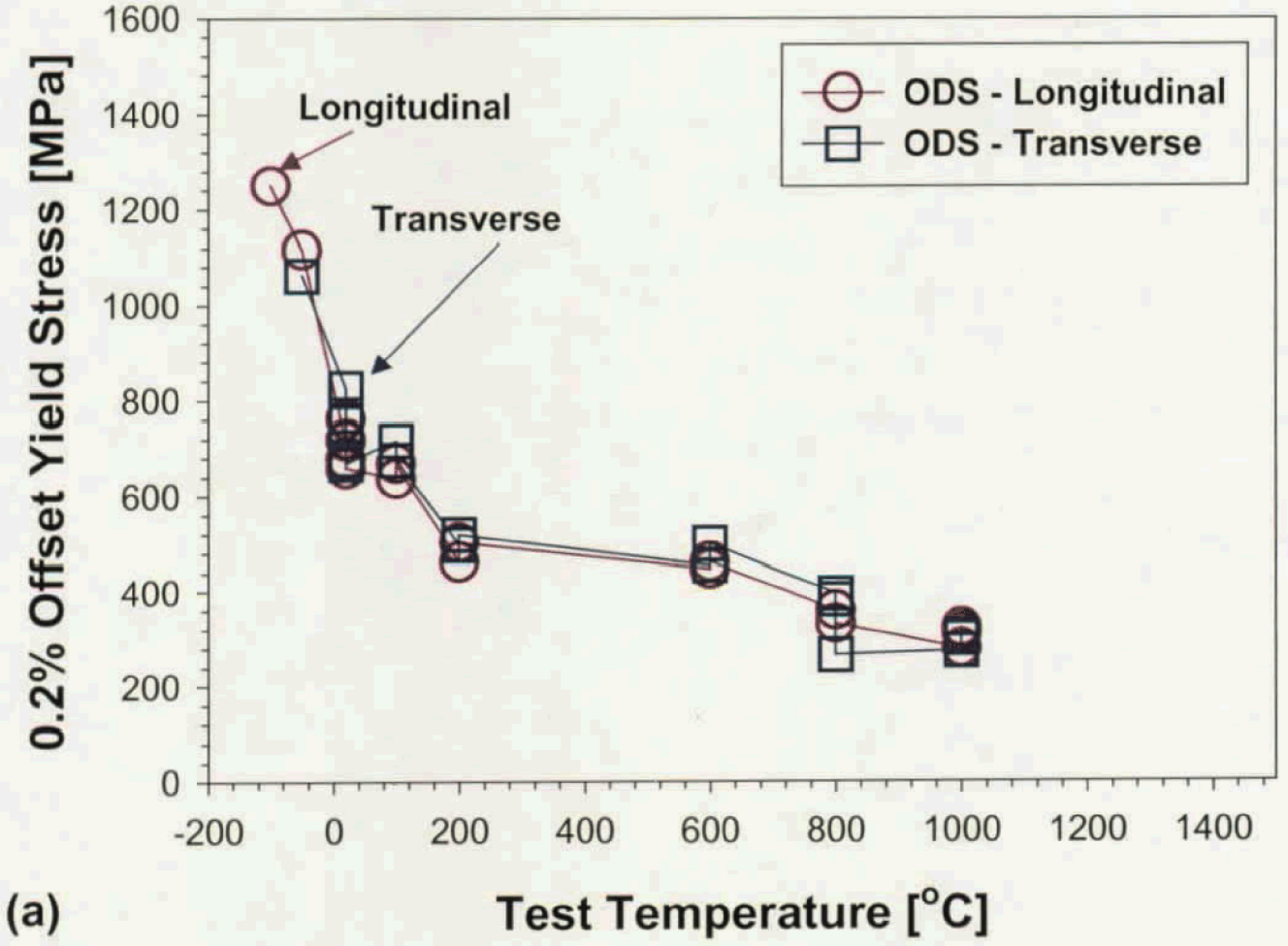

Figure 9. Comparison of tensile properties versus temperature for ODS molybdenum from -150°C to 1000°C for longitudinal (circle) and transverse (square) directions: (a) yield stress, and (b) total elongation. The tensile data are summarized in Tables V and VI. Engineering stress and engineering strain values are plotted. The scales for Figures 8 and 9 are the same.

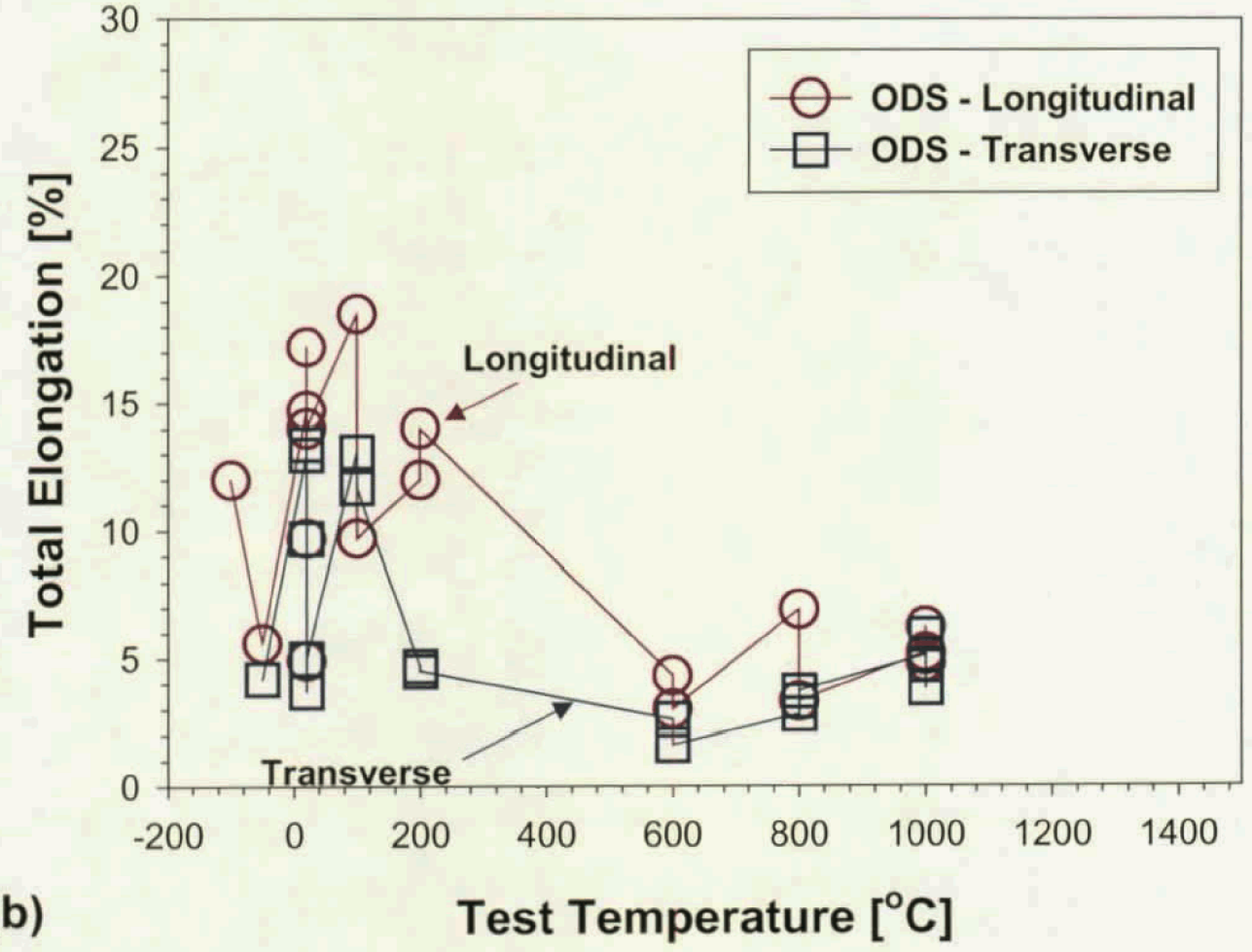

(b)

Figure 9. (Continued) Comparison of tensile properties versus temperature for ODS molybdenum from -150°C to 1000°C for longitudinal (circle) and transverse (square) directions: (a) yield stress, and (b) total elongation. The tensile data are summarized in Tables V and VI. Engineering stress and engineering strain values are plotted. The scales for Figures 8 and 9 are the same.

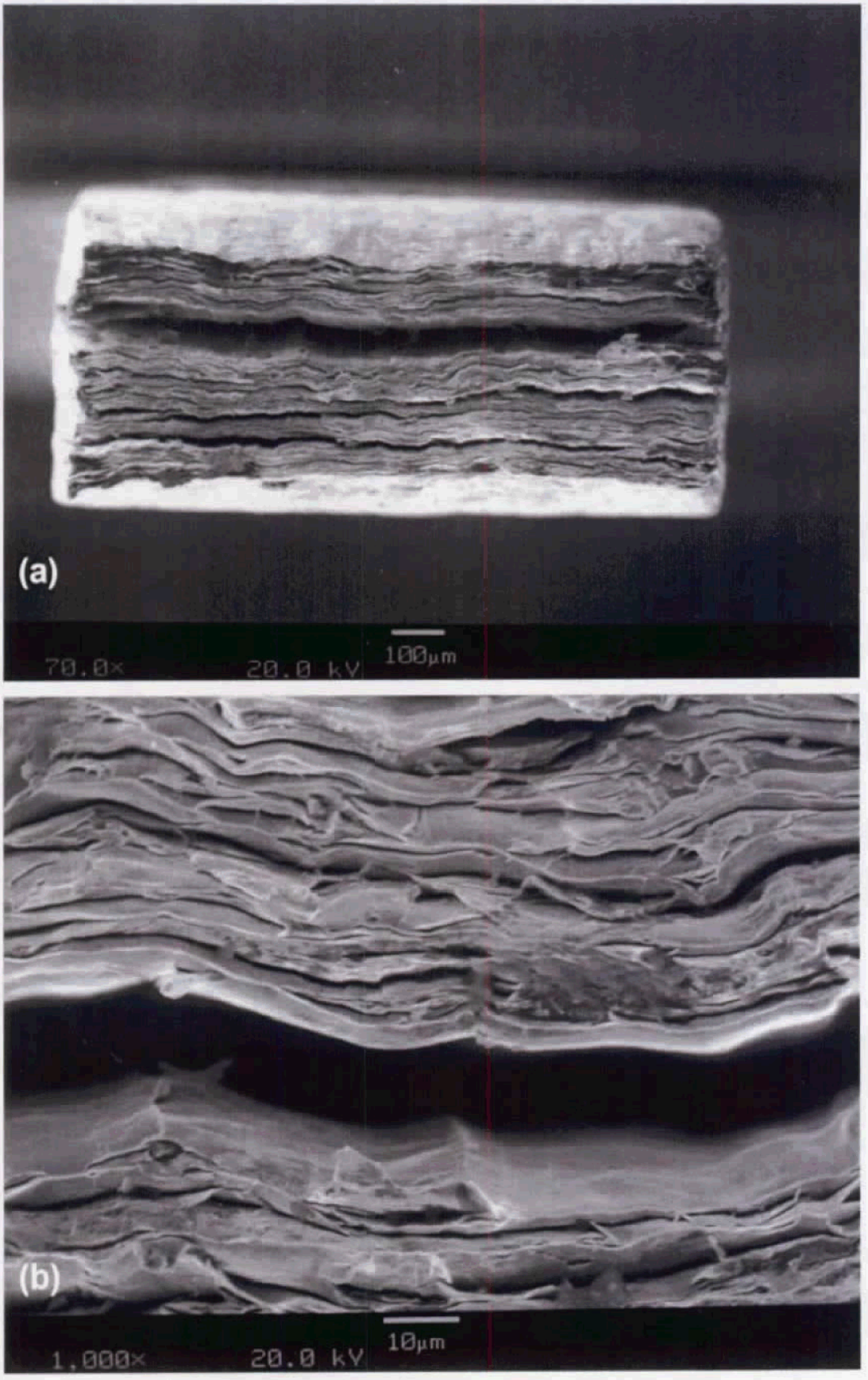

Figure 10. SEM fractography of TZM molybdenum tensile specimens in the longitudinal orientation after testing at : (a) room-temperature (low magnification image), (b) higher magnification image after room-temperature testing, (c) testing at 700°C for a low magnification image, and (d) higher magnification image following testing at 700°C.

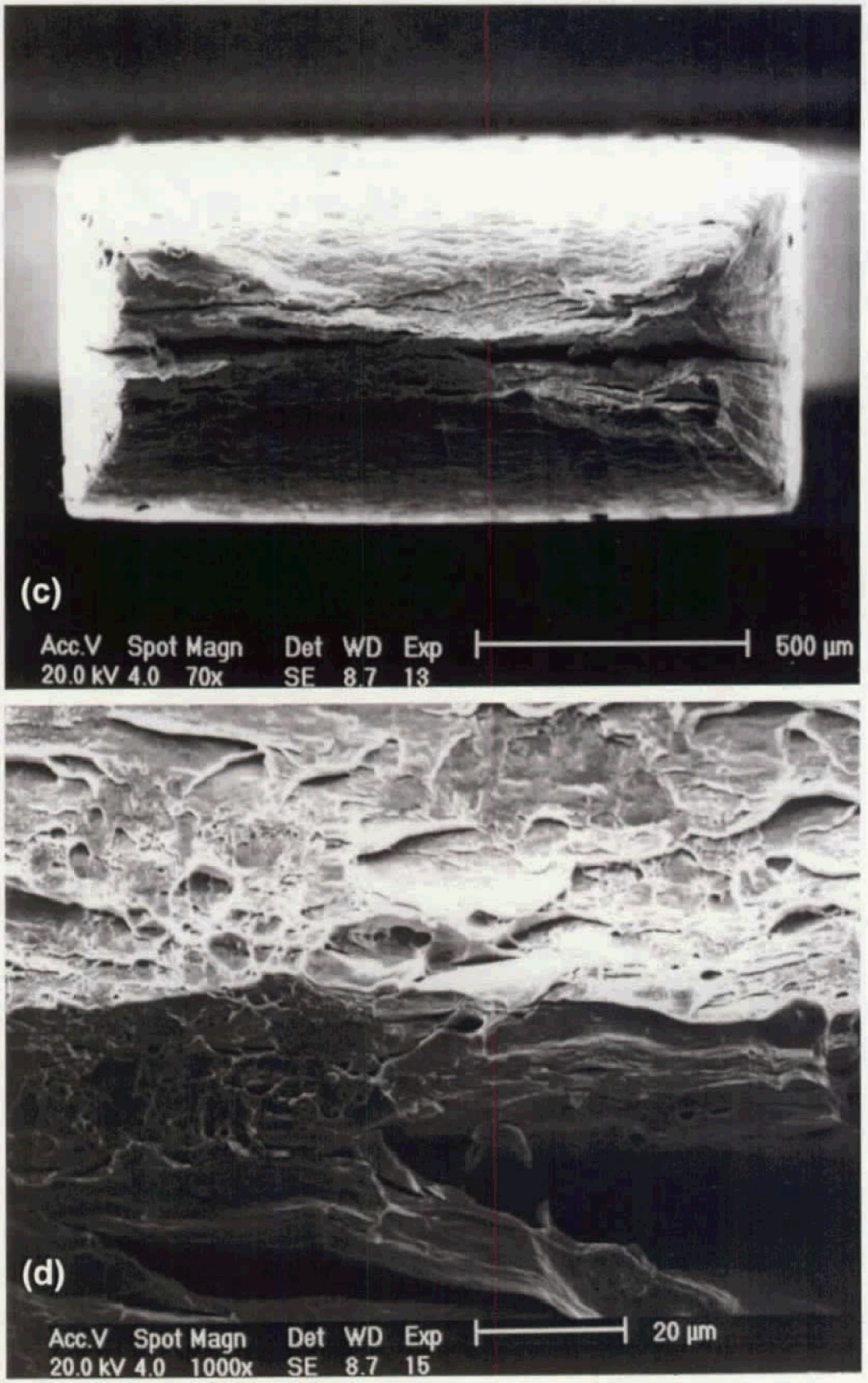

Figure 10. (Continued) SEM fractography of TZM molybdenum tensile specimens in the longitudinal orientation after testing at : (a) room-temperature (low magnification image), (b) higher magnification image after room-temperature testing, (c) testing at 700°C for a low magnification image, and (d) higher magnification image following testing at 700°C.

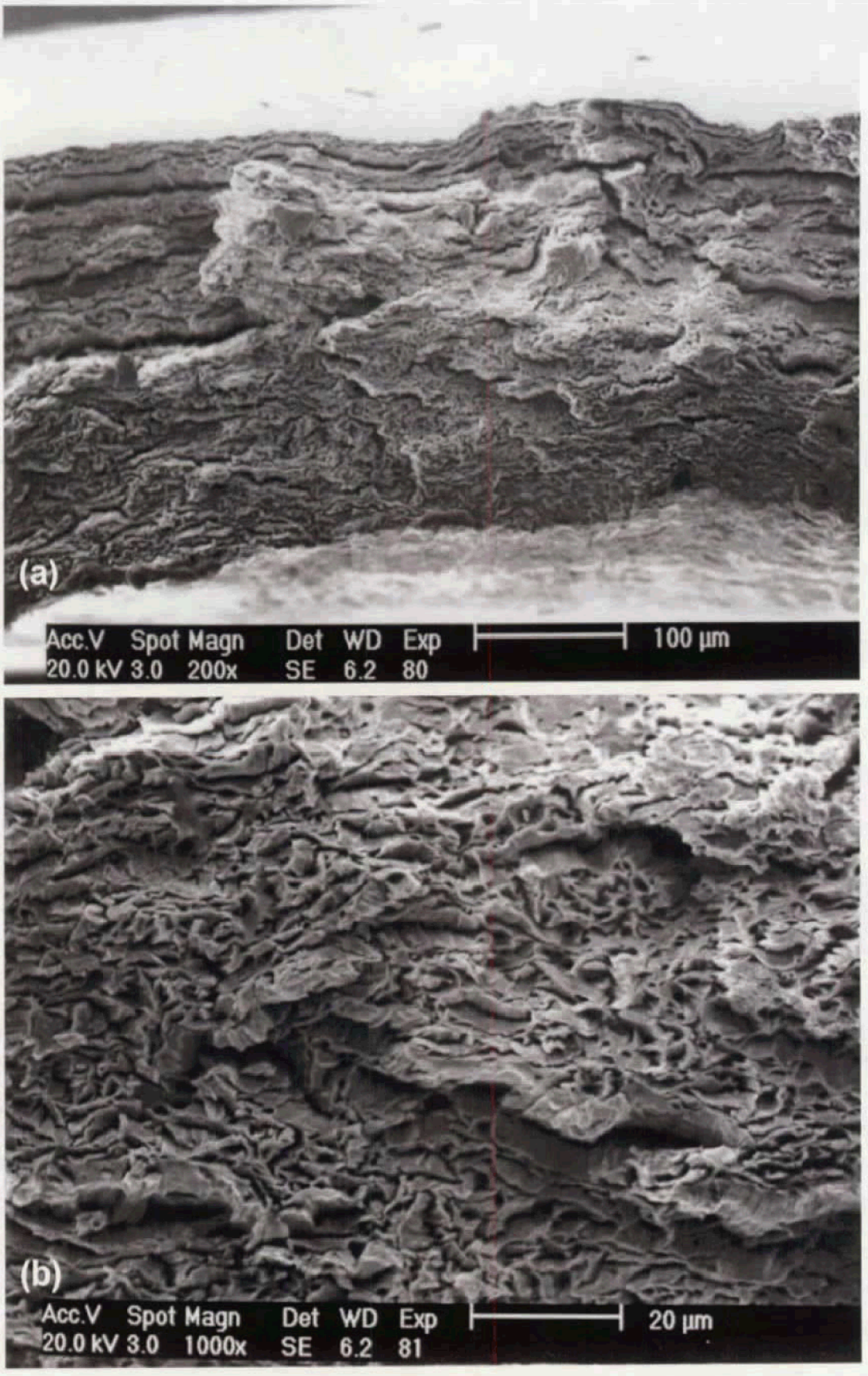

Figure 11. SEM fractography of longitudinal ODS molybdenum tensile specimens after testing at : (a) room-temperature (low magnification image), (b) higher magnification image after room-temperature testing, (c) testing at 1000°C (low magnification image), and (d) higher magnification image following testing at 1000°C.

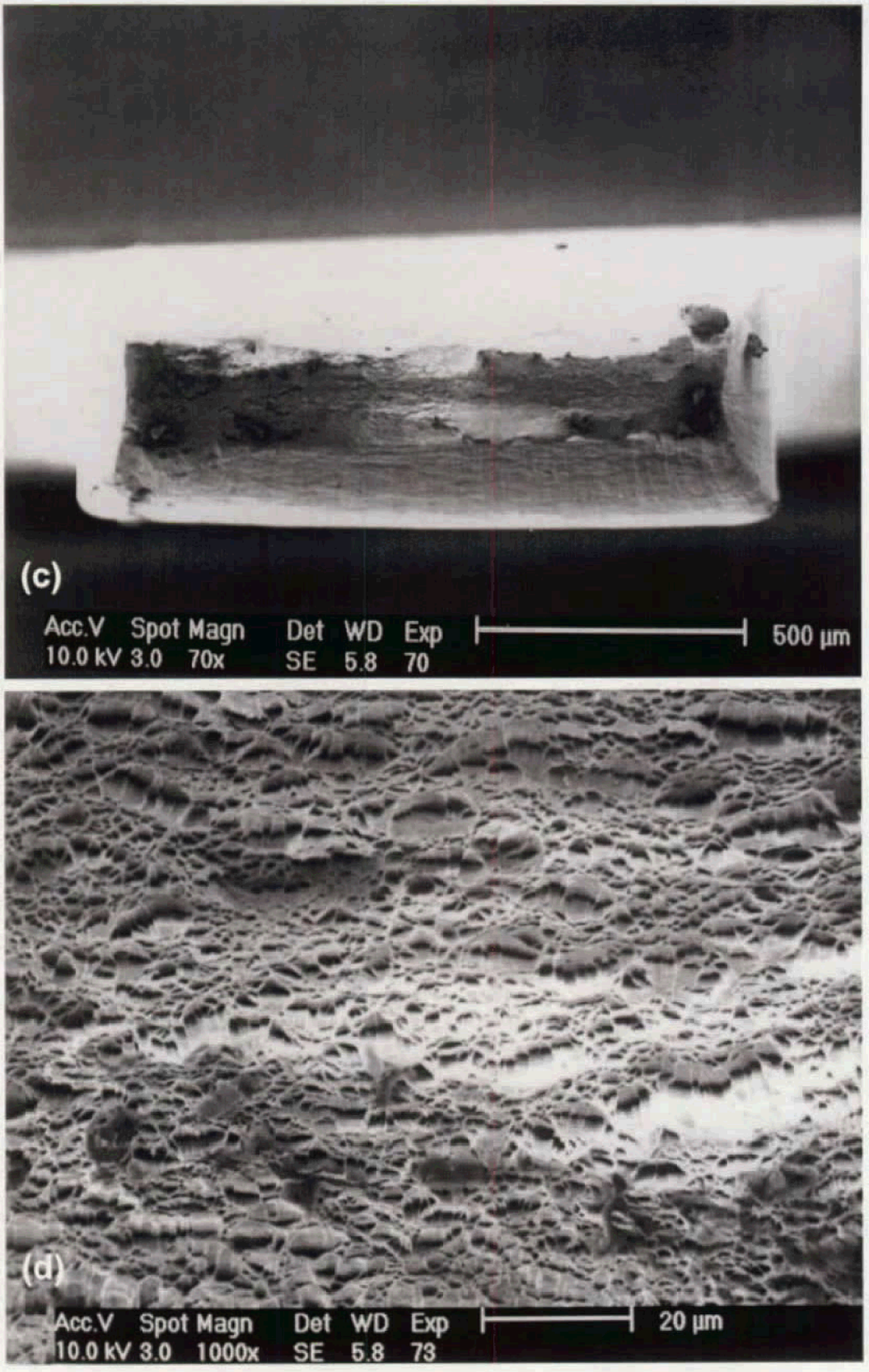

Figure 11. (Continued) SEM fractography of longitudinal ODS molybdenum tensile specimens after testing at : (a) room-temperature (low magnification image), (b) higher magnification image after room-temperature testing, (c) testing at 1000°C (low magnification image), and (d) higher magnification image following testing at 1000°C.

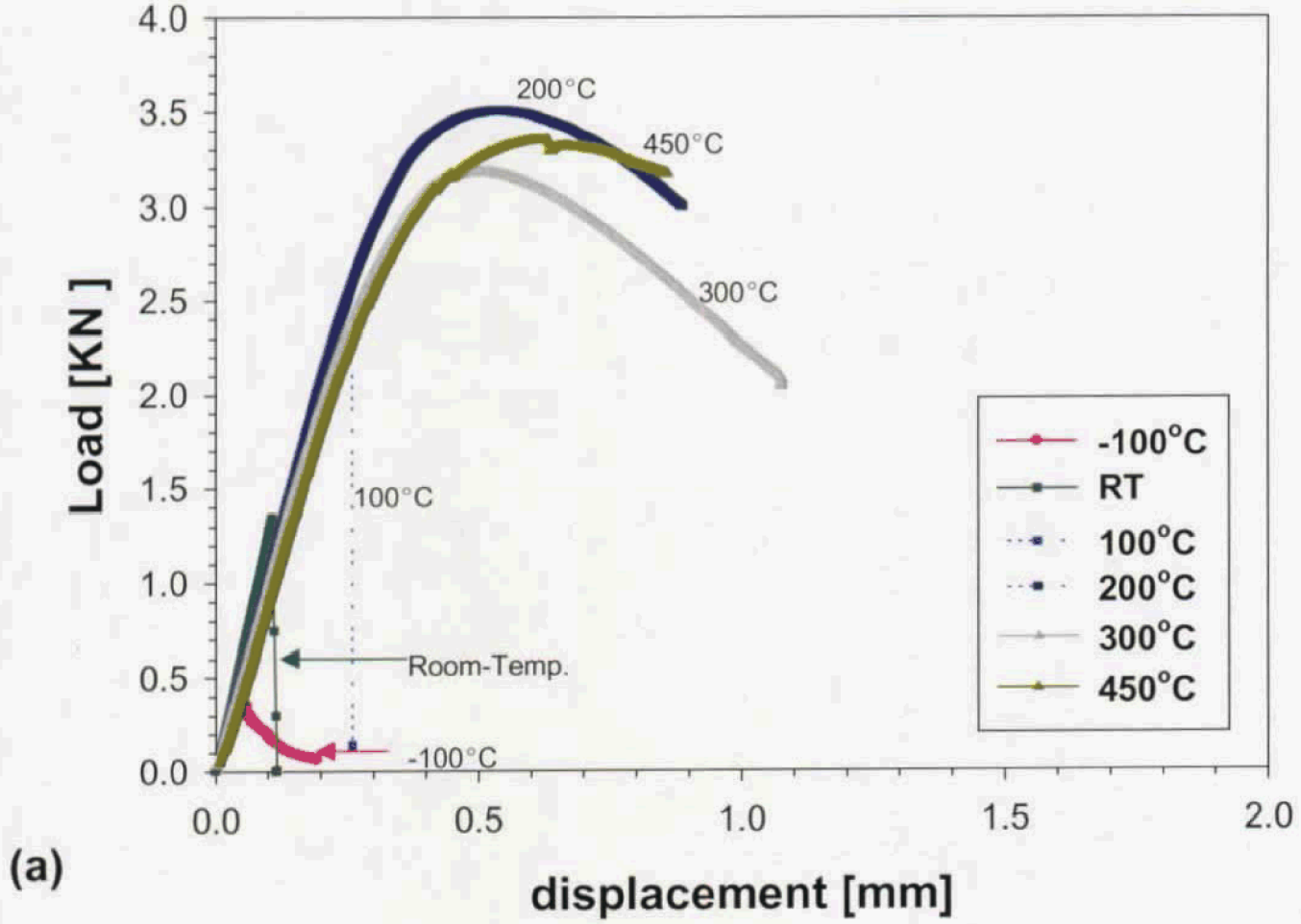

(a)

Figure 12. Representative load-displacement curves for fracture toughness testing at temperatures from -150°C to 450°C for: (a) TZM molybdenum in the longitudinal orientation, and (b) ODS molybdenum in the longitudinal orientation. All tests were performed at a displacement rate of 0.0025 mm/s. The scales of both graphs are identical.

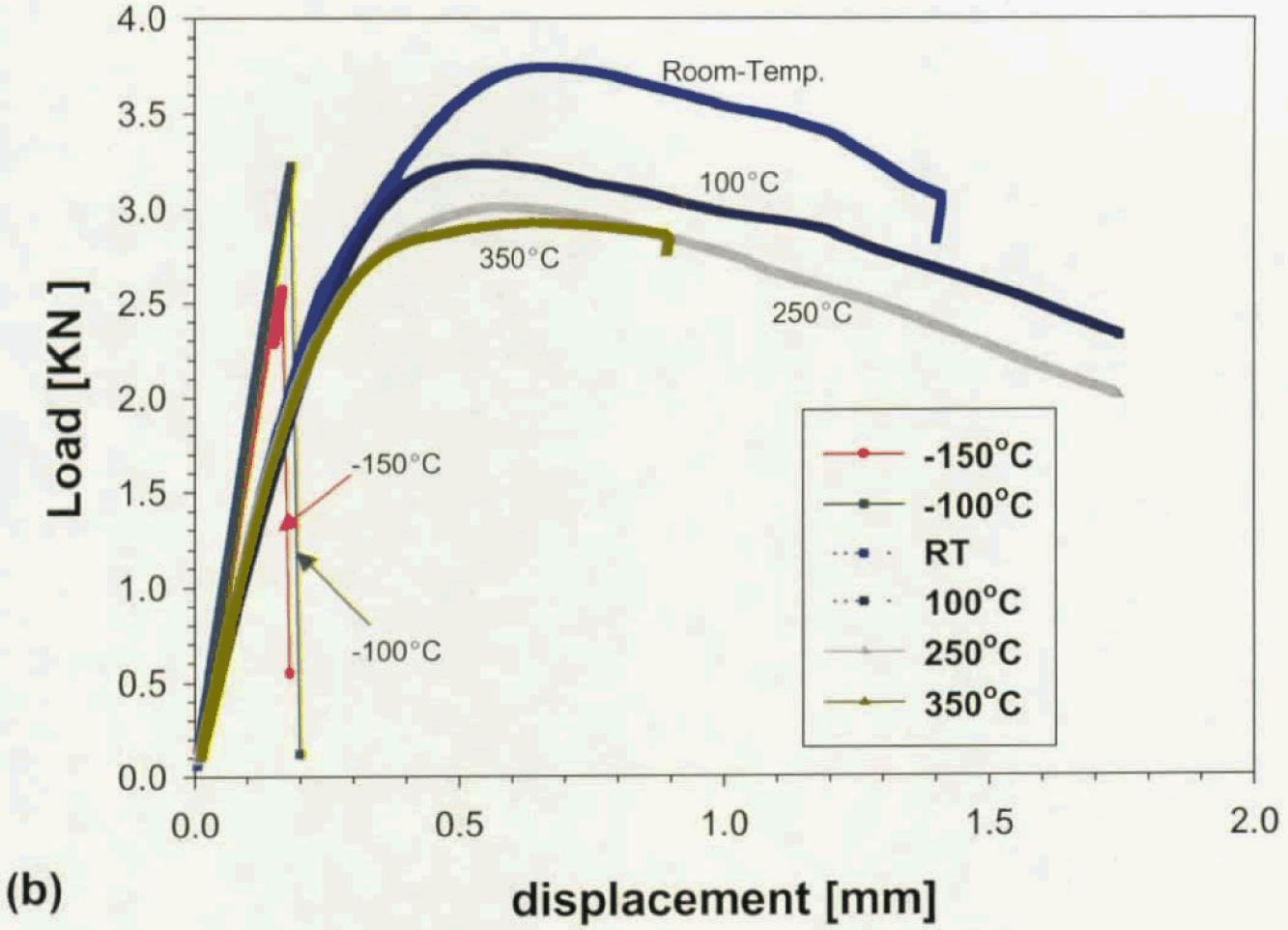

Figure 12. (Continued) Representative load-displacement curves for fracture toughness testing at temperatures from -150°C to 450°C for: (a) TZM molybdenum in the longitudinal orientation, and (b) ODS molybdenum in the longitudinal orientation. All tests were performed at a displacement rate of 0.0025 mm/s. The scales of both graphs are identical.

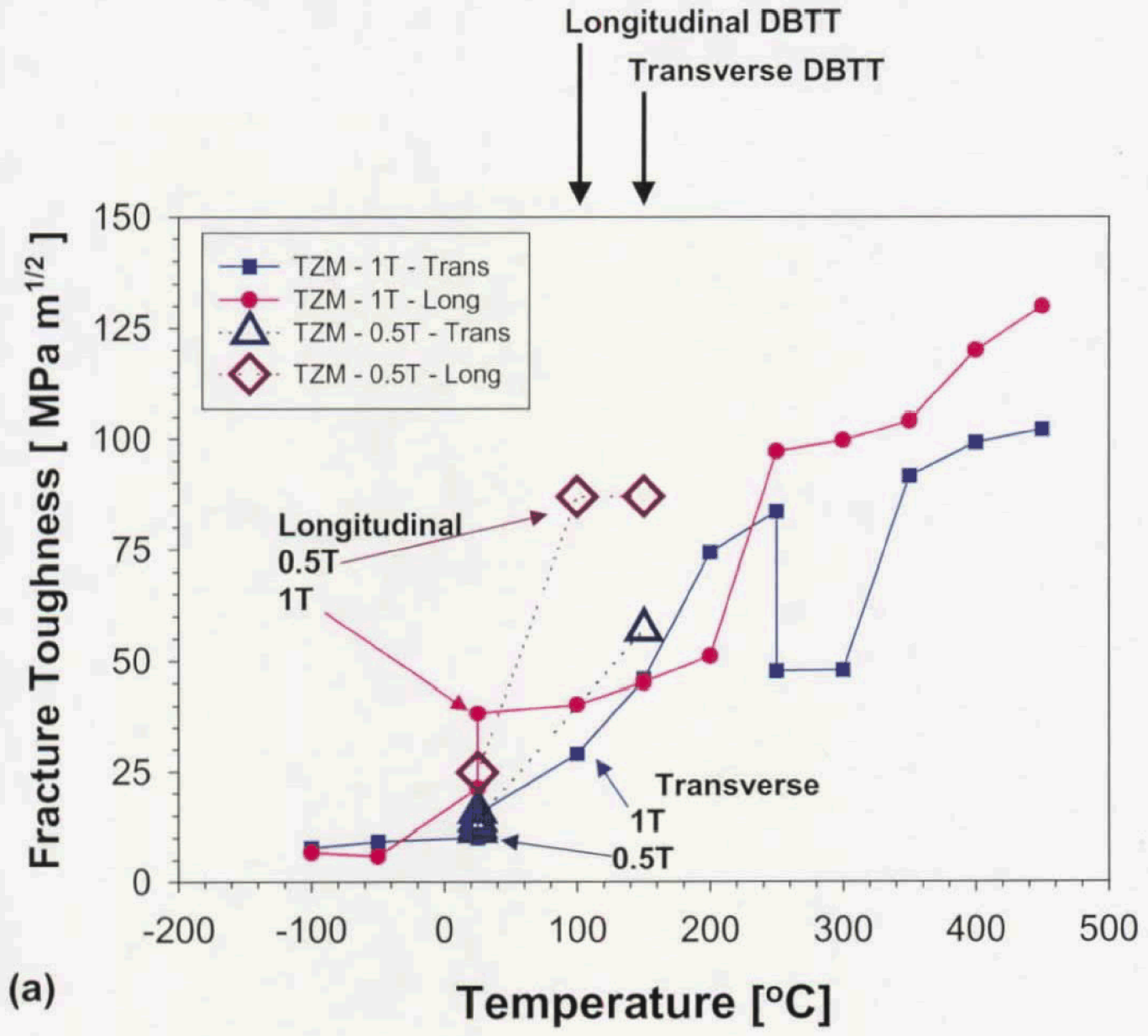

Figure 13. Fracture toughness values for TZM molybdenum as a function of temperature from -100°C to 450°C for longitudinal (circle) and transverse (square) orientations for results obtained from 1T Charpy specimens compared with results for: (a) 0.5T Charpy specimens in the longitudinal (open diamond) and transverse directions (open square), and (b) 0.25T Charpy specimens in the longitudinal (open diamond) and transverse directions (open square). The fracture toughness data are summarized in Tables VIII to XI. The results are shown for testing performed at a displacement rate of 0.0025 mm/s. The scales for Figures 13 and 14 are the same.

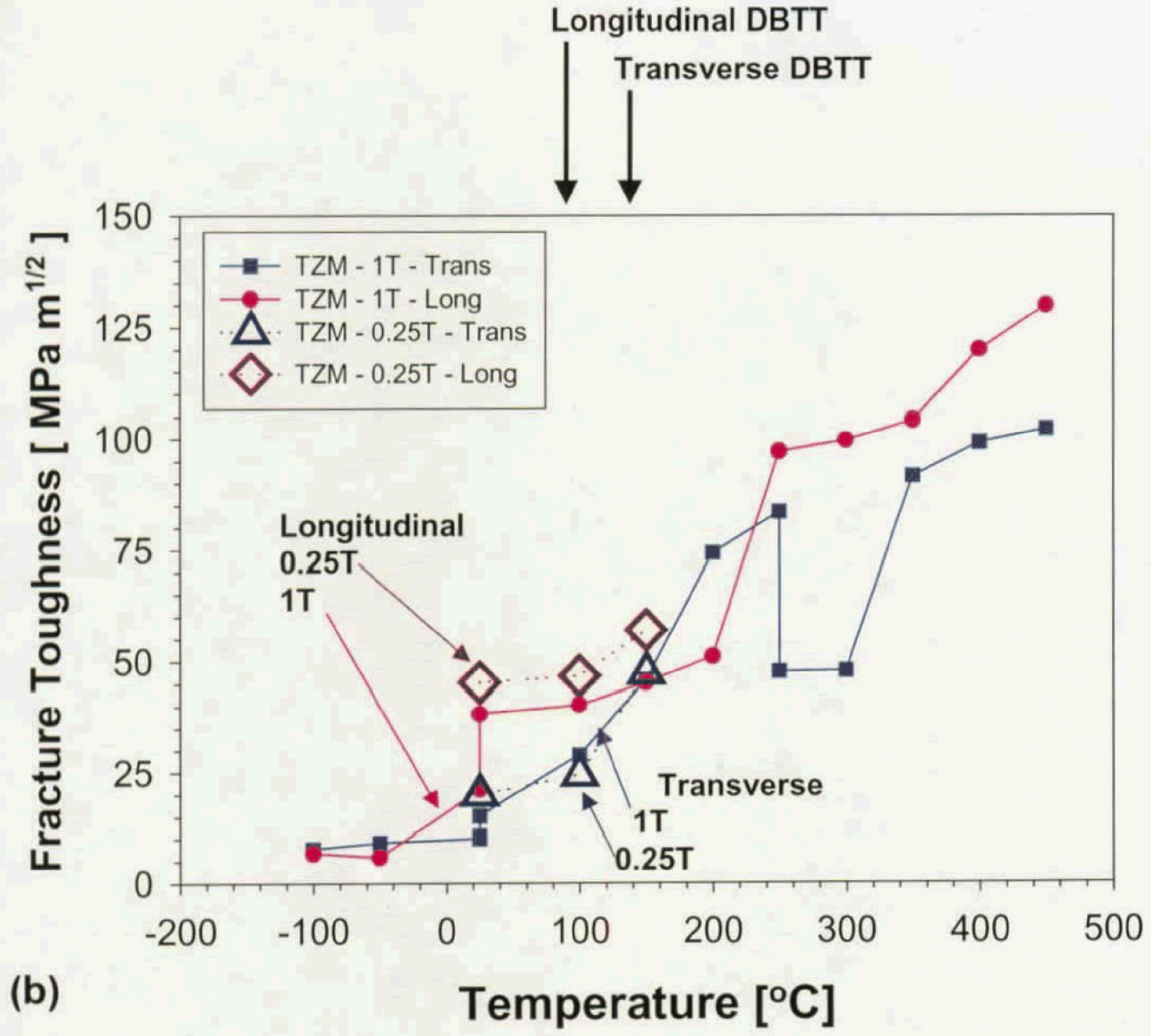

Figure 13. (Continued) Fracture toughness values for TZM molybdenum as a function of temperature from -100°C to 450°C for longitudinal (circle) and transverse (square) orientations for results obtained from 1T Charpy specimens compared with results for: (a) 0.5T Charpy specimens in the longitudinal (open diamond) and transverse directions (open square), and (b) 0.25T Charpy specimens in the longitudinal (open diamond) and transverse directions (open square). The fracture toughness data are summarized in Tables VIII to XI. The results are shown for testing performed at a displacement rate of 0.0025 mm/s. The scales for Figures 13 and 14 are the same.

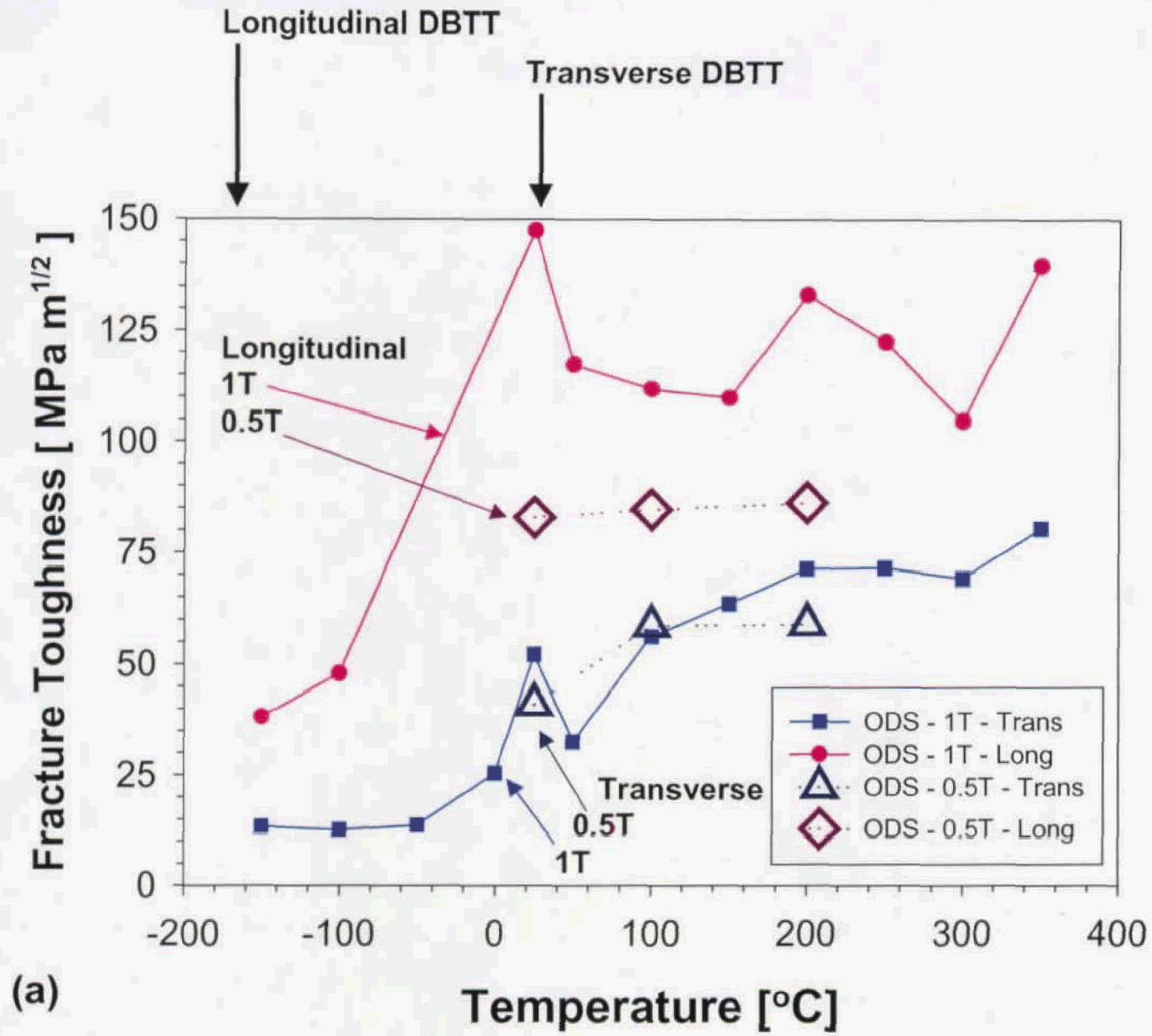

Figure 14. Plot of fracture toughness values for ODS molybdenum versus temperature from -150°C to 350°C for longitudinal (circle) and transverse (square) orientations for results obtained from 1T Charpy specimens compared with results for: (a) 0.5T Charpy specimens in the longitudinal (open diamond) and transverse directions (open square), and (b) 0.25T Charpy specimens in the longitudinal (open diamond) and transverse directions (open square). The fracture toughness data are summarized in Tables XII to XV. The results are shown for testing performed at a displacement rate of 0.0025 mm/s. The scales for Figures 13 and 14 are the same.

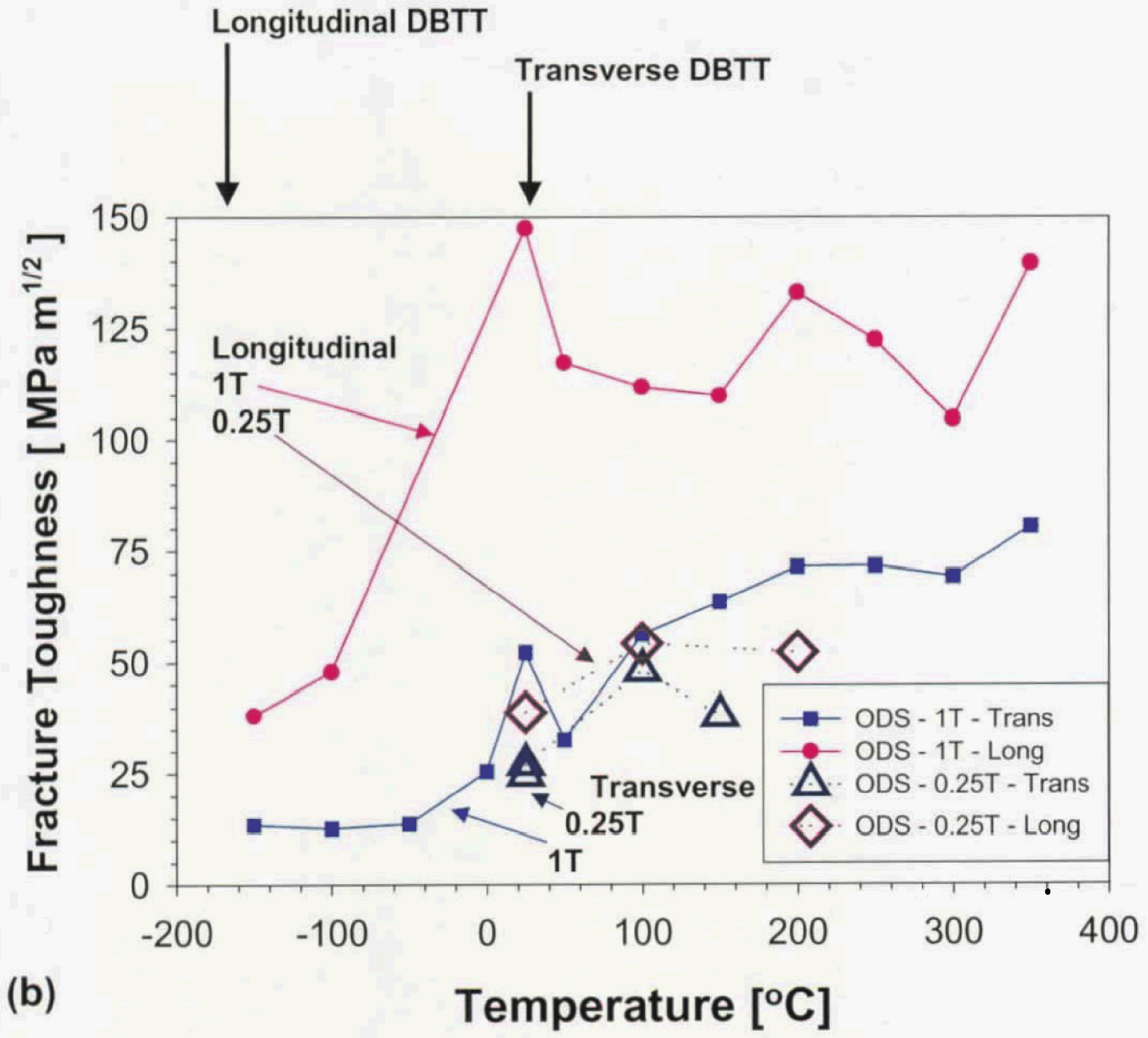

Figure 14. (Continued) Plot of fracture toughness values for ODS molybdenum versus temperature from -150°C to 350°C for longitudinal (circle) and transverse (square) orientations for results obtained from 1T Charpy specimens compared with results for: (a) 0.5T Charpy specimens in the longitudinal (open diamond) and transverse directions (open square), and (b) 0.25T Charpy specimens in the longitudinal (open diamond) and transverse directions (open square). The fracture toughness data are summarized in Tables XII to XV. The results are shown for testing performed at a displacement rate of 0.0025 mm/s. The scales for Figures 13 and 14 are the same.

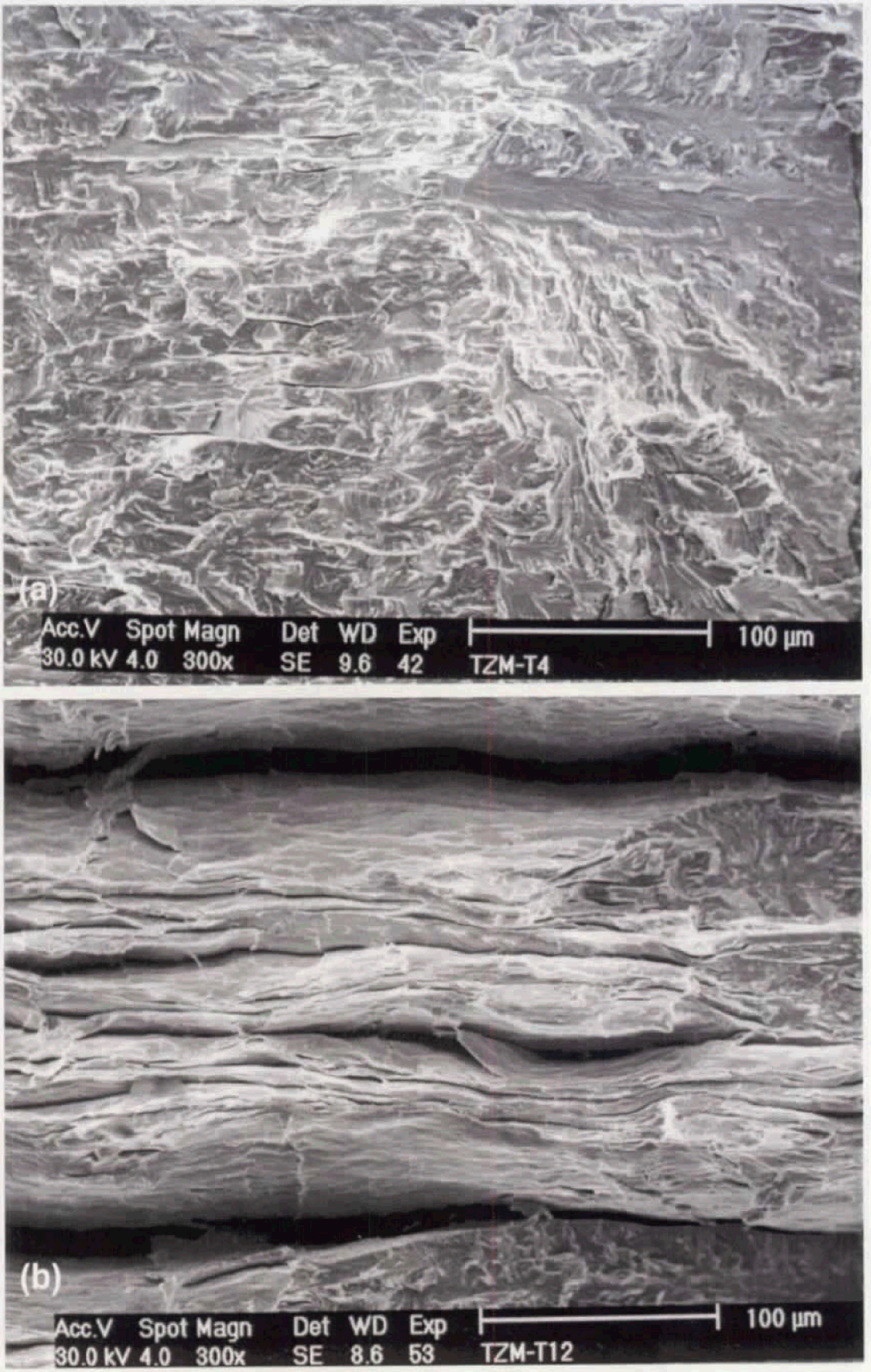

Figure 15. SEM fractography of TZM molybdenum 1T Charpy specimens after fracture toughness testing at: (a) room-temperature for the longitudinal (L-T) orientation, (b) 450°C for the longitudinal (L-T) orientation, (c) room-temperature for the transverse orientation (T-L), and (d) 150°C for the transverse (T-L) orientation.

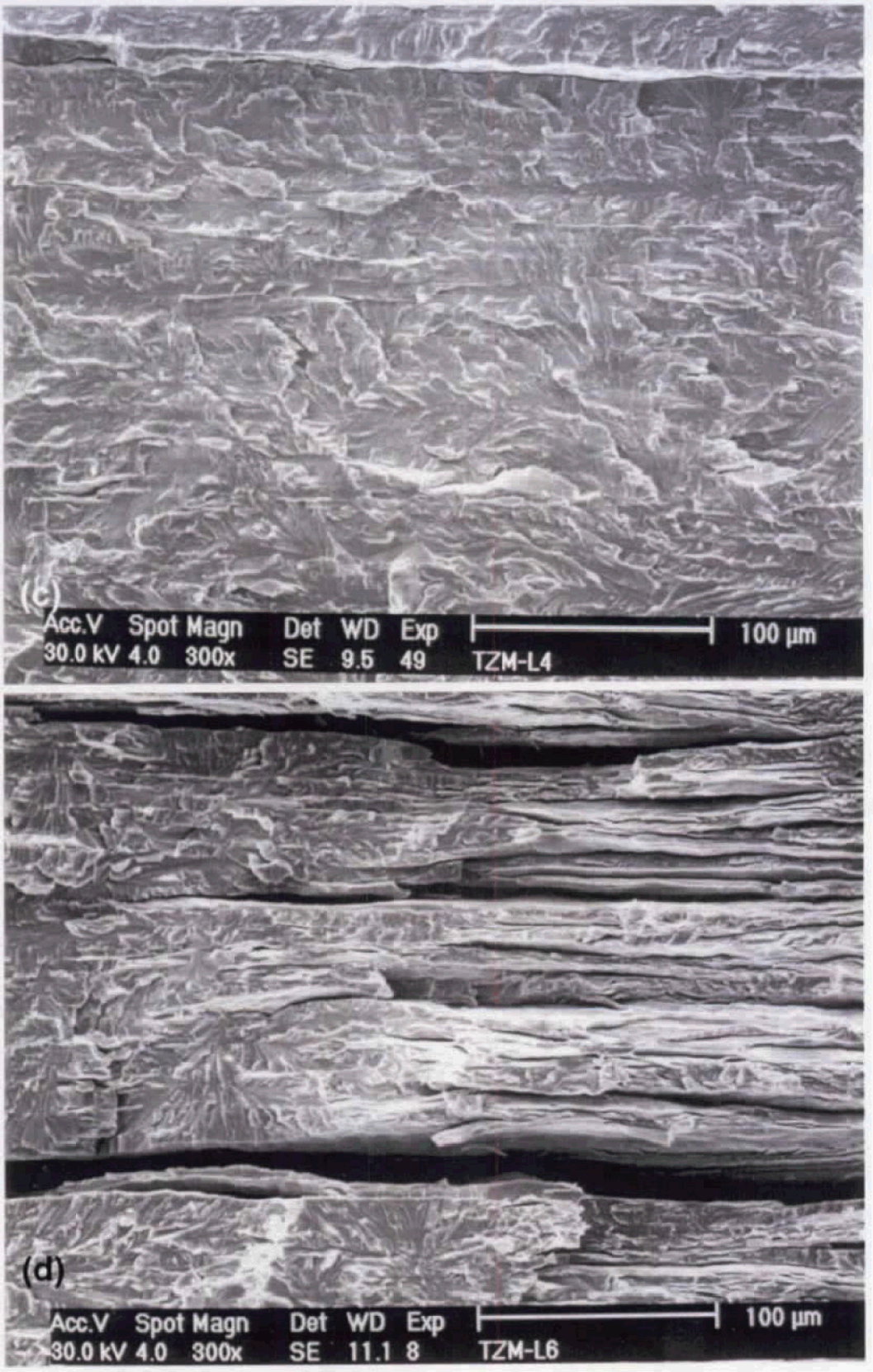

Figure 15. (Continued) SEM fractography of TZM molybdenum 1T Charpy specimens after fracture toughness testing at: (a) room-temperature for the longitudinal (L-T) orientation, (b) 450°C for the longitudinal (L-T) orientation, (c) room-temperature for the transverse orientation (T-L), and (d) 150°C for the transverse (T-L) orientation.

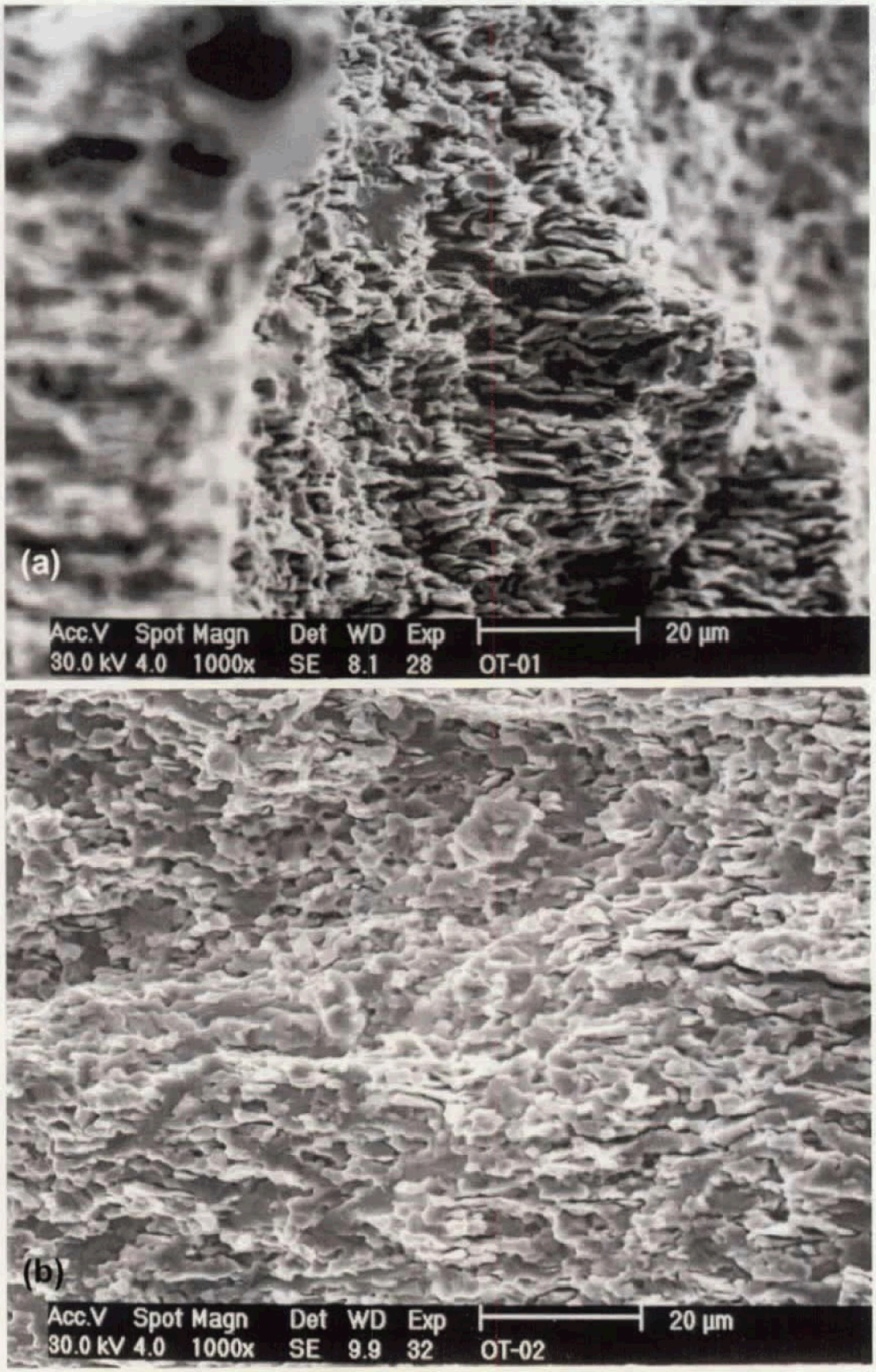

Figure 16. SEM fractography of ODS molybdenum 1T Charpy specimens following after fracture toughness testing at: (a) -150°C for the longitudinal (L-T) orientation, (b) -100°C for the longitudinal (L-T) orientation, (c) room-temperature for the longitudinal (L-T) orientation, (d) -50°C for the transverse orientation (T-L), (e) room-temperature for the transverse orientation (T-L), and (f) 350°C for the transverse (T-L) orientation.

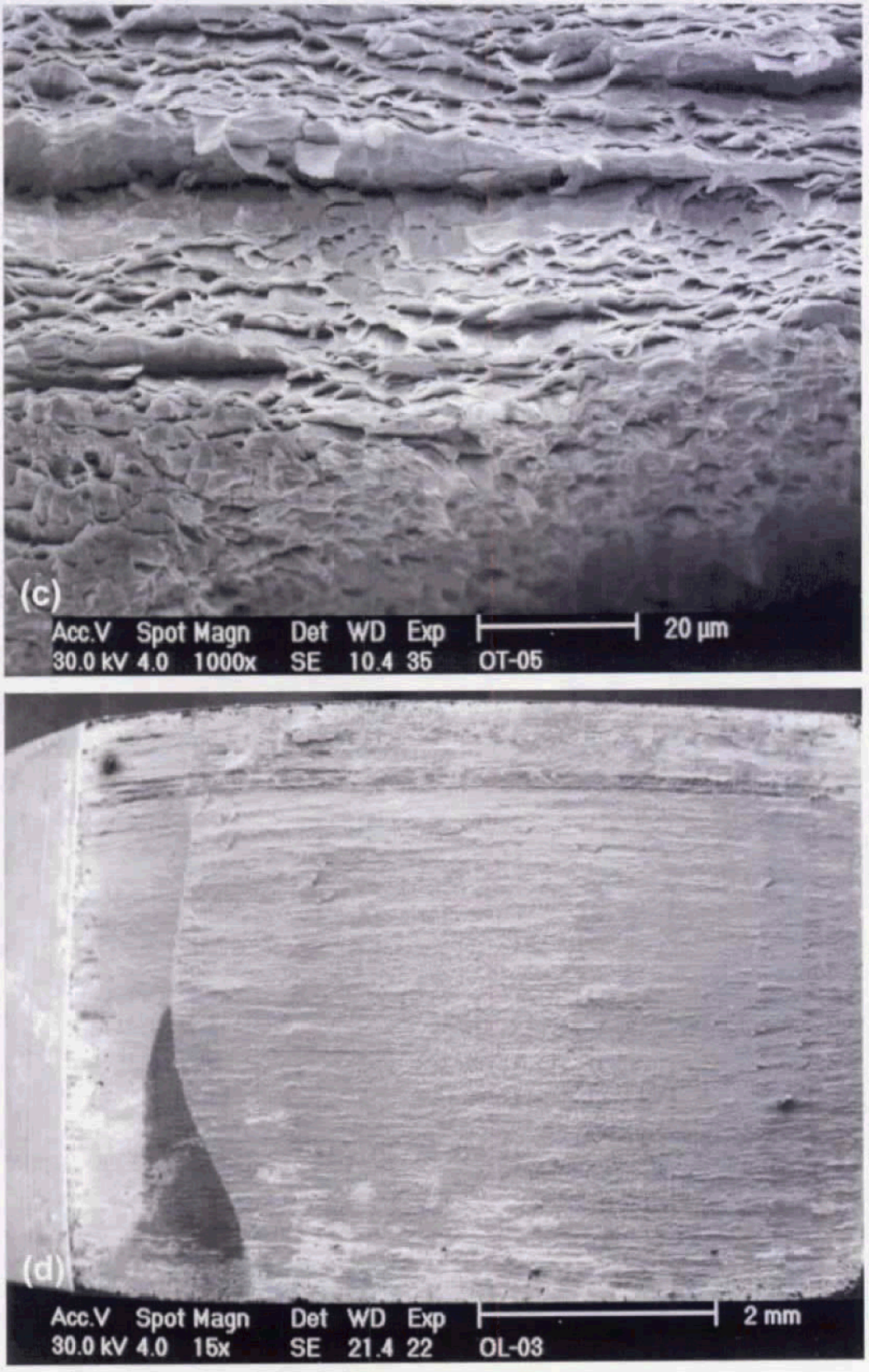

Figure 16. (Continued) SEM fractography of ODS molybdenum 1T Charpy specimens following after fracture toughness testing at: (a) -150°C for the longitudinal (L-T) orientation, (b) -100°C for the longitudinal (L-T) orientation, (c) room-temperature for the longitudinal (L-T) orientation, (d) -50°C for the transverse orientation (T-L), (e) room-temperature for the transverse orientation (T-L), and (f) 350°C for the transverse (T-L) orientation.

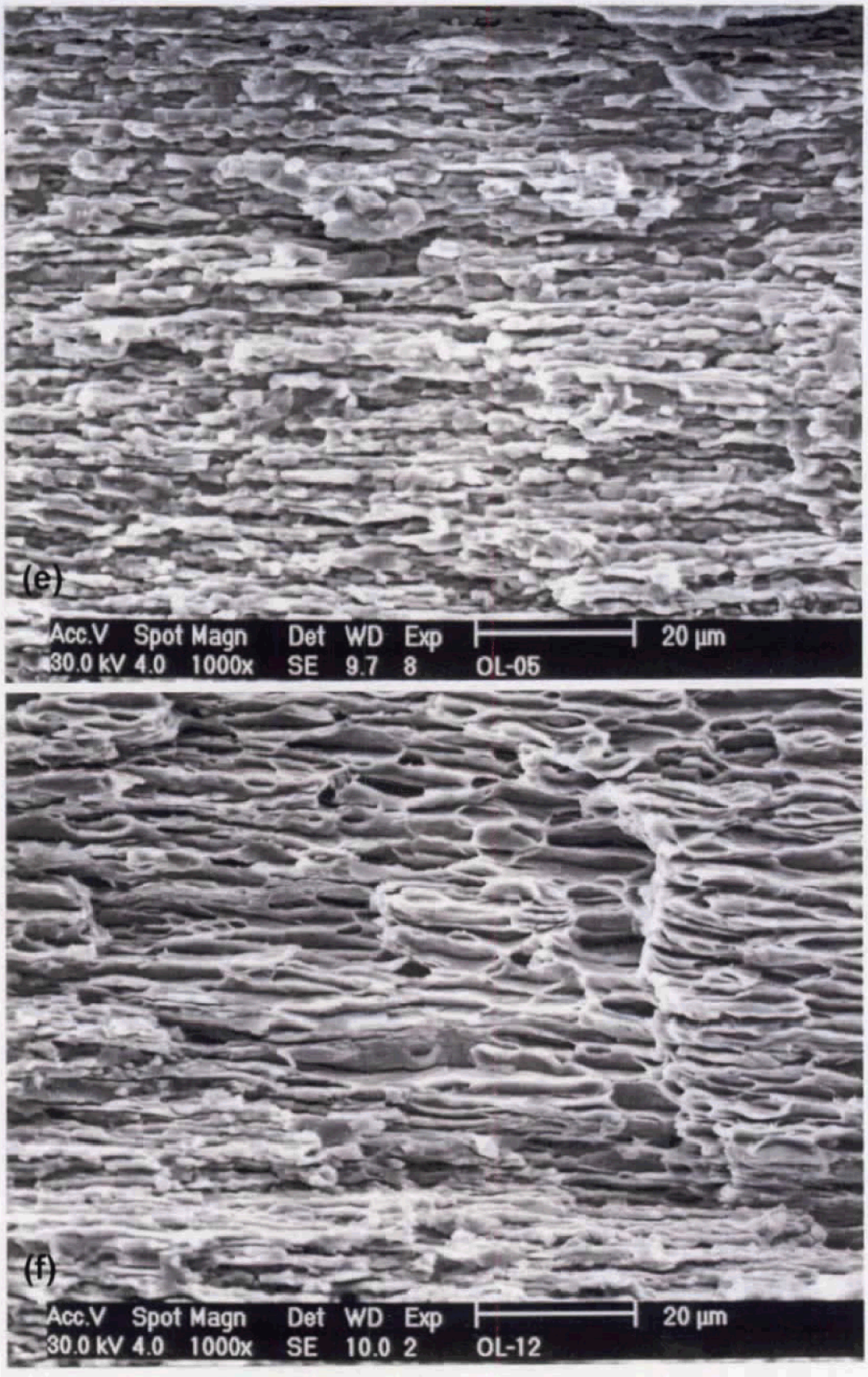

Figure 16. (Continued) SEM fractography of ODS molybdenum 1T Charpy specimens following after fracture toughness testing at: (a) -150°C for the longitudinal (L-T) orientation, (b) -100°C for the longitudinal (L-T) orientation, (c) room-temperature for the longitudinal (L-T) orientation, (d) -50°C for the transverse orientation (T-L), (e) room-temperature for the transverse orientation (T-L), and (f) 350°C for the transverse (T-L) orientation.

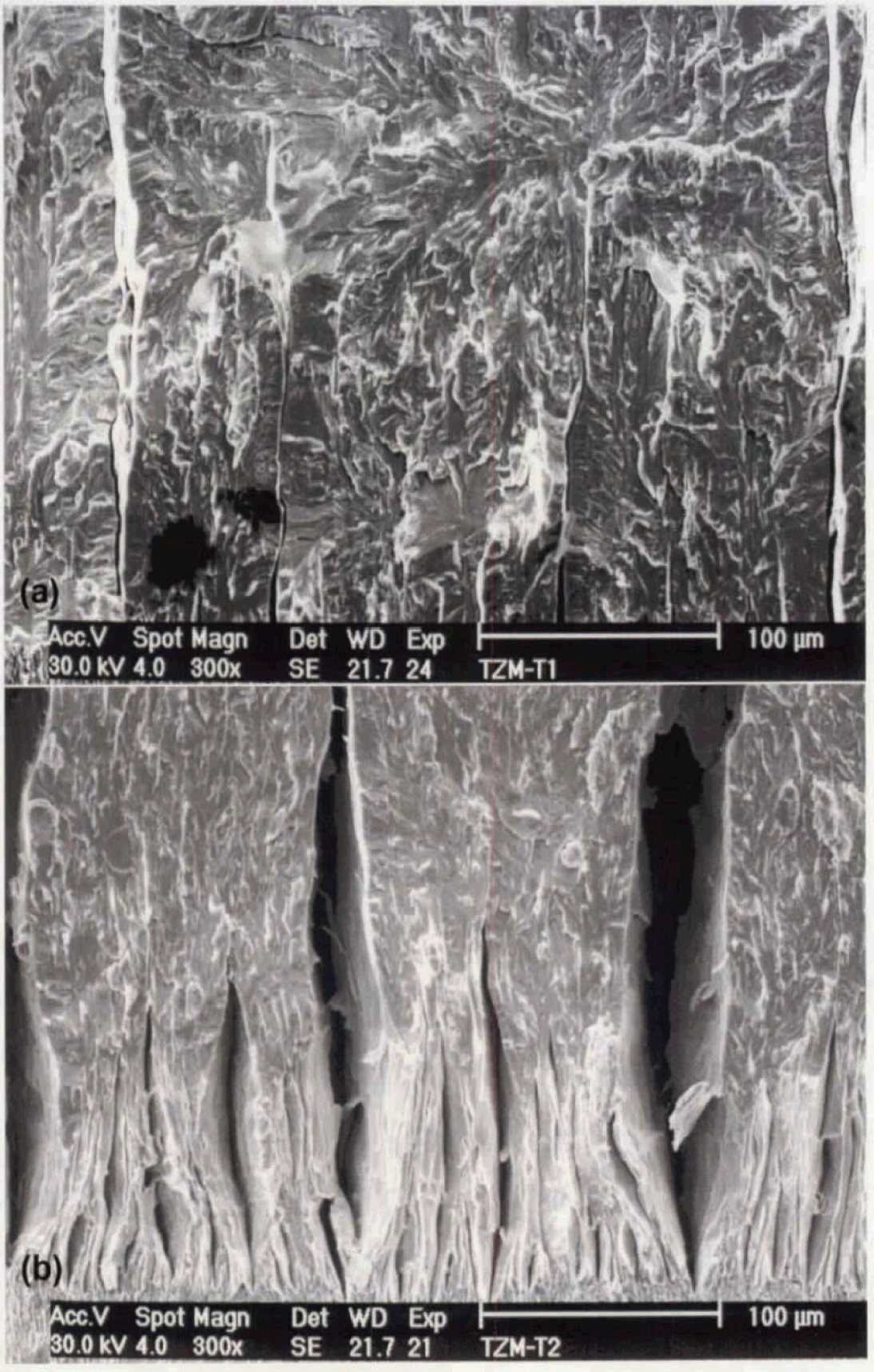

Figure 17. SEM fractography of TZM molybdenum specimens in the longitudinal (L-T) orientation after fracture toughness testing using a: (a) 0.5T Charpy for testing at room-temperature, (b) 0.5T Charpy tested at 100°C, (c) 0.25T Charpy tested at room-temperature, and (d) 0.25T Charpy for testing at 100°C.

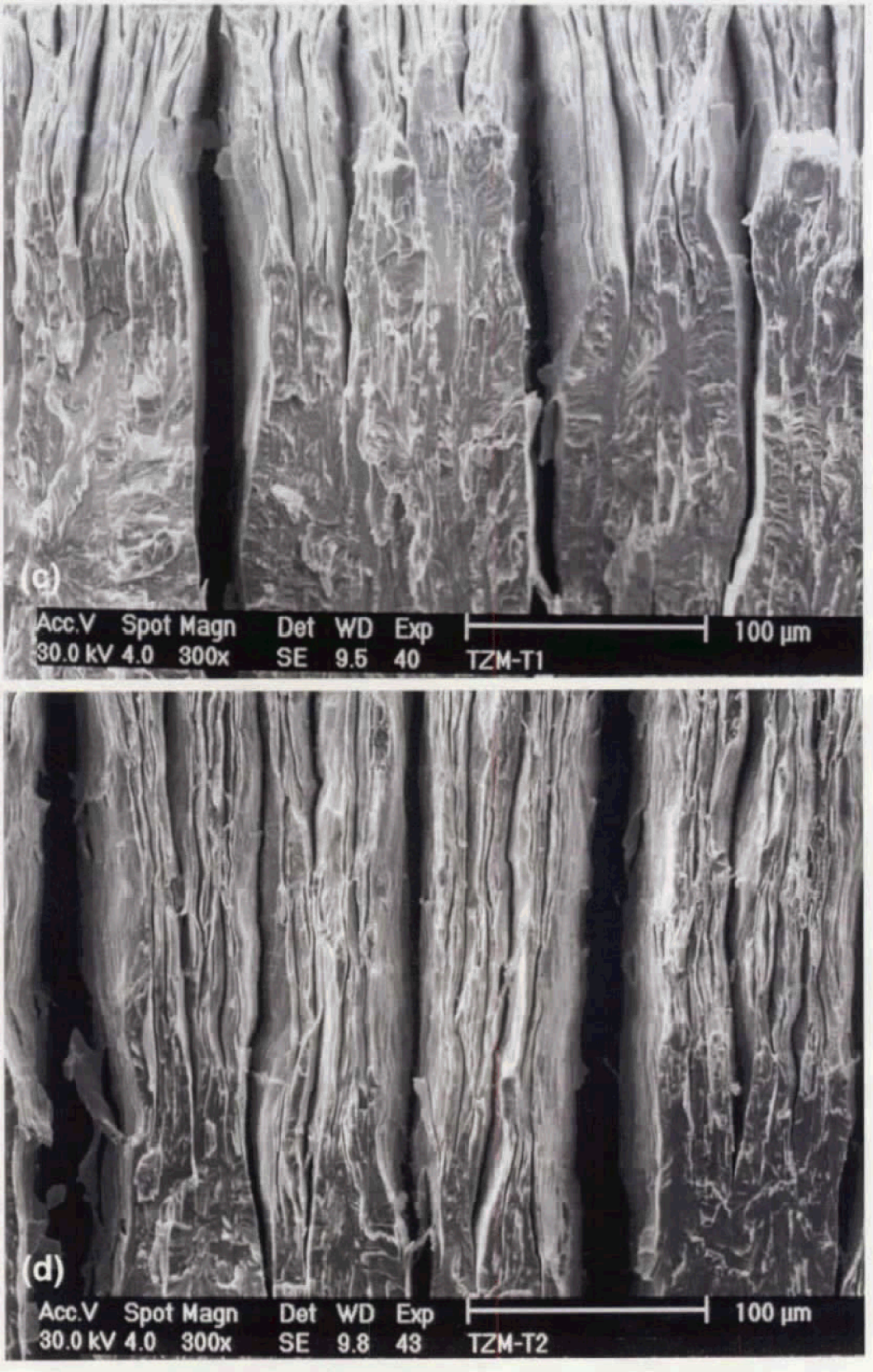

Figure 17. (Continued) SEM fractography of TZM molybdenum specimens in the longitudinal (L-T) orientation after fracture toughness testing using a: (a) 0.5T Charpy for testing at room-temperature, (b) 0.5T Charpy tested at 100°C, (c) 0.25T Charpy tested at room-temperature, and (d) 0.25T Charpy for testing at 100°C.

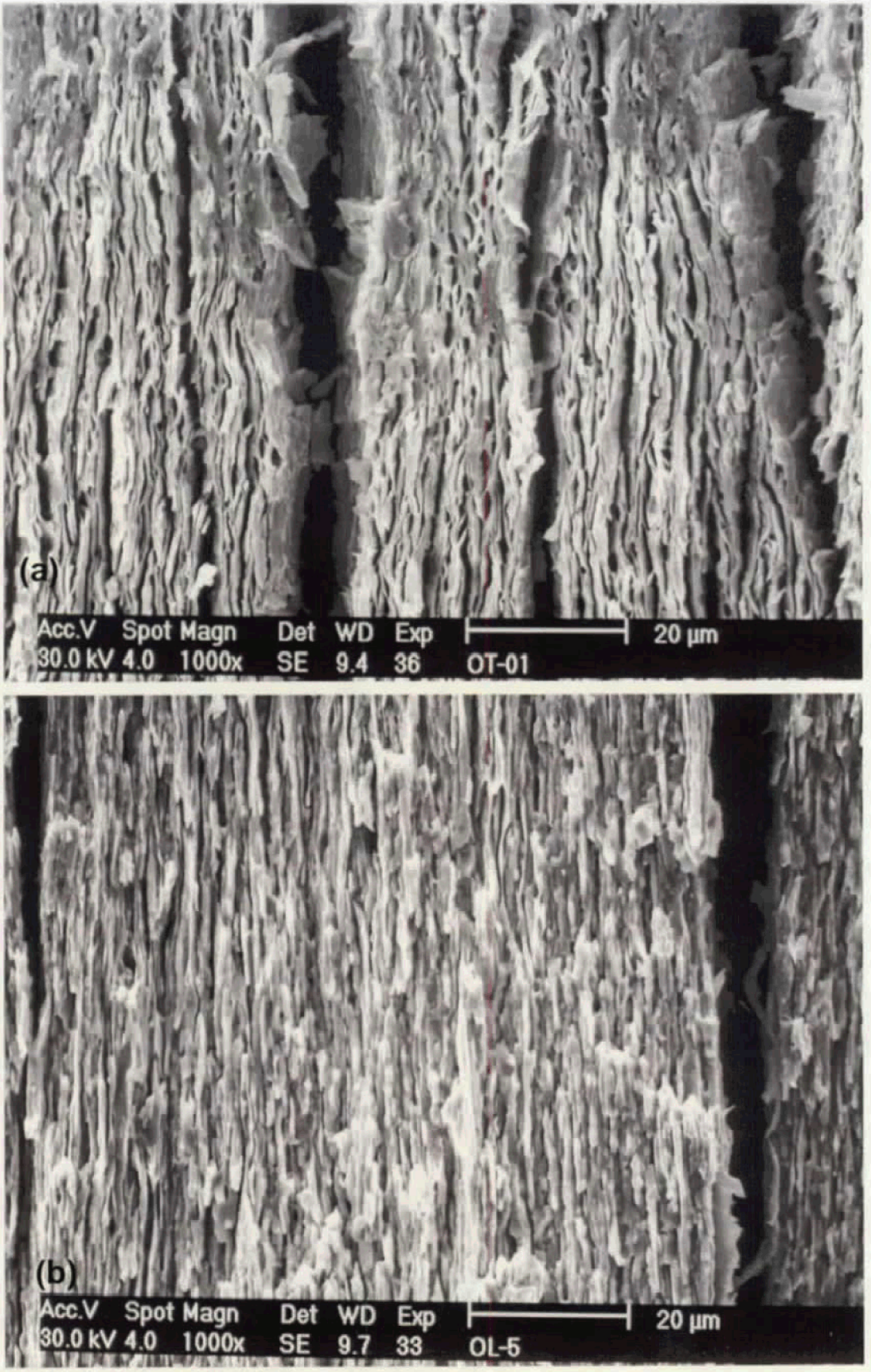

Figure 18. SEM fractography of ODS molybdenum specimens after fracture toughness testing at room-temperature using a: (a) 0.5T Charpy for the longitudinal (L-T) orientation, (b) 0.5T Charpy for the transverse (T-L) orientation, (c) 0.25T Charpy in the longitudinal (L-T) orientation, and (d) 0.25T Charpy for through thickness orientation (T-S).

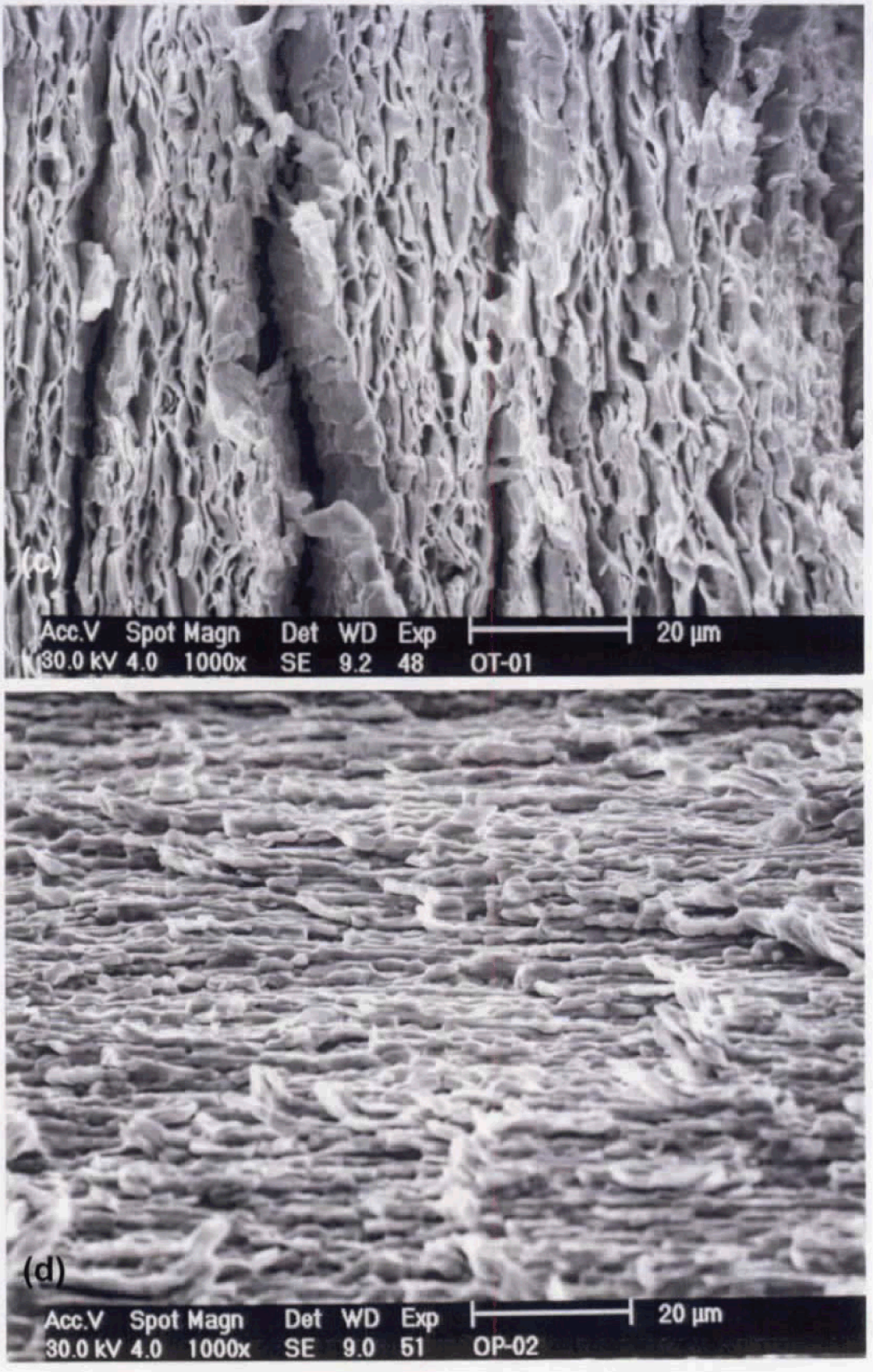

Figure 18. (Continued) SEM fractography of ODS molybdenum specimens after fracture toughness testing at room-temperature using a: (a) 0.5T Charpy for the longitudinal (L-T) orientation, (b) 0.5T Charpy for the transverse (T-L) orientation, (c) 0.25T Charpy in the longitudinal (L-T) orientation, and (d) 0.25T Charpy for through thickness orientation (T-S).